

# SPECTROSCOPY

## europa

*Spectroscopy since 1975*

**Were the Great Pyramids made of concrete?  
Raman study of interactions in multiferroics  
SERS for energetic material detection  
Representative sampling: the economic case**







PIGE and PIXE have been used to reveal that some blocks of the Khufu (Great) Pyramid at Giza were cast in situ: Egyptian concrete! Find out more in the article starting on page 21.

## Publisher

Ian Michael  
E-mail: [ian@impopen.com](mailto:ian@impopen.com)

## Advertising Sales

Ian Michael  
IM Publications Open, 6 Charlton Mill,  
Charlton, Chichester, West Sussex PO18 0HY,  
United Kingdom. Tel: +44-1243-811334,  
Fax: +44-1243-811711,  
E-mail: [ian@impopen.com](mailto:ian@impopen.com)

## Circulation

IM Publications Open, 6 Charlton Mill,  
Charlton, Chichester, West Sussex PO18 0HY,  
United Kingdom. Tel: +44-1243-811334,  
Fax: +44-1243-811711,  
E-mail: [katie@impopen.com](mailto:katie@impopen.com)

*Spectroscopy Europe* is published by  
IM Publications Open LLP, 6 Charlton  
Mill, Charlton, Chichester, West Sussex  
PO18 0HY, United Kingdom.

**Vol. 33 No. 5**  
**July/August 2021**

ISSN: 2634-2561

# CONTENTS

## 3 Editorial

## 4 News

## 21 Are carbon micro-clusters in the Khufu pyramid blocks of organic origin?

Guy Demortier

## 30 Structural, dielectric and Raman spectroscopic study of complex electric and magnetic interactions in multiferroic ionic crystals

Holger GIBHARDT, Fabian Ziegler and Götz Eckold

## 33 Surface-enhanced Raman spectroscopy for selected energetic material detection

Mohamed Mokhtar, Tamer Wafy and Mahmoud Abdelhafiz

## 41 Four generations of quality: "measuring up"

John P. Hammond

## 46 Sampling Column: "Sampling vs analytical error: where the money is ..."

Pentti Minkinen

## 51 Applications

## 53 Product Focus on Luminescence

## 54 Featured Product

## 55 New Products

## 63 Diary

## 64 Directory

*Spectroscopy Europe* is a digital magazine, published eight times a year and available free-of-charge to qualifying individuals in Europe and the Middle East.

Copyright 2021 IM Publications Open LLP

All rights reserved. No part of this publication may be reproduced, stored in a retrieval system, or transmitted, in any form or by any means, electronic, mechanical, photocopying, recording or otherwise, without the prior permission of the publisher in writing.

We have a bumper issue with three articles. Roman concrete is well known and has lasted well. Now, it seems that the Egyptians used concrete to build at least some of their pyramids. Guy Demortier reports that PIGE and PIXE analyses have revealed the presence of carbon clusters in the material used to build the Khufu (Great) pyramid at Giza. This fits with a model of construction in which the blocks were cast *in situ* rather than cut out of stone and somehow moved into place. There's always something new to be learnt!

Holger Gibhardt, Fabian Ziegler and Götz Eckold tell us about the use of Raman spectroscopy to understand complex electric and magnetic interactions in multiferroic ionic crystals. Multiferroics are a relatively new class of materials that exhibit magnetic and electrical ordering simultaneously. Both phenomena are coupled so that electric forces may be used to control the magnetic structure and vice versa. Raman enables understanding of the underlying processes on the atomic level, essential for the development of new materials with these properties.

Surface-enhanced Raman spectroscopy for selected energetic material detection is the topic of Mohamed Mokhtar, Tamer Wafy and Mahmoud Abdelhafiz. They have investigated various approaches to improve the SERS response of explosive materials and have come up with a simpler, one-step

method for the detection of natural, solid TNT.

John Hammond continues his series of Quality Matters Columns looking at Four Generations of Quality, with one on the developments of the ISO Technical Committee responsible for reference materials to its latest incarnation as a Technical Committee.

In the Sampling Column, Kim Esbensen has enlisted the support of another doyen of representative sampling, Pentti Minkkinen. In the commercial world, the reason for analysis comes down to money: whether ensuring you are getting what you paid for, but not providing more than necessary, or in regulatory compliance and the avoidance of fines. Kim's Column has been pushing the importance of not overlooking the sampling step since its beginnings, and this edition provides clear examples where the consequences are costly; very costly.

May I remind you that there is an online commenting facility if you wish to raise anything with authors. You must be logged in to use it, and there is likely to be a short delay for manual approval to avoid inappropriate posts appearing. As always, your private comments are most helpful and valued, so do feel free to contact me at [ian@impopen.com](mailto:ian@impopen.com).



## MS-based alien life detector

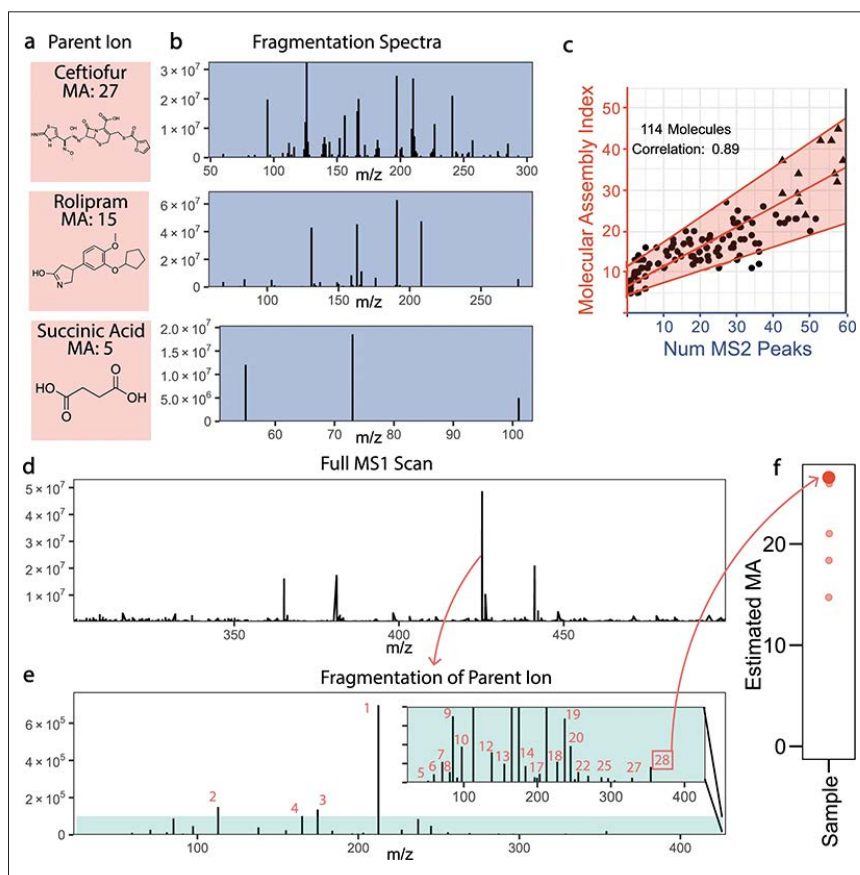
University of Glasgow researchers have developed a new method called Assembly Theory which can be used to quantify how assembled or complex a molecule is in the laboratory using techniques like mass spectrometry. The more complex the object, the more unlikely that it could arise by chance, and the more likely it was made by the process of evolution. The team, led by Professor Lee Cronin, developed Assembly Theory in partnership with collaborators at NASA and Arizona State University. Together, they have shown that the system works with samples from all over the Earth and extra-terrestrial samples.

The system uses mass spectrometry to analyse the molecule and counts the number of unique parts. The larger the number of unique parts, the larger the assembly number and the team have been able to show that life on Earth can only make molecules with high assembly numbers.

One of the main challenges of the search for extraterrestrial life has been identifying which chemical signatures are unique to life, leading to several ultimately unproven claims of the discovery of alien life. The metabolic experiments of NASA's Viking Martian lander, for example, only detected simple molecules whose existence could be explained by natural non-living processes in addition to living processes.

Professor Cronin, Regius Professor of Chemistry at the University of Glasgow, said: "Our system is the first falsifiable hypothesis for life detection. It's based on the idea that only living systems can produce complex molecules that could not form randomly in any abundance. This allows us to sidestep the problem of defining life—instead we focus on the complexity of the chemistry."

The theory of molecular assembly can also be used to explain that the larger the number of steps needed to deconstruct a given complex molecule, the more improbable it is that the molecule was created without life. This decomposition provides a complexity measure, called the molecular assembly number. Unlike all other complexity



Experimental correlation of mass spectrometry data to MA and MA analysis of mixtures. Reproduced from [doi.org/10.1038/s41467-021-23258-x](https://doi.org/10.1038/s41467-021-23258-x) under a CC-BY licence.

approaches, however, it is the first to be experimentally measurable. The team demonstrated that it was possible to experimentally observe the molecular assembly number of single molecules in the lab by deconstructing them using fragmentation tandem mass spectrometry. Thus, the complexity measure is distinct from all other complexity measures because it is both computable and directly observable.

A life detection instrument based on this method could be deployed on missions to extra-terrestrial locations to detect biosignatures, or even detect the emergence of new forms of artificial life in the lab.

Professor Cronin added: "This is important because developing an approach that cannot produce false positives is vital to support the first discovery of life beyond Earth, an event that will only happen once in human history."

This was reported in *Nature Communications* ([doi.org/gkcv4c](https://doi.org/gkcv4c)).

## ZooMS provides new insights on animals in the African past

In order to understand foodways and subsistence strategies of humans in the past, as well as distributions of ancient animal species, it is critical for archaeologists to accurately identify animal taxa in archaeological sites. Many sites across sub-Saharan Africa have fragmented and poorly preserved animal bones, leaving the majority of specimens unidentifiable. Sub-Saharan Africa is also home to the greatest diversity of bovids on Earth, including African buffalo, wildebeest, eland and duikers, as well as domestic sheep, goat and cattle. The sheer number of osteologically similar animals in Africa presents a major challenge for identifying animal bones.

During the past decade, archaeologists have increasingly used a bone collagen peptide fingerprinting technique called *Zooarchaeology by Mass Spectrometry (ZooMS)* to identify



UV-VIS Spectrophotometer  
**UV-1900i**



# Push the limits

With its new features, the UV-1900i spectrophotometer pushes the limits of UV-Vis analysis applications. It integrates 'Analytical Intelligence' automated support functions utilizing digital technology, such as M2M, IoT, and Artificial Intelligence (AI) that enable higher productivity, maximum reliability and better connectivity. Several measurement modes and accessories support a wide range of measurements in food, pharmaceutical, life sciences and chemical markets' labs.

**High-accuracy quantitative analysis**

featuring high resolution and high sensitivity based on the patented LO-RAY-LIGH technology

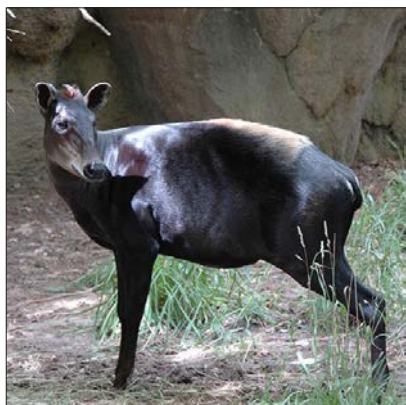
**The industry's fastest scan functions**

providing measurement within three seconds and following even fast chemical reactions

**Easy-to-use operability for fast complete analysis**  
through color touch panel with large and intuitive icons

**Compliant with advanced regulations**  
through LabSolution DB and CS software supporting FDA 21 CFR Part 11, GMP and more





A yellow backed duiker at the Knoxville Zoo.  
Credit: University of Tennessee, Knoxville

ambiguous or unidentifiable bone fragments. However, the lack of complete reference peptide markers for African animals has hindered its application in Africa. In a new study, researchers have presented a complete set of confirmed ZooMS peptide markers for all groups of African bovids, revealing new opportunities for archaeologists to identify these species in archaeological sites.

"Our new reference dataset has the potential to revive research interest in, and add value to, assemblages previously considered too poorly preserved for traditional zooarchaeological analysis", said Anneke Janzen, assistant professor in the Department of Anthropology at the University of Tennessee, Knoxville, and lead author on the study.

Using these new peptide markers, Janzen and her team applied the ZooMS method to extremely fragmented animal bone assemblages from six Iron Age archaeological sites in Zambia and discovered the number of species present is greater than expected. Their work is published in *PLOS One* ([doi.org/gj6bwv](https://doi.org/gj6bwv)).

"With this new data, we discovered that Iron Age populations continued to hunt wild bovids, especially small duikers, in addition to relying on cattle-based pastoralism", Janzen said. "Our research opens new opportunities for addressing questions of paleoenvironment, subsistence strategies, foodways, the spread of and development of herding economies in the African past."

## Raging Raman

Researchers from the Single-Cell Center at the Qingdao Institute of Bioenergy and Bioprocess Technology (QIBEBT) of the Chinese Academy of Sciences have developed a technique to sort and sequence the genome of bacteria in soil one bacterial cell at a time, while also identifying what its function is in the soil environment.

Soil is home to a vast and complex microbiome, which features arguably the highest genomic diversity and widest heterogeneity of metabolic activities of cells on Earth. In turn, these metabolic activities can, in principle, provide the foundation for industrial production of numerous compounds of value. The ability to pinpoint "who is doing what" in the soil microbiome has until now been extremely difficult at the resolution of a single cell, as normally a great many cells, typically millions of them, have had to be analysed at the same time.

In 2020, researchers from the QIBEBT Single-Cell Center developed a bacteria-profiling technique called

Raman-Activated Gravity-driven single-cell Encapsulation and Sequencing, or RAGE sequencing. This sequencing technique uses laser tweezers and takes advantage of the properties of gravity to permit analysis of bacteria cells one by one. The form and structure of a bacterium are then investigated using Raman spectroscopy. They have now developed their RAGE sequencing technique into a new scientific instrument they are calling a Raman-activated Cell Sorter-Sequencer or RACS-Seq. It is the first instrument that can pinpoint "who is doing what" at one-cell resolution in complex ecosystem. And they applied it to the bacteria in soil.

The Raman spectrum of a single cell offers an intrinsic biochemical fingerprint, and this in turn can be used as a proxy of its metabolic activity. When this single-cell Raman spectrum is coupled with probing of the isotopes involved in this activity, the technique can reveal the amount of chemical from the cell's environment that it is taking up.

Isotopes are often used track or trace chemical processes. By feeding the



A technique to sort and sequence the genome of bacteria in soil one bacterial cell at a time.  
Credit: Liu Yang



bacteria with D<sub>2</sub>O, the general metabolic activity of the cells can be tracked via their Raman spectra. The technique can also detect not only uptake of D<sub>2</sub>O but also different isotopes of carbon or nitrogen. This can even reveal the particular cellular profile of synthesis of biological molecules. This metabolic tracking can then be linked via the RAGE technique to individual cells whose genome can be sequenced. The results of the work are published in *mSystems* ([doi.org/gnjh](https://doi.org/gnjh)).

"This should allow researchers to 'mine' soil to find bacteria of interest that are in the business of producing particular carotenoids, lipids, polysaccharides, protein and even antibiotics", said Jing Xiaoyan, a microbiome scientist at the QIBEBT Single-Cell Center. The researchers now want to further improve the throughput of their technique, currently a few cells per minute, to speed up and fully automate the process.

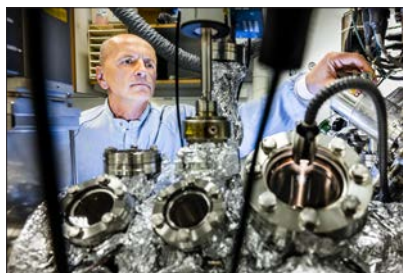
"Our goal ultimately is to keep optimising the RACS-Seq instrument, so that it becomes a universal and highly versatile tool for precisely probing target cells or metabolic activities of interest", added Xu Jian, Director of the QIBEBT Single-Cell Center. "And not just from soil, but from any other complex natural ecosystem."

## Have we been doing XPS wrong?

X-ray photoelectron spectroscopy (XPS) was developed in the 1960s and is accepted as a standard method in materials science. Researchers at Linköping University, Sweden, however, have shown that the method is often used erroneously.

"It is, of course, an ideal in research that the methods used are critically examined, but it seems that a couple of generations of researchers have failed to take seriously early signals that the calibration method was deficient. This was the case also for a long time in our own research group. Now, however, we hope that XPS will be used with greater care", says Grzegorz Greczynski, senior lecturer in the Department of Physics, Chemistry and Biology at Linköping University.

Grzegorz Greczynski and his colleague in the department, Professor Lars Hultman, have shown that XPS can give



Grzegorz Greczynski, senior lecturer in the Department of Physics, Chemistry and Biology at Linköping University. Credit: Thor Balkhed

misleading analysis results due to an erroneous assumption during calibration. XPS is a standard method in materials science, and more than 12,000 scientific articles with results obtained by XPS are published each year. The technique was developed during the 1960s by Professor Kai Siegbahn at Uppsala University to become a useful and powerful method for chemical analysis, and the work led to him being awarded the Nobel Prize in physics in 1981.

"The pioneering work that led to the Nobel Prize is not in question here. When the technique was developed initially, the error was comparatively small, due to the low calibration precision of the spectrometers used at the time. However, as spectroscopy developed rapidly and spread to other scientific fields, the instruments have been improved to such a degree that the underlying error has grown into a significant obstacle to future development", says Lars Hultman.

What the researchers have discovered is that the original method is being used wrongly, through an erroneous assumption used in the calibration process. When calibrating the experiment, the signal from elemental carbon accumulating on the sample surface is often used.

It turns out that the carbon-based compounds that are formed naturally by condensation onto most samples give rise to signals that depend on the surroundings and the substrate onto which they are attached, in other words, the sample itself. This means that a unique signal is not produced, and large errors arise when a more or less arbitrary value is used as reference to calibrate the measuring instrument.

Criticism of the method was raised as early as the 1970s and into the early 1980s. After that, however, knowledge about the error fell into oblivion. Lars Hultman suggests that several factors have interacted to allow the error to pass unnoticed for nearly 40 years. He believes that the dramatic increase in the number of journals that digital publishing has made possible is one such factor, while deficient reviewing procedures are another.

"Not only has a rapidly growing number of scientists failed to be critical, it seems that there is a form of carelessness among editors and reviewers for the scientific journals. This has led to the publishing of interpretations of data that are clearly in conflict with basic physics. You could call it a perfect storm. It's likely that the same type of problem with deficient critical assessment of methods is present in several scientific disciplines, and in the long term this risks damaging research credibility", says Lars Hultman.

Grzegorz Greczynski hopes that their discovery can not only continue to improve the XPS technique, but also contribute to a more critical approach within the research community. This has been published in *Scientific Reports* ([doi.org/gnjj](https://doi.org/gnjj)).

"Our experiments show that the most popular calibration method leads to nonsense results and the use of it should therefore be terminated. There exist alternatives that can give more reliable calibration, but these are more demanding of the user and some need refinement. However, it is just as important to encourage people to be critical of established methods in lab discussions, in the development department, and in seminars", Grzegorz Greczynski concludes.

## NMR and MS provide new insights into "long COVID"

A clinical research collaboration on COVID-19 pheno-conversion and subsequent pheno-reversion has discovered transient and persistent systemic changes of the molecular signatures in patient blood samples three months after the acute COVID-19 disease phase. These biochemical abnormalities, identified by

a quantitative, label-free assay platform integrating nuclear magnetic resonance (NMR) spectroscopy and mass spectrometry (MS), relate to ongoing “long COVID” symptoms, which persist post-acute infection and can affect more than half of the recovered COVID patients—even six months after infection.

The integrated, quantitative NMR and MS assay platform has revealed metabolic abnormalities, interactions of metabolic markers with cytokines, as well as interactions of lipoproteins with inflammation markers, caused by acute COVID-19. It enabled the creation of a multi-assay panel of pheno-conversion markers that change significantly during disease progression. This molecular phenomics panel can now also provide a measure of a patient’s partial recovery, or of emerging chronic PACS risks, e.g., for new-onset diabetes or for new-onset atherosclerosis, and for other persistent or reoccurring symptoms, including chronic fatigue, “brain fog” and numerous other reported long COVID symptoms.

Post-acute follow up studies on non-hospitalised and mildly affected COVID-19 patients revealed that the majority of these patients is not back to normal health or normal biochemistry three months on and suffers from PACS characterised by persistent symptoms and health dysfunction after the acute infection. More than 57% of these patients show one or more symptoms up to six months following the acute phase, and many of them have metabolic abnormalities as revealed by the NMR- and MS-based pheno-reversion panel.

Professor Jeremy Nicholson, Pro Vice Chancellor for the Health Futures Institute at Murdoch University and Director of the Australian National Phenome Centre (ANPC) explained: “Advanced NMR- and MS-screening of blood plasma provides complementary insights into the complex COVID-19 systemic pattern. There were multiple but variable biochemical abnormalities in the follow up patients with a variety of partial recovery phenotypes. We noted that most of the follow up COVID-19 patients had metabolic abnormalities irrespective of whether they were still symptomatic, but symptomatic

patients were statistically more likely to have biochemical abnormalities. This is an immensely dangerous disease that is not only costing lives today, but as we’re discovering now, may have serious health consequences for some patients long into the future, even in relatively mild original cases.”

The majority of patients at three months post-acute phase have a variety of blood metabolic abnormalities that differ between symptomatic and asymptomatic at six months. The researchers found that plasma lipoproteins in the blood of COVID-19 patients changed during infection and came closer to patterns typically found in patients with diabetes and atherosclerosis. Some abnormalities were reduced in the follow up patients and were reversible, whereas markers related to liver, energy metabolism and neuro-pathologies were often not completely reversed.

The latest research is consistent with earlier findings from the ANPC that showed COVID-19 is a systemic disease with multi-organ effects. The concept of pheno-conversion, as expressed in the lipoprotein and metabolic profile of blood plasma, establishes molecular phenotype biomarkers that can be analysed for disease progression, severity and treatment. This underlines the importance of longitudinal studies on recovered patients for PACS effects and long-term health risks.

ANPC also devised a novel relaxation and diffusion edited NMR method that refined selectivity and led to the discovery of novel phospholipid signals from supramolecular clusters. “This is the first example of motional editing of complex blood plasma spectra to enhance the selectivity of a diagnostic procedure and opens the door to other NMR approaches to classification based on the dynamics of molecules, as well as on concentrations”, added Professor Nicholson.

The COVID-19 pheno-conversion and pheno-reversion signatures are detected by combined NMR and MS assays, providing complementary insights into potential biomarkers for cardiology, metabolism, diabetes, kidney disease, liver function, neurological effects and inflammation.

Bruker has begun validation of this integrated NMR/MS clinical research assay set in Europe, with the goal of developing PACS personalised risk screening and longitudinal patient monitoring diagnostic methods.

Dr Óscar Millet, Principal Investigator at CIC bioGUNE in Bilbao, Spain, commented: “As one of the key clinical research labs for precision medicine in Europe, we see huge potential for the PACS research enabled by high performance NMR and MS technology. We are an active member of the International COVID-19 research network, which is led by the ANPC. The harmonised research approach, which is based on standardised operating procedures developed by ANPC and Bruker, has allowed us to study PACS on Spanish patient cohorts and cross-validate our data with those of the ANPC at both the analytical and biological level.”

The studies were conducted using Avance™ IVDr NMR 600 MHz spectrometers integrated in the ANPC class II biosecurity laboratory, together with Bruker and CIC bioGUNE *in vitro* diagnostics NMR research (IVDr) technology methods. The ANPC has also equipped its molecular phenomics lab with mass spectrometers, including Bruker impact II and timsTOF™ Pro QTOF-MS, and a solarix™ MRMS system. Results were reported in *Journal of Proteome Research* ([doi.org/gj9qvf](https://doi.org/gj9qvf)).

## Graphene and Raman spectroscopy can detect COVID-19 quickly

The researchers combined sheets of graphene with an antibody designed to target the infamous spike protein on the coronavirus. They then used Raman spectroscopy to measure the atomic-level vibrations of these graphene sheets when exposed to COVID-positive and COVID-negative samples in artificial saliva. These sheets were also tested in the presence of other coronaviruses, such as Middle East respiratory syndrome or MERS-CoV.

They found that the vibrations of the antibody-coupled graphene sheet changed when treated with a COVID-positive sample, but not when treated with a COVID-negative sample or with



# Partner with the experts in advanced Silicon Drift Detectors Science at the speed of light

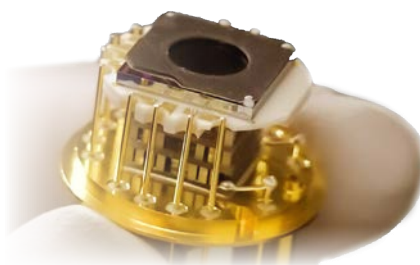
With over 40 years' experience in XRF-detector R&D and manufacturing, Hitachi High-Tech detector products are used worldwide. Proven reliability and radiation hardness, low power consumption and competitive pricing make Hitachi detectors the complete package. From at our production facilities in the USA and Finland, our teams offer flexibly scalable manufacturing capabilities and agile R&D to deliver the custom solutions to your requirements.

Now, our expanded detector product range includes the SAANA as well as the Vortex SDD; offering a wider choice of designs, fully customizable to your needs:

	<b>SAANA SDD</b>	<b>Vortex SDD</b>
<b>Resolution</b>	<140 eV	<140 eV
<b>Sensor Thickness</b>	1.0 mm	0.5, 1.0 and 2.0 mm
<b>Sensor sizes</b>	50 mm <sup>2</sup>	50 to 100mm <sup>2</sup>
<b>Input Count rates</b>	2000 Kcps	>5,000 Kcps



▶ **SAANA SDD**



▶ **SAANA TO8**



▶ **VORTEX ME-7 SDD**

Find out more about partnering with Hitachi for your detector supply:

**Hitachi High-Tech Science America, Inc.**

20770 Nordhoff St. Chatsworth, CA 91311

[www.hitachi-hightech.com/hhs-us/](http://www.hitachi-hightech.com/hhs-us/)

Email: [del.redfern@hitachi-hightech.com](mailto:del.redfern@hitachi-hightech.com); Call: +44 747 1086 241

## Company News

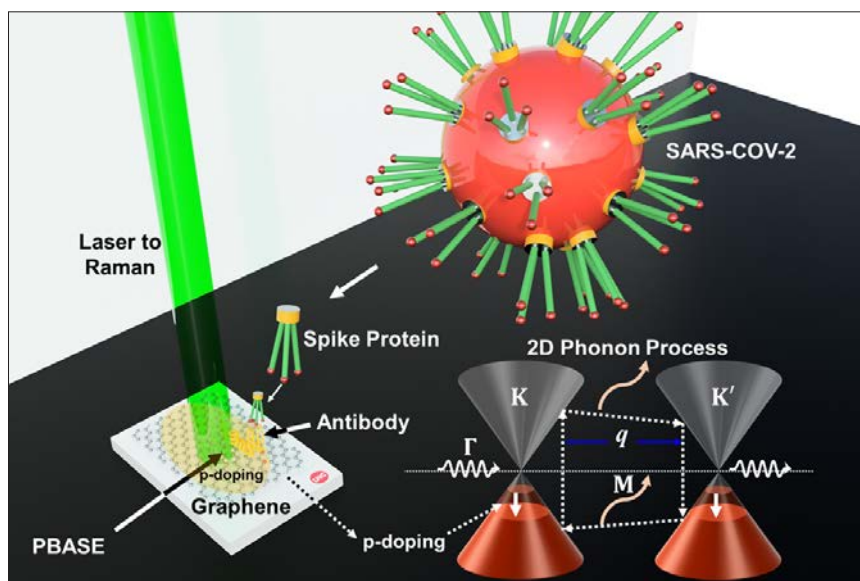
### Oxford Instruments acquires WITec

Oxford Instruments has acquired WITec for a cash-free, debt-free consideration of €42m, of which €5m is conditional on trading performance over a period of 12 months following completion. Completion is subject to regulatory approval of the transaction by the Federal Ministry for Economic Affairs and Energy (BMWi) in Germany. These conditions are expected to be satisfied during the second quarter of the Group's financial year.

The acquisition is in line with Oxford Instruments' strategy of supporting customers in attractive end markets, enhancing its portfolio of solutions for a range of applications including semiconductors, life science and advanced materials. It will enable WITec GmbH to build on its success to date, benefitting from the global reach of Oxford Instruments, alongside its complementary technology and application knowledge.

Dr Ian Barkshire, Chief Executive, Oxford Instruments said, "We are delighted to welcome WITec colleagues to Oxford Instruments. WITec's leading Raman microscopy solutions are a great complement to our existing products and techniques. Raman microscopy is an important and widely used technique across academic and commercial customers for fundamental research, applied R&D and quality assurance/quality control. The technique is used in conjunction and alongside our existing characterisation solutions and broadens the capabilities that we can bring to existing customers whilst expanding opportunities into new market areas. Providing a broader range of solutions helps us support our customers in facilitating a greener economy, increased connectivity, improved health and achieve leaps in scientific understanding."

Dr Joachim Koenen and Dr Olaf Hollricher, WITec's founders and managing directors said: "We look back on a



An illustration of the graphene-based COVID-19 spike protein detection process. The white rectangle represents the substrate with graphene functionalised with SARS-CoV-2 antibody (shown in yellow). When this graphene detector interacts with the virus' spike protein in a COVID-positive sample, its atomic vibration frequency changes. Illustration: Vikas Berry

other coronaviruses. Results were evident in under five minutes. Their research was published in *ACS Nano* ([doi.org/gknzwm](https://doi.org/10.1021/acsnano.1c01234)).

"We have been developing graphene sensors for many years. In the past, we have built detectors for cancer cells and ALS. It is hard to imagine a more pressing application than to help stem the spread of the current pandemic", said Vikas Berry, professor and head of chemical engineering at the UIC College of Engineering. "There is a clear need in society for better ways to quickly and accurately detect COVID and its variants, and this research has the potential to make a real difference. The modified sensor is highly sensitive and selective for COVID, and it is fast and inexpensive."

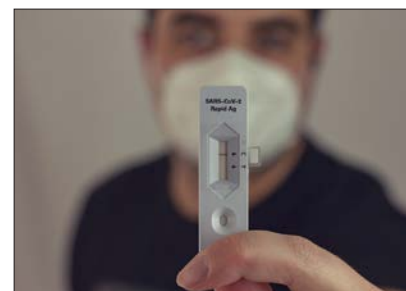
"This project has been an amazingly novel response to the need and demand for detection of viruses, quickly and accurately", said study co-author Garrett Lindemann, a researcher with Carbon Advanced Materials and Products, or CAMP. "The development of this technology as a clinical testing device has many advantages over the currently deployed and used tests."

"Graphene is just one atom thick, so a molecule on its surface is relatively enormous and can produce a specific change

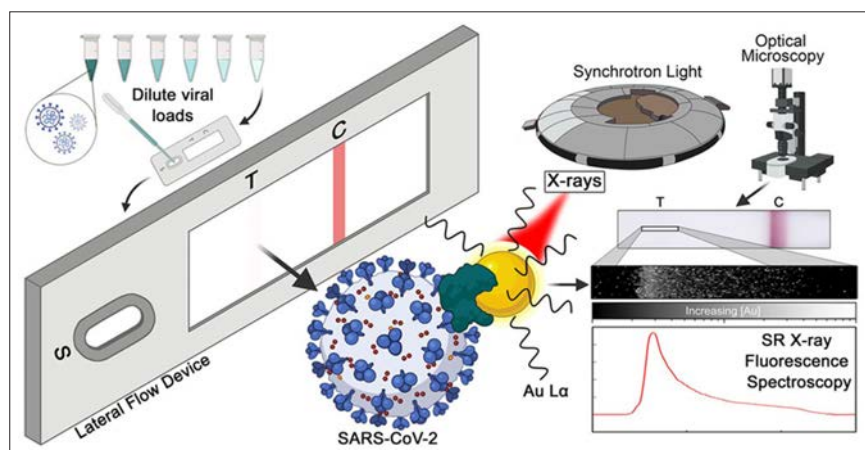
in its electronic energy", Berry said. "In this experiment, we modified graphene with an antibody and, in essence, calibrated it to react only with the SARS-CoV-2 spike protein. Using this method, graphene could similarly be used to detect COVID-19 variants."

### XRF imaging helps improve accuracy of lateral flow tests

Using X-ray fluorescence imaging at Diamond, the UK's national synchrotron, researchers from King's College London set out to identify what could be causing the false-negative results in lateral flow tests, and what potential modifications could enable increased accuracy. They identified that the underlying technology of the lateral flow devices is highly accurate and able to theoretically detect trace amounts of the COVID-19 virus, but







the limitations are in the read-out of the device.

The study suggests several potentially simple modifications to lateral flow devices that could lead to improved performance. Professor Owen Addison, Professor of Oral Rehabilitation from King's College London, said: "Methods to detect infectious individuals who do not show or are yet to show symptoms remain essential for the management of the current pandemic. Lateral flow devices are the simplest and most accessible tests available, and our findings show great scope for improving the deficiencies that these tests have been recently criticised for."

The research was a collaboration between King's College London, Guy's and St Thomas' Hospital Trust and Diamond. Using Diamond's Microfocus Spectroscopy Beamline, I18, researchers used X-ray light to image how the virus interacts with the tests. Diamond also supported the project by a rapid award of experimental time.

Konstantin Ignatyev, Principal Beamline Scientist on I18, said: "This is a very timely research that sheds a light on the inner mechanisms of the lateral flow devices for COVID-19 testing and highlights the deficiencies that need addressing in order to improve their accuracy. The measurements with spatial resolution and sensitivity that this study required are only possible at a synchrotron such as Diamond. An equally important factor to the success of this study was the close collaboration between scientists from academia

and the beamline staff, including beamline scientists and technicians as well as the continuing user support from various groups at Diamond."

Lateral flow devices were introduced late in 2020 on a global scale to help detect COVID-19 infection in asymptomatic or pre-symptomatic individuals, with test results produced rapidly in half an hour or less. However, their potential has been somewhat hindered by inadequate sensitivity, with a high number of false-negative results.

Just over a year ago, little was known about the COVID-19 virus, how it worked to infect us, how it was passed on, and furthermore the possible solutions and therapies. For over a year, Diamond has been committed to working with global experts and has contributed to unlocking some of the virus's secrets. The work has been published in *ACS Applied Materials & Interfaces* ([doi.org/gj8t85](https://doi.org/gj8t85)).

### ATR FT-IR spectroscopy part of the answer to medication errors

Medication errors are one of the most important problems that can significantly influence patient safety in health care. A very common source of medication errors is the mix-up of "Look-Alike and Sound-Alike" (LASA) medication. Scientists at the Groupement Hospitalier Centre Edouard Herriot, Lyon, France have developed a new tool called Medicine Identification New Database (MIND) to quickly and accurately identify unlabelled medication, even by untrained individuals. This is especially

24-year track record of making WITec a prosperous and innovative Raman imaging company. Now that we are joining the Oxford Instruments Group, we look forward to continuing this success together with a strong partner to grow even faster and to use the existing synergies to further expand our reach into the range of markets that will benefit from our wide product portfolio."

"WITec developed ground-breaking solutions in confocal Raman microscopy and correlative Raman microscopy. Oxford Instruments' key technologies in AFM and scientific spectroscopic cameras with the brands Asylum and Andor puts WITec in an even better position for future developments," Holtricher added.



WITec's representatives following the official announcement at WITec Headquarters in Ulm, Germany. From left to right: Joachim Koenen (Managing Director at WITec), Alexandra Lipes (HR Generalist at Oxford Instruments), Dirk Keune (Managing Director Germany and Director Sales EMEA at Oxford Instruments) and Olaf Holtricher (Managing Director at WITec).

WITec will, of course, fulfil its obligations toward existing customers and business partners in the usual manner and the management team will work to make the transition as smooth as possible.

### Ibsen celebrates 30 years

Transmission grating and OEM spectrometer manufacturer Ibsen Photonics celebrates 30 years in business on 1 July 2021. They manufacture their gratings in a Class 10 cleanroom for customers in the telecom, laser and analytical industries. This grating technology has enabled them to build compact, sensitive and ruggedised spectrometers for the UV to NIR wavelength range (175–2500 nm) for a broad range of applications in diverse industries.

## JEOL and SCiLS sign distribution agreement for MSI software

SCiLS Lab is software for mass spectrometry imaging, providing analysis and visualisation. The SCiLS Lab MVS (Multi-Vender Support) can be used for the analysis of mass spectrometry imaging datasets based on the open imzML data format. SCiLS Lab MVS offers all features of SCiLS Lab and it allows the statistical analysis and visualisation of mass spectrometry imaging data of virtually unlimited size in two and three spatial dimensions.

"We're very excited to work with JEOL to jointly disseminate the technology of mass spectrometry imaging and to support JEOL's further development of their MALDI imaging solution", Dennis Trede, co-founder of SCiLS and Director at Bruker Daltonics commented.

"We are excited to offer SCiLS lab MVS software through our own sales channels", said Yoshihisa Ueda, general manager of the mass spectrometry business unit of JEOL Ltd.

## IonSense appoints Jeff Zonderman as CEO

IonSense has appointed Jeffrey Zonderman as President and Chief Executive Officer. Mr Zonderman brings experience gained from commercialising disruptive technologies at early-stage ventures including RedShift Bioanalytics and Cohesive Technologies, as well as major instrument manufacturers including Thermo Fisher Scientific and Waters Corporation.



Jeff Zonderman

important after the medication has been removed from its initial packaging and blister and then been placed in unlabelled dispensers for individual patients.

MIND consist of three modules to identify (1) commercial information (manufacturer, CAS number and active pharmaceutical ingredient), (2) organoleptic properties (type, shape, colour, size, weight) and (3) collect an ATR-FT-IR spectrum of the medication to precisely identify the medication and counterfeit medication.

The backbone of the ATR-FT-IR module is a reference spectra database containing more than 500 entries with extensive sample information. The spectra in this database were measured in the hospital laboratories and then transferred to S.T. Japan-Europe, who converted it into the data formats for use with most instruments/software packages in the market. With the combination of these three modules, counterfeit medication and also medication with questions about its physico-chemical integrity and stability after long storage in varying conditions of temperature and humidity can be reliably discriminated, characterised and identified.

## Fast IR imaging-based AI identifies tumour type in lung cancer

Lung tumours are divided into various types, such as small cell lung cancer, adenocarcinoma and squamous cell carcinoma. Many rare tumour types and sub-types also exist. This diversity

hampers reliable rapid diagnostic methods in everyday clinical practice. In addition to histological typing, the tumour samples also need to be comprehensively examined for certain changes at a DNA level. "Detecting one of these mutations is important key information that influences both the prognosis and further therapeutic decisions", says co-author Professor Reinhard Büttner, head of the Institute of General Pathology and Pathological Anatomy at University Hospital Cologne.

Patients with lung cancer clearly benefit when the driver mutations have previously been characterised: for instance, tumours with activating mutations in the EGFR (epidermal growth factor) gene often respond well to tyrosine kinase inhibitors, whereas non-EGFR-mutated tumours or tumours with other mutations, such as KRAS, do not respond at all to this medication. The differential diagnosis of lung cancer previously took place with immunohistochemical staining of tissue samples and a subsequent extensive genetic analysis to determine the mutation.

The potential of infrared imaging as a diagnostic tool to classify tissue, called label-free digital pathology, has already been shown by the group led by Klaus Gerwert in previous studies. The procedure identifies cancerous tissue without prior staining or other markings and functions automatically with the aid of artificial intelligence (AI). In contrast to the methods used to determine tumour shape and mutations in tumour tissue



Frederik Großerüschkamp, Nina Goertzen and Klaus Gerwert (from left) are part of the research team. © RUB, Marquard



in everyday clinical practice, which can sometimes take several days, the new procedure only takes around half an hour. In that time it is not only possible to ascertain whether the tissue sample contains tumour cells, but also what type of tumour it is and whether it contains a certain mutation.

The Bochum researchers were able to verify the procedure on samples from over 200 lung cancer patients. When identifying mutations, they concentrated on by far the most common lung tumour, adenocarcinoma, which accounts for over 50% of tumours. Its most common genetic mutations can be determined with a sensitivity and specificity of 95% compared to laborious genetic analysis. "For the first time, we were able to identify spectral markers that allow for a spatially resolved distinction between various molecular conditions in lung tumours", explains Nina Goertzen from PRODI. A single IR spectroscopic measurement offers information about the sample which would otherwise require several time-consuming procedures. The research was reported in *The American Journal of Pathology* ([doi.org/gnjik](https://doi.org/gnjik)).

### Raman spectroscopy monitors stem cell reprogramming

The 2012 Nobel prize-winning discovery that ordinary cells could be coaxed to revert to their earliest pluripotent stage ushered in the era of ethical stem cell research. Suddenly, scientists can have

an inexhaustible supply of pluripotent stem cells—the most versatile of stem cells—that can become any type of cell, much like how embryonic stem cells function but without the ethical troubles that hampered research in the past.

These reprogrammed cells called induced pluripotent stem cells, or iPS cells, hold great promise for regenerative medicine, where they can be used to develop tissue or organ replacement-based treatments for life-threatening diseases.

Artificially inducing ordinary cells to reset back to pluripotency, however, is a lengthy and delicate process. Obtaining iPS cells depends on chance. And knowing all they can about the complex chemical changes happening inside during reprogramming can help scientists improve the odds of attaining viable iPS cells for clinical applications. Current methods that track reprogramming status, however, use destructive and costly techniques.

A study led by Dr Tomonobu Watanabe, professor at Hiroshima University's Research Institute for Radiation Biology and Medicine, has shown how Raman spectroscopy could be a low-cost, simpler and non-intrusive technique in monitoring what goes on inside the cell as it transitions.

"The quality evaluation and sorting of existing cells have been carried out by investigating the presence or absence of expression of surface marker genes. However, since this method requires a fluorescent antibody, it is expensive and

"We are thrilled Jeff has joined IonSense as his experience positions him well to lead the company and achieve our strategic vision", said Bob Linke, Executive Chairman of the Board. "I'd also like to thank Dr Brian Musselman whose contributions in founding and leading the company to establish the DART technology in labs around the world have been tremendous. We are pleased to announce Dr Musselman will take on the newly created role as IonSense's Chief Technology Officer to guide proprietary DART technology through its next stage of growth outside the central lab. Brian's vision will continue to play a key role developing IonSense's technologies to achieve our strategic goals."

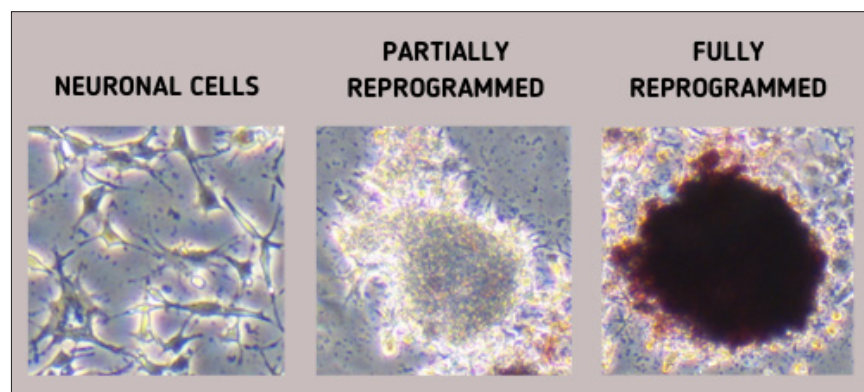
### Senorics GmbH raises more than 8 million euros in funding for expansion

Senorics GmbH, a spin-off from the University of Technology Dresden (TU Dresden) and a startup in the ZEISS Ventures Portfolio has successfully closed a new financing round. Senorics specialises in designing and manufacturing optical spectroscopic sensor solutions for mass market applications. Senorics will use the new funds to accelerate the roll-out of its innovative near infrared spectroscopy sensors based on organic semiconductor technology.

In 2019 ZEISS and Senorics entered a technological cooperation to further develop the technology and to identify new application fields which laid the foundation for the current investment by ZEISS Ventures.

The new investment round is led by the FIDURA Private Equity Fonds and all existing investors such as TGFS (Technologiegründerfonds Sachsen) and public funding from the Development Bank of Saxony (Sächsische Aufbaubank).

"With these powerful new partner and investments, we will be able to commercialise our solution in the initial target application fields and further develop our patented optical sensor technology", said Dr Ronny Timmreck Founder and CEO of Senorics.



Raman spectroscopy has been used to train an AI so it can monitor if the reprogramming of ordinary cells into stem cells is on track and check for markers that will verify a successful return to their earliest pluripotent stage. Courtesy of Professor Tomonobu Watanabe

causes a problem of bringing the antibody into the cells", Watanabe said.

"Solution of these problems can accelerate the spread of safe and low-cost regenerative medicine using artificial tissues. Through our method, we provide a technique for evaluating and sorting the quality of iPS cells inexpensively and safely, based on scattering spectroscopy", he added.

The team used Raman spectroscopy to obtain the "chemical fingerprints" of mouse embryonic stem cells, the neuronal cells they specialised into and the iPS cells formed from those neuronal cells. These data were then used to teach an AI model so it can track if the reprogramming is progressing without a hitch and verify iPS cell quality by checking for a "fingerprint" match with the embryonic stem cell.

To measure the progress, they assigned the "chemical fingerprint" of neuronal cells as the transformation starting point and the embryonic stem cell's patterns as the desired end goal. Along the axis, they used "fingerprint" samples collected on days 5, 10 and 20 of the neuronal cells' reprogramming as reference points on how the process is advancing. The research was published in *Analytical Chemistry* ([doi.org/gnjm](https://doi.org/gnjm)).

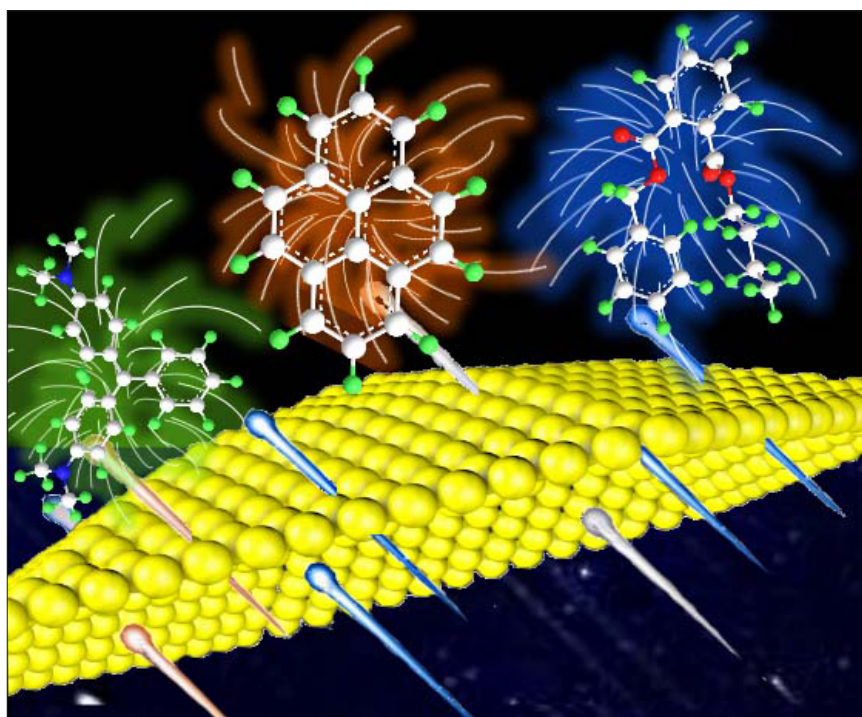
"The Raman scattering spectrum contains comprehensive information on molecular vibrations, and the amount of information may be sufficient to define cells. If so, unlike gene profiling, it allows for a more expressive definition of cell function", Watanabe said.

"We aim to study stem cells from a different perspective than traditional life sciences."

model. In this research, published in the *Journal of the American Chemical Society* ([doi.org/gkrg2i](https://doi.org/gkrg2i)), using the principle of capillary suction, they constructed a nanocapillary pumping model, for the first time, with abundant hot spots, leading to the first systematic study of small gaps to actively capture molecules.

"What makes this method stand out is the highly universal characteristic of it", said Yang. It could be used for highly sensitive detection of almost all types of molecules, including plasticisers, organic contaminants, anti-tumour drugs, poisons, toxins, pesticide residues, dyes, antibiotics, explosives and amino acids. This general method has provided a new way for stimulating active transport of target molecules to optimal hot spots to achieve ultrasensitive detection and real-time monitoring of cell behaviour or chemical kinetics.

## New SERS method actively captures target molecules in small gaps



Schematic diagram of the principle of the general surface enhanced Raman spectroscopy method for actively capturing target molecules in small gaps with the solvent. Image: Ge Meihong

Professor Yang Liangbao, from the Institute of Health and Medical Technology, Hefei Institutes of Physical Science (HFIPS), has developed a

general surface-enhanced Raman spectroscopy (SERS) method for actively capturing target molecules in small gaps based on a nano-capillary pumping

## Synchrotron X-ray spectromicroscopy shows metallic particles in Alzheimer's brains

An international team of researchers has discovered elemental metallic copper and iron in the human brain for the first time. The team, comprised of scientists from Keele University and the University of Warwick in collaboration with the University of Texas at San Antonio (UTSA), used Diamond Light Source and the Advanced Light Source located in California to identify elemental metallic copper and magnetic elemental iron within the amyloid plaques, chemical forms of copper and iron previously undocumented in human biology.

The study looked at amyloid plaques isolated from the brain tissue of deceased Alzheimer's patients. Amyloid plaques, a hallmark feature of Alzheimer's disease (AD), act as a site of disrupted metal chemistry in the Alzheimer's brain, and are believed by many to be integral to disease progression.

Neil Telling, Professor of Biomedical Nanophysics at Keele University, said: "The discovery of these elemental metallic particles in the brain tissue we studied, was very much unexpected, and made possible only by using specialist X-ray techniques at Diamond that





The experimental team at I08 Diamond left to right: James Everett, Jake Brooks and Frederik Lermyte. Credit: Keele University

can detect chemical variations at length scales much smaller than a human cell. There is no reason to think that everyday exposure to these metals could cause

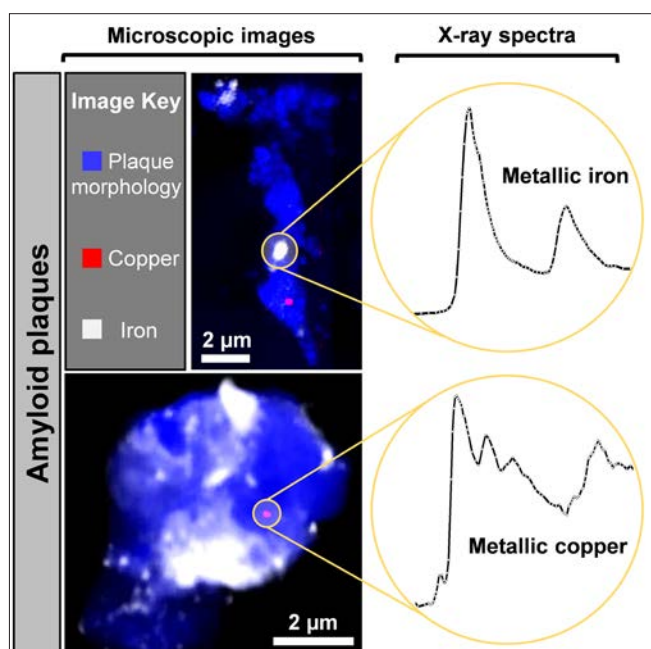
their presence in the brain, and in fact it is not yet clear whether such particles are indeed linked to disease. They may be present in normal brains. However, their

very presence underlines the importance of the future work now needed to learn about the way in which metals are processed in the brain."

The research, published in *Science Advances* ([doi.org/gkzv8n](https://doi.org/gkzv8n)) identified nanoscale deposits of the metals in post-mortem brain tissue donated by AD patients, using synchrotron X-ray spectromicroscopy. The surfaces of metallic copper and iron are usually highly unstable and readily react with oxygen from their surroundings to form oxides and other compounds. Chemical compounds of copper and iron and about eight other metals occur naturally in the body and are vital for brain well-being. However, when faults develop in the body's biochemistry, these metals can also cause damage to the brain. Metal imbalances may be linked to the development of numerous dementia-causing neurodegenerative diseases including AD and Parkinson's, which afflict millions of individuals worldwide.

The identification of previously undocumented metallic copper and iron deposits within human brain tissue, indicates that metallic elements, previously observed only in microorganisms, viruses and plants, can also occur in humans. These metallic forms of iron and copper have distinctly different chemical and magnetic properties from their oxide forms, in which they are predominately stored in tissues. The role of the expected highly reactive surfaces of nanodeposits of copper and iron in natural or pathological processes remains to be seen. Their discovery, therefore, potentially offers new insights into the roles played by metals in normal neurochemistry and neurobiology, as well as in neurodegenerative diseases.

Dr Burkhard Kaulich, Principal Beamline Scientist on the I08 Beamline at Diamond Light Source, comments: "This impressive scientific project on fundamental synchrotron and lab-based medical research will hopefully contribute to improve human life conditions by shedding light on the chemical environment within the brains of those with neurodegenerative disease. Additionally, the collaboration with the team at Keele and Warwick opened important new



X-ray microscope images and X-ray absorption spectra obtained from two AD plaque cores, measured at Diamond Light Source beamline I08. X-images showed the plaques to contain both iron and copper deposits. X-ray absorption spectra from the highlighted regions were consistent with metallic elemental iron (top spectrum) and copper (bottom spectrum). Credit: *Science Advances*

paths for the instrumental performance of the Diamond I08 Scanning X-ray Microscopy Beamline."

These new findings offer a potential step-change in our understanding of how metals contribute to the pattern of brain cell death that underpins neuro-degenerative disease. In turn, this could facilitate the development of new therapies designed to restore metal balance in diseased brains, potentially slowing or preventing the progression of these currently incurable diseases.

Professor Collingwood, co-author and project lead at the University of Warwick said: "This is a fascinating and unexpected discovery, enabled by the sensitivity and precision of the synchrotron techniques we have used to study these human-brain-derived samples. The findings raise detailed questions about how these forms of iron and copper can be produced in the human brain. We know that certain living systems can produce elemental forms of metals, so it will be important to discover if these arise from equivalent but previously undiscovered pathways in humans, or if the metallic forms arise as a direct consequence of disease."

Outstanding questions remain regarding the origins of the metallic brain metals, including whether they are uniquely associated with amyloid plaques or are more widely distributed throughout the brain. The team believe the presented findings will stimulate new and exciting research into the role of metal biochemistry in the human brain, whilst the state-of-the-art techniques used could be adapted to examine a variety of biological systems and problems.

### Award for development batteries through NMR spectroscopy

The Körber European Science Prize 2021, worth one million euros, is to be awarded to University of Cambridge chemist Professor Clare Grey, one of the UK's leading battery researchers. Grey pioneered the optimisation of batteries with the help of NMR spectroscopy.

Her NMR studies have helped to significantly increase the performance



Professor Clare Grey. Credit: Gabriella Bocchetti; ©Cambridge University

of lithium-ion batteries. She has been instrumental in the development of next-generation batteries and cost-effective, durable storage systems for renewable energy. She sees her fundamental research as an important contribution to achieving net-zero emissions by 2050.

"There have been significant advances in lithium-ion batteries since they were commercialised in the 1990s", said Grey. "Their energy density has tripled and prices have fallen by 90 %."

Grey's research has made key contributions to these developments. She is a pioneer in the study of solids with the help of NMR spectroscopy, which she has developed and applied to allow researchers to observe the electrochemical processes at work during charging and discharging of batteries.

Clare Grey, 56, studied chemistry at the University of Oxford. At the age of 22, she published her first scientific article in *Nature*. After completing her doctoral studies in 1991, she went to Radboud University in Nijmegen, the Netherlands, and has also worked as a visiting scientist at the US chemical company Dupont. In 1994, she joined the State University of New York at Stony Brook as an assistant professor, and she became a full professor in 2001. In 2009, she became Geoffrey Moorhouse Gibson Professor at the University of Cambridge's Yusuf Hamied Department of Chemistry. She is a Fellow of Pembroke College, and has been a Fellow of the Royal Society since 2011.

At the time Grey was still a student, most chemist and physicists used X-rays to determine the internal structure of solids. Grey was one of the first in her field to use solid state NMR instead: during her time in the USA, she met researchers from the Duracell company who inspired her to use the technology to study materials in batteries.

"Previously, the usual investigations with X-rays only provided an average picture", Grey said. "With the help of NMR, I was able to detect the local structural details in these often-disordered materials."

Initially, she examined individual materials by opening the batteries at a certain stage of their charging and discharging cycle. The aim was to find out which chemical processes cause the batteries to age and how their lifespan and capacity could be increased. Later, she improved the NMR technology so that she could use it to examine batteries during operation without destroying them, which helped speed up the studies enormously.

Now, in addition to her work improving lithium-ion batteries, Grey is developing a range of different next-generation batteries, including lithium-air batteries (which use oxidation of lithium and reduction of oxygen to induce a current), sodium, magnesium and redox flow batteries.

Her NMR studies allow her to follow the processes at work inside these batteries in real time and help determine the processes that cause batteries to degrade. She is working on further



optimising the NMR method to design even more powerful, faster-charging and more environmentally friendly batteries.

In 2019, Grey co-founded a company (Nyobolt) for ultra-fast charging batteries. To achieve climate goals and transition away from fossil fuels, Grey believes it is vital that “basic research into new battery technologies is already in full swing today—tomorrow will be too late.”

The Körber European Science Prize 2021 will be presented to Professor Clare Grey on 10 September in the Great Festival Hall of Hamburg City Hall. Since 1985, the Körber Foundation has honoured a breakthrough in the physical or life sciences in Europe with the Körber Prize. It is awarded for excellent and innovative research approaches with high application potential. To date, six Körber Prize winners have been awarded the Nobel Prize.

### FT-IR spectroscopy shows molecular orientation in very thin films

Using laboratory-grade equipment with 3D printable optical setups, the research group of Professor Masahide Takahashi of the OPU Graduate School of Engineering at Osaka Prefecture University has established an easy, versatile, yet highly sensitive approach to identify the orientation

of molecules and chemical bonds in crystalline organic–inorganic hybrid thin films deposited on a substrate as small as 10 nm, “even film with three molecular layers”. They used an FT-IR spectrometer and polarised IR light with their own designed 3D-printed attenuated total reflectance (ATR) unit. FT-IR spectrometers have not been able to reveal the three-dimensional orientation of these molecules relative to the substrates. This is important to the manufacturing of thin-film devices that can be nanometres in size, as an unpredicted shift in molecular orientation at that level can cause the entire structure of the device to break down.

“We realised that by re-orienting the sample, we could introduce polarised light directly into the substrate of the thin film, generating an evanescent wave that heats up the sample, exciting certain molecules and betraying their orientation”, states Bettina Baumgartner, a visiting researcher on the team, “we just needed a new kind of sample interface”, adds Associate Professor Kenji Okada. This is where the team designed a brand-new ATR optical setup that bounces polarised infrared light through the entirety of the sample substrate allowing the team to observe the vibration of all molecules aligned with the electric field component of the infrared

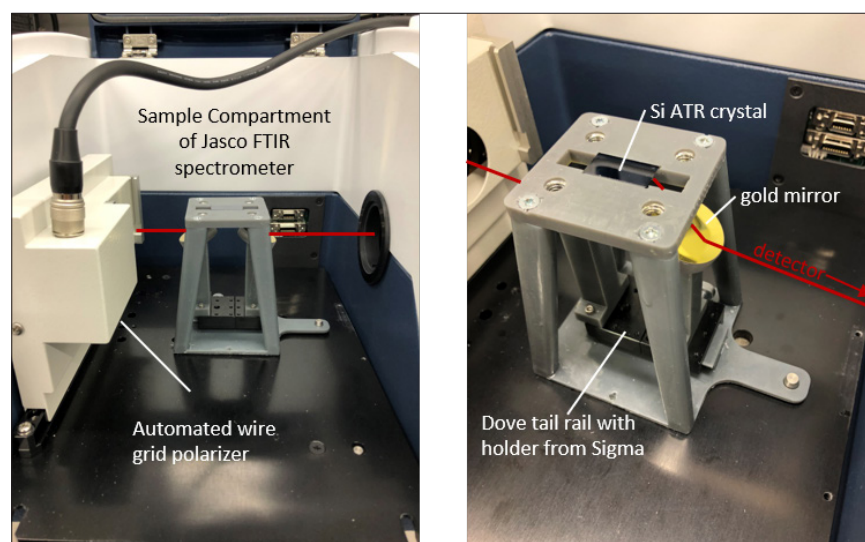
light, revealing their orientation. Any lab with a 3-D printer can make these ATR optical setups.

This method, which the team used to obtain the structural information of metal–organic framework thin film with a degree of crystal orientation comparable to X-ray structural analysis and was published in *Chemical Science* ([doi.org/gnpx](https://doi.org/gnpx)), is expected to be a useful method in many situations in materials science, such as where orientation control is linked to controlling physical properties, the functional improvement of porous materials used for CO<sub>2</sub> capture and the development of new heterogeneous catalysts.

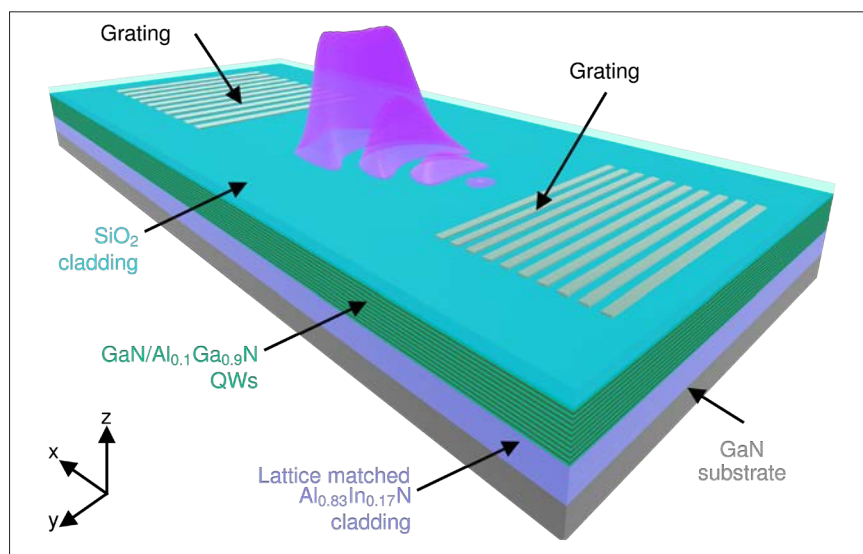
### Achieving UV non-linearity with a wide bandgap semiconductor waveguide

The field of ultrafast non-linear photonics has become the focus of numerous studies, as it enables a host of applications in advanced on-chip spectroscopy and information processing. The latter, in particular, requires a strongly intensity-dependent optical refractive index that can modulate optical pulses faster than even picosecond timescales and on sub-millimetre scales suitable for integrated photonics.

Despite the tremendous progress made in this field, there is currently no platform providing such features for the ultraviolet (UV) spectral range, which is where broadband spectra generated by non-linear modulation can be used for new on-chip ultrafast chemical and biochemical spectroscopy devices. Now, an international team of scientists have achieved giant non-linearity of UV hybrid light–matter states (“exciton-polaritons”) up to room temperature in a waveguide made of AlInGa<sub>N</sub>, a wide bandgap semiconductor material behind the solid-state lighting technology (e.g. white LEDs) and blue laser diodes. The study, published in *Nature Communications* ([doi.org/gkhf45](https://doi.org/gkhf45)), is a collaboration between the University of Sheffield, ITMO Saint Petersburg, Chalmers University of Technology, the University of Iceland and the LASPE at Ecole Polytechnique Federale de



3D printable optical setup with built-in sample chamber for an FT-IR spectrometer. Sample is put on the Si ATR crystals for measurement. © M. Takahashi and K. Okada, Osaka Prefecture University



Schematic of AlInGaN polariton waveguide structure. Courtesy of Dr Paul Walker, University of Sheffield.

Lausanne's Institute of Physics of the School of Basic Sciences.

The scientists used a compact 100 mm-long device, to measure an ultrafast non-linear spectral broadening of UV pulses with a non-linearity 1000× larger than that observed in common UV non-linear materials, which is comparable to non-UV polariton devices. Using AlInGaN is a significant step toward a new generation of integrated UV non-linear light sources for advanced spectroscopy and measurement. "The

AlInGaN system is a highly robust and mature semiconductor platform that shows strong excitonic optical transitions up to room temperature in the UV spectral range", says EPFL's Raphaël Butté, who worked on the study.

The authors state: "The non-linear exciton interactions in our system are comparable to those in other polariton material systems, such as GaAs and perovskites, which, however, do not simultaneously operate in the UV and up to room temperature."

key to the device's success. Moreover, an advanced algorithm plays an equally important role in this spectrometer, partly shifting the innate complexity in spectroscopy from hardware to software.

The spectrometer's dimensions of  $9 \times 16 \mu\text{m}$  are comparable to the wavelength of light that it measures. Even if it were possible to make the device smaller, it would not show much improvement due to the diffraction limit. The development is described in *Nature Photonics* ([doi.org/gnjz](https://doi.org/gnjz)).

"It is very exciting to realise such a high-performance spectrometer with the ultimate compactness", said Professor Doron Naveh of Bar-Ilan University. "We expect that the principle of leveraging advances in hardware and software simultaneously as shown in this work will lead to commercial applications in medicine, agriculture and food quality control."

"This spectrometer shows an advantage over conventional light-splitting spectrometers because the light doesn't need to be split into different parts spatially", said Shaofan Yuan.

Unlike conventional spectrometers, the system does not rely on optical components such as interferometers or tuneable infrared lasers. That opens the possibility for an extreme miniaturisation of spectrometers and could enable on-chip, affordable mid-infrared spectroscopy and spectral imaging.

## Ultracompact on-chip computational infrared spectrometer

With potential applications that range from detecting greenhouse gases to making self-driving vehicles safer, there has been a great deal of interest in recent years in developing compact, on-chip spectrometers. An on-chip spectrometer would greatly expand the applications and accessibility of the technology. Toward this goal, a team of researchers in the US, Israel and Japan has developed an ultracompact mid-infrared spectrometer. The work is the result of a collaboration between Yale University, Bar-Ilan University, Israel and the National Institute for Materials Science, Japan.

The device incorporates black phosphorus (BP) for a spectrometer that is

operational at a 2–9  $\mu\text{m}$  wavelength range, based on a single tuneable photodetector. The material, which is about 10 nm thick, allows users to tune the light-matter interaction to capture the different spectral components—a



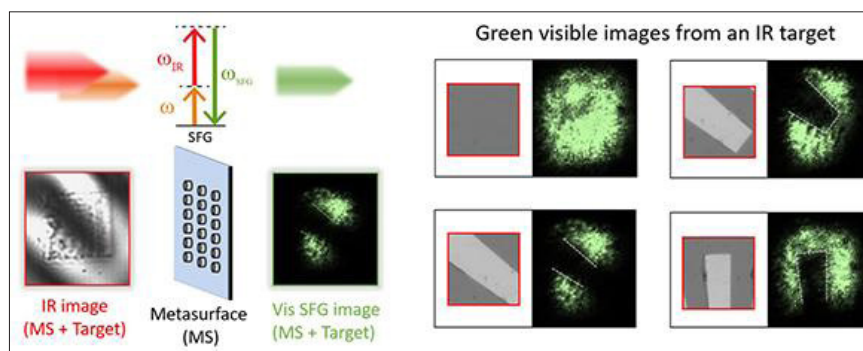
An optical micrograph of two typical on-chip spectrometers. Scale bar: 8  $\mu\text{m}$

## Infrared imaging by non-linear optics

The demand for detecting infrared (IR) light continues to grow, due to a wide variety of applications ranging from food quality control and remote sensing to night vision devices and lidar. Commercial IR cameras require the conversion of IR light to electrons and the projection of the resultant image on a display. This display blocks the transmission of visible light, thereby disrupting normal vision. Moreover, such IR detectors require low temperature and even cryogenic cooling due to the low energies of the IR photons, making IR detectors bulky and heavy.

An all-optical alternative to traditional cameras is the use of a non-linear optical process to convert IR light into visible. In this case, electrical signals are no longer





Through the sum-frequency generation (SFG) non-linear optical process, two incident photons, one of them in the IR spectrum, interact within the metasurface to generate emission at green visible frequencies. More importantly, an IR image of a target is mixed with a second beam, within the metasurface, generating a green visible image via SFG. Optical microscope images of different transverse positions of the target (left-hand side) and their corresponding up-converted images (right-hand side). Credit: Camacho-Morales *et al.*, <https://doi.org/10.1117/1.AP.3.3.036002>

involved in the IR detection process, and the image, converted to the visible, can be captured by eye or a phone-type camera. The optical process employed in this technique is non-linear sum-frequency generation (SFG). In the SFG process, two incident photons, one of them in the IR spectrum, interact within a non-linear material to generate emission at higher and visible frequencies. However, in the usual approaches this conversion relies on bulky and expensive non-linear crystals.

A very attractive platform to overcome these limitations is the use of ultrathin nanocrystal layers known as metasurfaces. Metasurfaces are planar arrays of densely packed nanoantennas, designed to manipulate various properties of the incident light including its frequency. Among various examples, dielectric and semiconductor metasurfaces have shown great promise to enhance non-linear optical processes at the nanoscale. Such metasurfaces can exhibit enhanced frequency conversion due to the excitation of optical resonances and good coupling to free space. Thus, the use of non-linear metasurfaces is a promising way to up-convert IR photons to visible and thereby image IR objects through coherent conversion using ultrathin and ultralight devices. Importantly, transparent metasurfaces could perform IR imaging in a transmission configuration and simultaneously transmit visible light to allow for normal vision.

With this idea in mind, researchers from The Australian National University, Nottingham Trent University and collaborators worldwide managed to demonstrate IR imaging via non-linear metasurfaces composed of small semiconductor nanocrystals. The researchers designed a multiresonant metasurface to enhance the field at all the frequencies participating in the SFG process. The designed metasurface was fabricated and transferred to a transparent glass, forming a layer of nanocrystals on the glass surface. They report their results in *Advanced Photonics* ([doi.org/gkznzz](https://doi.org/gkznzz)).

In the experiment, an IR image of a Siemens-star target illuminated the metasurfaces. The IR image of the target was mixed with a second beam and, through the SFG process, up-converted to a visible wavelength at 550 nm. The visible green images, captured with a conventional camera, correspond to different transverse positions of the target, including the case when the target was fully removed from the path of the IR beam and the SFG emission from the metasurface was observed. Despite different parts of the IR signal beam being up-converted by independent nanocrystals composing the metasurface, the images were well-reproduced into the visible.

The proposed metasurface-based IR imaging approach offers novel opportunities not possible in conventional up-conversion systems. For example,

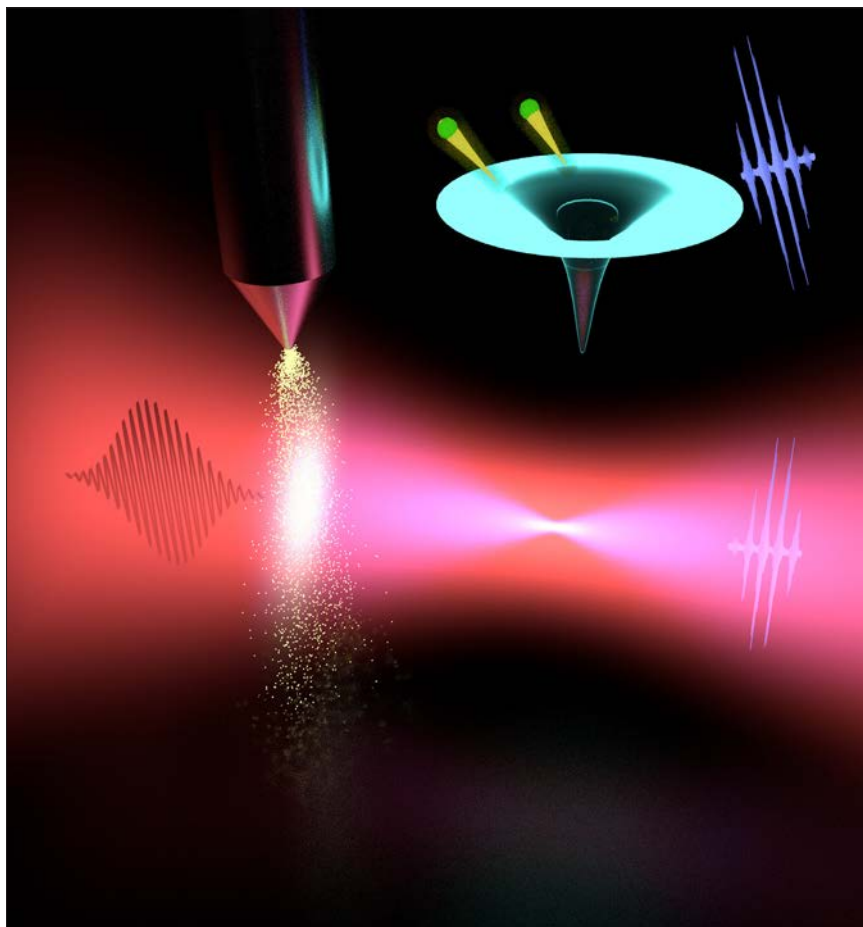
the use of counter-propagating excitation beams, as well as incidence at different angles and, most importantly, multicolour IR imaging by an appropriately designed metasurface. Therefore, the results obtained by the researchers can benefit the future development of compact instruments and sensors, offering an ultrathin and ultracompact platform and new functionalities such as multicolour IR imaging at room temperature.

## Benchtop XUV laser

An international team of researchers has demonstrated a new concept for the generation of intense extreme-ultraviolet (XUV) radiation by high-harmonic generation (HHG). Its advantage lies in the fact that its footprint is much smaller than currently existing intense XUV lasers. The new scheme is straightforward and could be implemented in many laboratories worldwide, which may boost the research field of ultrafast XUV science.

The invention of the laser has opened the era of non-linear optics, which today plays an important role in many scientific, industrial and medical applications. These applications all benefit from the availability of compact lasers in the visible range of the electromagnetic spectrum. The situation is different at XUV wavelengths, where very large facilities (so-called free-electron lasers) have been built to generate intense XUV pulses. One example of these is FLASH in Hamburg that extends over several hundred metres. Smaller intense XUV sources based on HHG have also been developed. However, these sources still have a footprint of tens of metres, and have so far only been demonstrated at a few universities and research institutes worldwide.

A team of researchers from the Max Born Institute (Berlin, Germany), ELI-ALPS (Szeged, Hungary) and INCDTIM (Cluj-Napoca, Romania) has recently developed a new scheme for the generation of intense XUV pulses. Their concept is based on HHG, which relies on focusing a near infrared (NIR) laser pulse into a gas target. As a result, very short light bursts with frequencies that are harmonics of the NIR driving laser are emitted, which thereby are



Compact intense XUV source. An NIR pulse (red) is focused, and high harmonics are generated in a gas jet that is placed before or behind the NIR focus. In this way, the generated XUV light has a size and a divergence that is similar to that of the NIR beam. Due to the shorter wavelength, the focus of the XUV beam is then much smaller than the focus of the NIR beam. This allows the generation of intense XUV pulses which are used for XUV multi-photon ionisation of atoms (see upper part). Image credit: Balázs Major

typically in the XUV region. To be able to obtain intense XUV pulses, it is important to generate as much XUV light as possible. This is typically achieved by generating a very large focus of the NIR driving laser, which requires a large laboratory.

Scientists from the Max Born Institute have demonstrated that it is possible to shrink an intense XUV laser by using a setup which extends over a length of only 2m. To be able to do so, they used the following trick: instead of generating XUV light at the focus of the NIR driving laser, they placed a very dense jet of atoms relatively far away from the NIR laser focus, as shown in the image. This has two important advantages. (1) Since the NIR beam at the position of the jet is large, many XUV photons

are generated. (2) The generated XUV beam is large and has a large divergence and can, therefore, be focused to a small spot size. The large number of XUV photons in combination with the small XUV spot size makes it possible to generate intense XUV laser pulses. These results, published in *Optica* ([doi.org/gk6m69](https://doi.org/gk6m69)) were confirmed by computer simulations that were carried out by a team of researchers from ELI-ALPS and INCDTIM.

To demonstrate that the generated XUV pulses are very intense, the scientists studied multi-photon ionisation of argon atoms. They were able to multiply ionise these atoms, leading to ion charge states of  $\text{Ar}^{2+}$  and  $\text{Ar}^{3+}$ . This requires the absorption of at least two

and four XUV photons, respectively. In spite of the small footprint of this intense XUV source, the obtained XUV intensity of  $2 \times 10^{14} \text{Wcm}^{-2}$  exceeds that of many already existing intense XUV sources.

The new concept can be implemented in many laboratories worldwide, and various areas of research may benefit. This includes attosecond-pump attosecond-probe spectroscopy, which has so far been extremely difficult to do. The new compact intense XUV laser could overcome the stability limitations that exist within this technique, and could be used to observe electron dynamics on extremely short timescales. Another area that is expected to benefit is the imaging of nanoscale objects such as biomolecules. This could improve the possibilities for making movies in the nano-cosmos on femtosecond or even attosecond timescales.

### Algorithm uses MS data to predict identity of molecules

An algorithm designed by researchers from Carnegie Mellon University's Computational Biology Department and St Petersburg State University in Russia could help scientists identify unknown molecules. The algorithm, called MolDiscovery, uses mass spectrometry data from molecules to predict the identity of unknown substances, without relying on a mass spectral database, telling scientists early in their research whether they have stumbled on something new or merely rediscovered something already known. This could save time and money in the search for new naturally occurring products that could be used in medicine and was reported in *Nature Communications* ([doi.org/gj953k](https://doi.org/gj953k)).

"Scientists waste a lot of time isolating molecules that are already known, essentially rediscovering penicillin", said Hosein Mohimani, an assistant professor and part of the research team. "Detecting whether a molecule is known or not early on can save time and millions of dollars, and will hopefully enable pharmaceutical companies and researchers to better search for novel natural products that could result in the development of new drugs."



# Are carbon micro-clusters in the Khufu pyramid blocks of organic origin?

## PIXE and PIGE reveal the construction of Giza's pyramids

**Guy Demortier**

SPS and LARN, University of Namur and 61, rue de Bruxelles, B-5000 Namur, Belgium

The presence of carbon clusters of size ranging between 5  $\mu\text{m}$  and 50  $\mu\text{m}$  in samples of the Khufu pyramid identified with a nuclear microprobe seems to indicate that they are of organic origin. Their location in the pyramid samples coincide with the position of other clusters containing sodium. This situation is completely absent in limestone samples collected from Egyptian quarries. The interpretation of the results could shed some light on the technique of construction of this huge monument.

### Introduction

The interdisciplinary approach of the technique of construction of the Big Pyramids of Egypt is a subject of debate giving rise to passionate arguments. Increasingly, scientific teams are now being accepted on Egyptian sites to perform non-destructive investigations of monuments. Recent discoveries by Morishima and co-workers of large cavities in the Khufu's pyramid using cosmic-ray muons<sup>1</sup> have encouraged the Egyptian authorities to cooperate with Egyptologists around the World. The former reported length of the "big void" (around 30 m long) is now believed to be larger and continuous.<sup>2</sup> The size of this void is so large that it is clear that all the surrounding structure must be highly rigid: this rigidity can only be achieved with perfectly overlapping blocks. Zahi

Hawass, former minister of the Egyptian Antiquities who was initially sceptical about the Morishima's conclusions of muon scans, is now ready to fully accept them and suggest that this void could be the location of the Khufu burial as reported in the *Daily Express*.<sup>3</sup> ruption are to look at the structure of the monument as made by Bertho<sup>4</sup> and by materials analysis as reported by Davidovits.<sup>5</sup> These last two authors conclude that the monument was constructed with blocks moulded on site using local limestone and binder (to produce a kind of concrete) and not with hewn blocks. We have recently considered this point of view on the basis of the distribution maps of six major elements (C, O, Na, S, Cl and Ca) with a nuclear microprobe.<sup>6,7</sup> This view is also supported by Barsoum *et al.* who have used various X-ray and electron microscopies to demonstrate that pyramid blocks contain calcium oxides and magnesium oxides with crystallographic structures which are not found in natural materials.<sup>8</sup> Recent measurements of the orientation of iron compounds in pyramid samples using paleo-magnetic methods support the hypothesis of a man-made technique giving rise to a rapid solidification

of mixed materials.<sup>9</sup> In addition to the already reported elemental analysis of Na, S and Cl associated with natural limestone we present here a possible interpretation of abnormally incrustated 5–50  $\mu\text{m}$  carbon clusters.

### Experimental arrangement

Non-vacuum proton-induced X-ray emission (PIXE) and proton-induced gamma-ray emission (PIGE) analyses of Egyptian pyramid blocks with low-energy protons produced by electrostatic accelerators at the Universities of Namur and Lecce have shown abnormal concentrations of F, Na, S and Cl.<sup>10–12</sup> More recently, micro-PIXE and micro-PIGE investigations with a (in vacuum) scanning nuclear microprobe at ATOMKI (Debrecen, Hungary) (Figure 1) have been performed to locally quantify the composition in lighter elements, down to carbon. The spatial resolution and uniformity of irradiation were regularly checked on a copper grid deposited on a carbon substrate during the analysis (Figure 2).

Samples were taken from the inside of chunks of Egyptian pyramid blocks and from stone in the limestone quarries of Tura and Maadi (north of Egypt).

DOI: [10.1255/sew.2021.a21](https://doi.org/10.1255/sew.2021.a21)

© 2021 The Author

Published under a Creative Commons BY-NC-ND licence



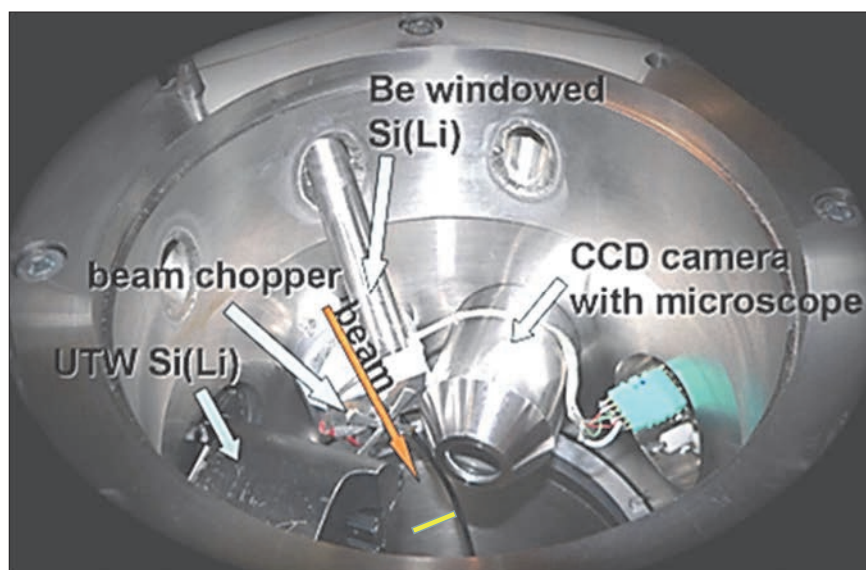


**Figure 1.** The PIXE microprobe chamber at Atomki (Debrecen, Hungary).

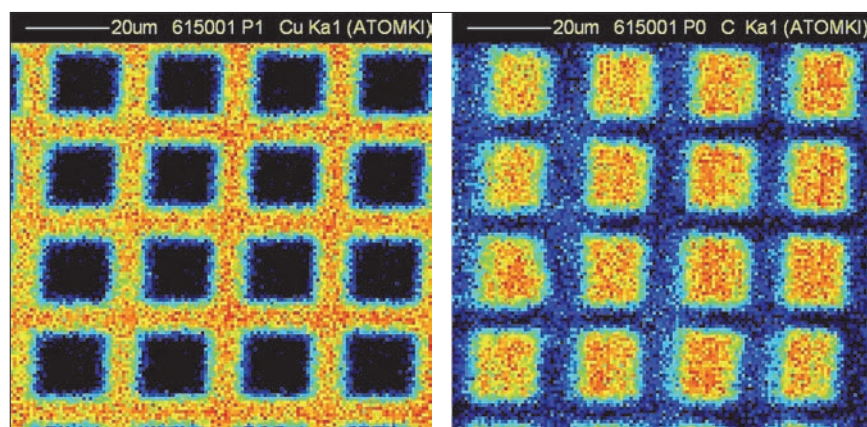


**Figure 2.** Micro-PIXE maps of a copper grid on a carbon substrate. Left: copper; data collected with the Be windowed detector). Right: carbon; data collected with the SUTW detector.



**Figure 3.** Pellet samples on their target holder.

They were crushed and pressed to obtain flat circular pellets without any additional binder (Figure 3). The sampling process ensured that any contamination with foreign material was excluded. The flat surfaces were irradiated with protons at normal incidence with the following experimental conditions: 2.5 MeV proton beam focussed to a spot size of  $\sim 3 \mu\text{m}$ , beam current  $\sim 100\text{--}200 \mu\text{A}$ , size of the scanned region  $1 \times 1 \text{ mm}^2$ . The measurement times were typically  $\sim 500\text{--}900 \text{ s}$  corresponding to  $\sim 0.1\text{--}0.2 \mu\text{C}$  accumulated charge.

Incident 2.5 MeV protons offer a maximum cross-section (100 %) for K-shell ionisation of Al; 61 %, 84 %, 93 %, 98 %, 99.5 % for K-shell ionisation of C, O, F, Na, Mg and F, respectively (region of decreasing slope of the K-shell ionisation cross-section at  $E_p = 2.5 \text{ MeV}$ ); and 87 %, 80 %, 73 %, 60 % and 53 %, respectively, for Si, P, Cl, K and Ca (region of increasing slope of the K-shell ionisation cross-section). This choice of proton energy is optimum to partially compensate for the unavoidable loss of low-energy X-ray signals from light elements (277 eV for  $\text{CK}\alpha$  to 1.25 keV for  $\text{MgK}\alpha$ ) in the material, since the K-shell ionisation cross-section increases as protons enter deeper into matter. The information depth for  $\text{CK}\alpha$ ,  $\text{OK}\alpha$  and  $\text{CaK}\alpha$  X-ray lines in pure  $\text{CaCO}_3$  is given in Figure 4.

The micro-PIXE detection setup consisted of a super ultra-thin windowed (SUTW) Si(Li) X-ray detector and a Be-windowed detector which were operated simultaneously, allowing the efficient detection of light elements down to carbon (in the 0.28–8 keV range) as well as heavier ones (from K upwards), respectively. The SUTW detector was protected from backscattered particles with a permanent magnetic unit. In the case of the Be-windowed detector (solid angle  $\sim 100 \text{ msr}$ ) the intense soft characteristic x-rays ( $< 3 \text{ keV}$ ) were attenuated with a Kapton<sup>®</sup> filter (375  $\mu\text{m}$  thick). Characteristic X-ray spectra of samples were evaluated and elemental compositions were determined with the PIXEKLIM-TPI (Atomki) software package.<sup>13</sup> With this, the K, L (and M)



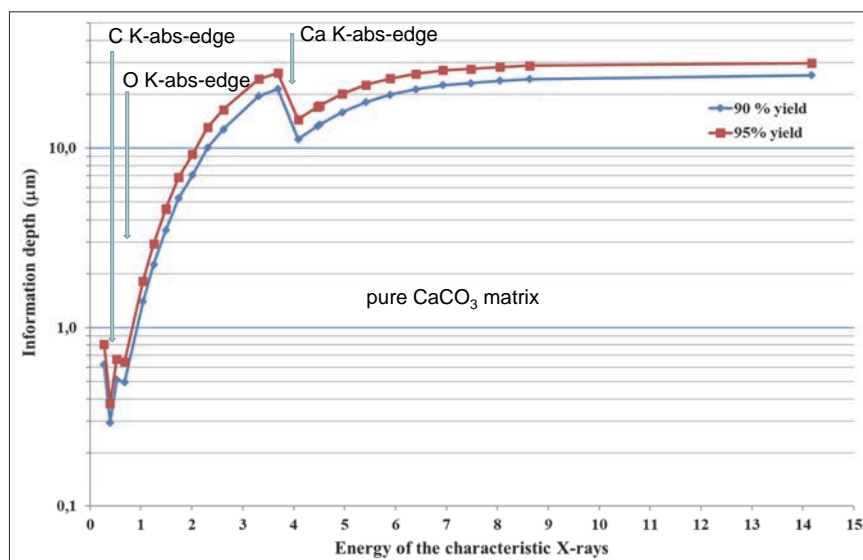


**Figure 4.** Information depth for C, O and Ca in  $\text{CaCO}_3$ .

## Micro-PIXE analysis of Egyptian pyramid blocks

The choice of the positions of the SUTW and Be-windowed detectors installed on either side of the proton beam direction (see Figure 1) was essential to check the uniformity of the irradiated surface. In order to avoid any misinterpretation of the collected X-ray maps, it was necessary to be sure that the structure of the  $\text{CaK}\alpha$  maps was the same in both detectors. Shadowing effects due to potential irregularities along the pellet surface would give rise to signal loss of X-rays emitted by the lightest elements. It is shown in Figure 8 that both  $\text{CaK}\alpha$  maps are similar for homogeneous (quarry) and for non-homogeneous (pyramid) samples. The  $\text{CaK}\alpha$  maps collected in both detectors are similar but not identical in their intensity (counts are less important in the Be-windowed detector than in the SUTW detector which covers a higher solid angle). It can be seen that a Si cluster takes the place of Ca in the top maps (Tura quarry). In the middle maps (an outside block from the Khufu pyramid), clusters of Na and S are present in those regions missing Ca. For the bottom maps (an outside block from the Khafra pyramid), large Na clusters are present. These Na clusters have a very irregular shape that induces some apparent fuzziness which is certainly not due to the proton beam being out of focus, but to large variations of thickness at their edges.

The spatial distribution of all the elements is uniform in all quarry samples (Figures 9 and 10). Small inclusions

characteristic lines of elements from  $\text{CK}\alpha$  upwards as well as escape and pile-up peaks present in the spectra are fitted. However, elemental concentrations are calculated from the  $\text{K}\alpha$  or  $\text{L}\alpha$  X-ray intensities of elements, considering the absorption-enhancement effects for characteristic X-rays within the samples as well as experimental parameters (proton beam energy, detector solid angle, X-ray filters etc.) as described in References 13 and 14. The micro-PIGE setup consisted of a NaI(Tl) detector (diam. = 110 mm) placed outside the vacuum chamber at  $90^\circ$  relative to the direction of the beam. It was chosen for the detection of the 6–7.1 MeV  $\gamma$ -ray group of the  $^{19}\text{F}(\text{p}, \alpha \gamma)^{16}\text{O}$  nuclear reaction, because  $\text{FK}\alpha$  (677 eV) detection

in the SUTW detector could indeed suffer from partial interference with the  $\text{L}\alpha$  line of Fe (705 eV): iron is indeed present in all the analysed samples.

The whole measurement procedure was calibrated and tested thoroughly with standard reference materials (RMs), e.g. NIST 610, "Corning D" archaeological glass and some homemade RMs, as well as pure chemical compounds such as quartz, NaCl etc. On average, ~5–10 rel.% accuracy can be achieved for the concentrations of major and minor elements and 10–20 rel.% for the trace element data.

Selected X-ray spectra of RMs, quarry and pyramid samples are given in Figures 5–7.

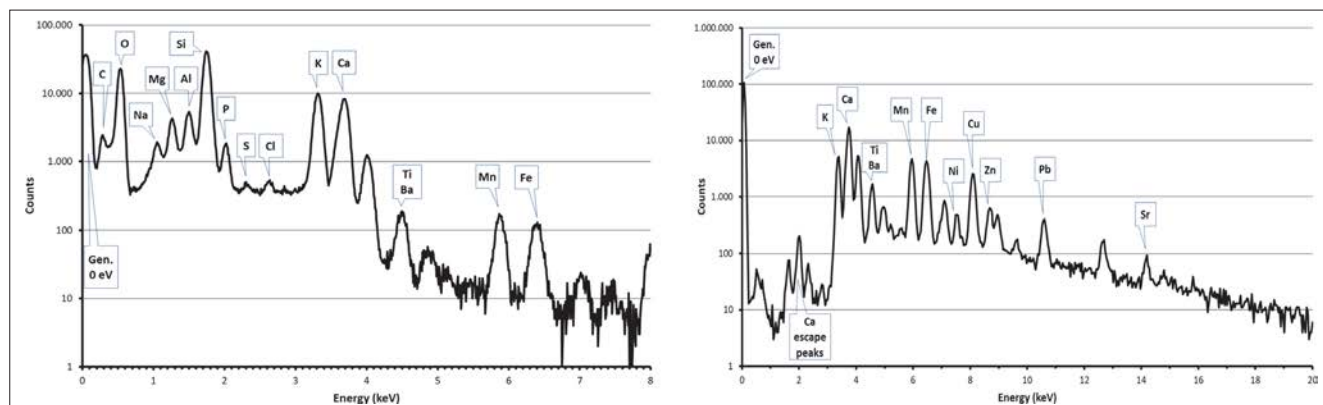


**Figure 5.** PIXE spectra collected by SUTW detector (left) and Be-windowed detector (right) on the homogeneous Corning reference material.

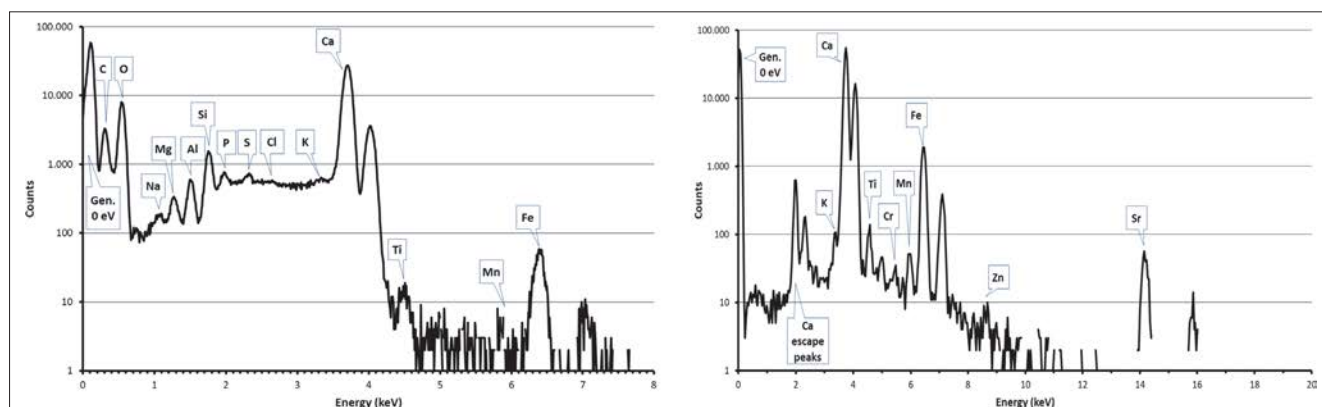


**Figure 6.** PIXE spectra collected by SUTW detector (left) and Be-windowed detector (right) on a limestone sample from Maadi quarry.

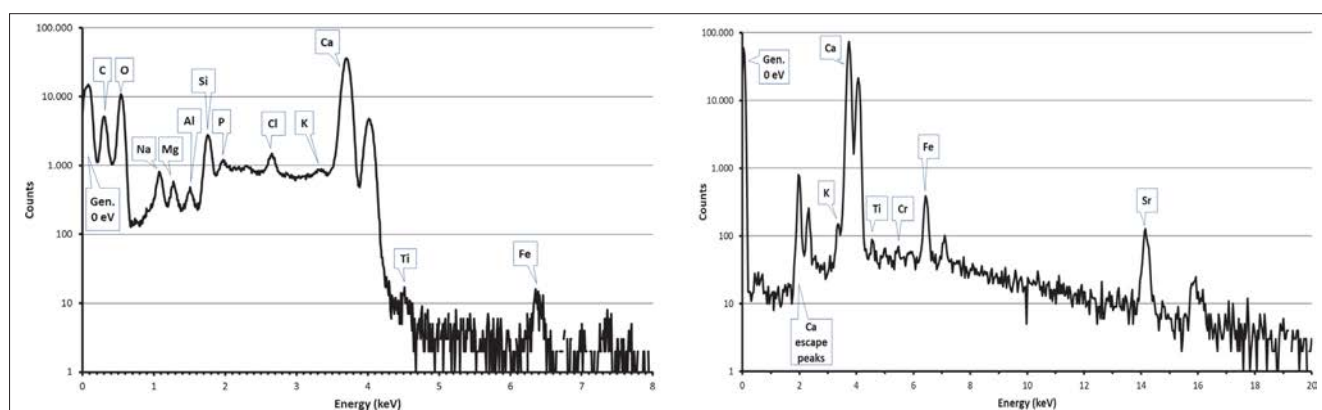


**Figure 7.** PIXE spectra collected by SUTW detector (left) and Be-windowed detector (right) on a sample of the external block of the Khufu pyramid.

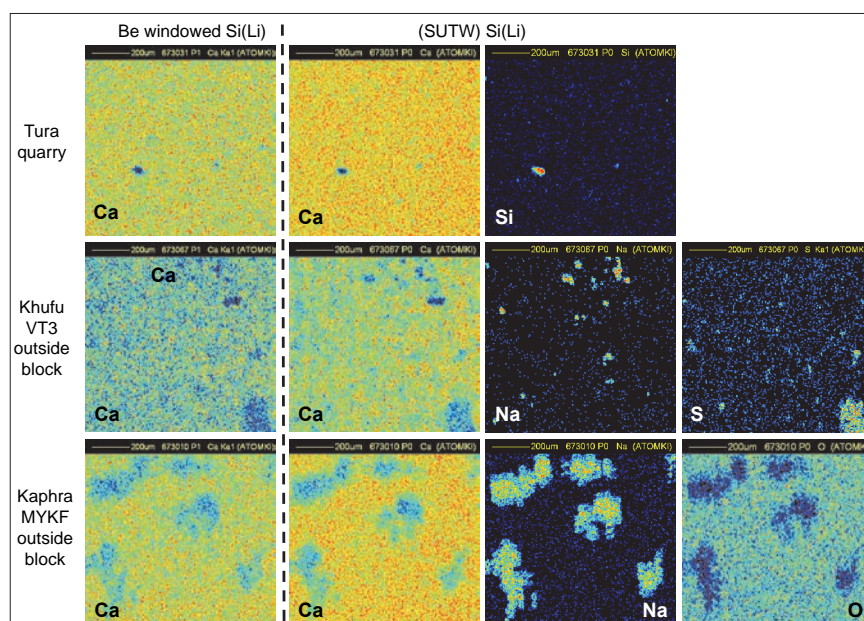


**Figure 8.** Flatness check of pellet samples by comparison of CaK $\alpha$  maps in both detectors.

(around 15–30  $\mu\text{m}$  in diameter) of Al, Si and Fe can also be observed in addition to nearly pure calcium carbonate (C, O and Ca maps). Traces of Na, Mg, P, S, Cl and K show no specific spatial distribution. The elemental concentrations in Ca, Mg, Al and Si were combined with the appropriate O concentration to obtain the most probable chemical compounds:  $\text{CaCO}_3$ ,  $\text{MgO}$ ,  $\text{Al}_2\text{O}_3$  and  $\text{SiO}_2$ .

On the contrary, the distribution is very non-homogeneous in most of the pyramid samples, as shown in Figures 11–14. Beside abundant calcium carbonate, there are inclusions (about 20  $\mu\text{m}$  wide or larger) of Na, Cl and/or S which are correlated with a lack of Ca and O. Sodium and chlorine (about 4–6 % and sometimes more) are systematically correlated and could at first sight be interpreted as inclusions



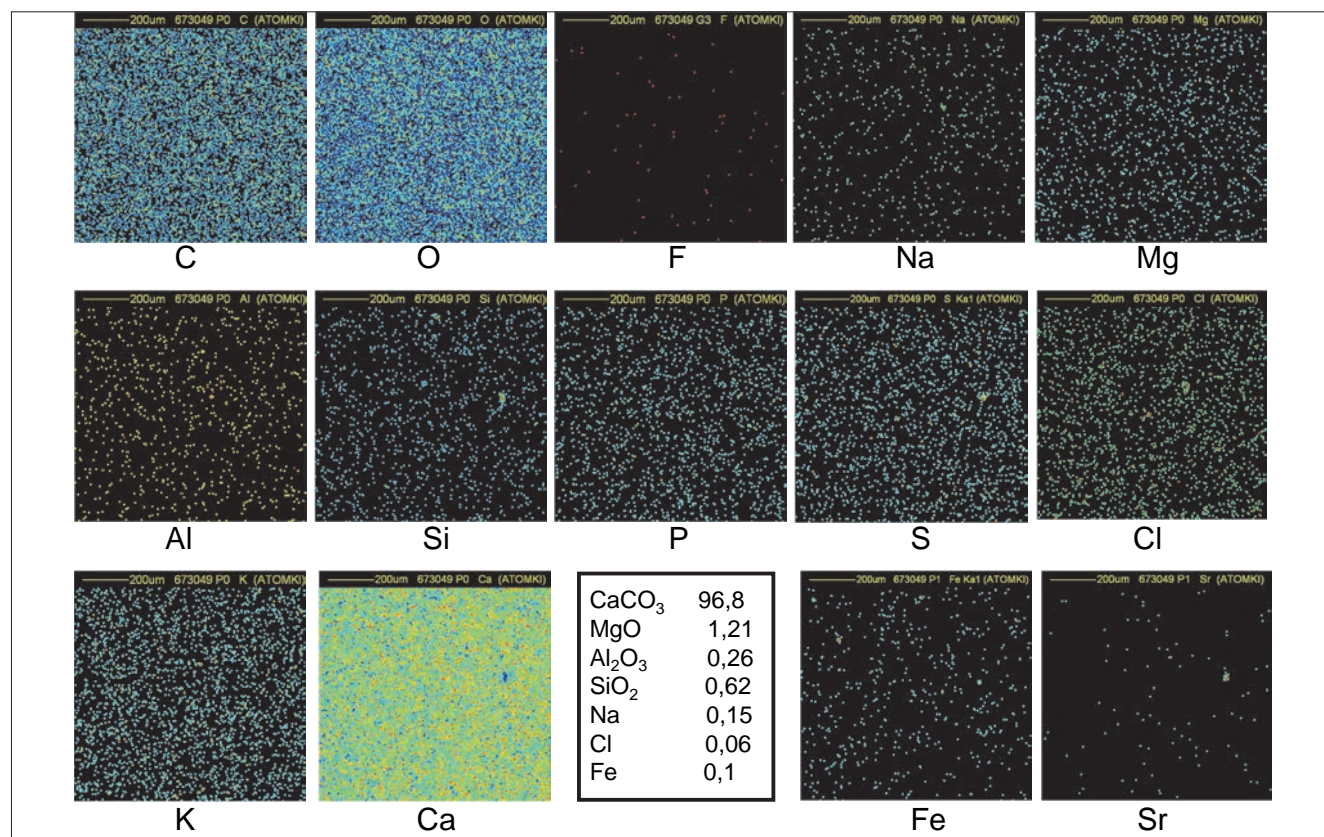


**Figure 9.** Distribution maps of 14 elements in Tura quarry sample (1 mm × 1 mm).

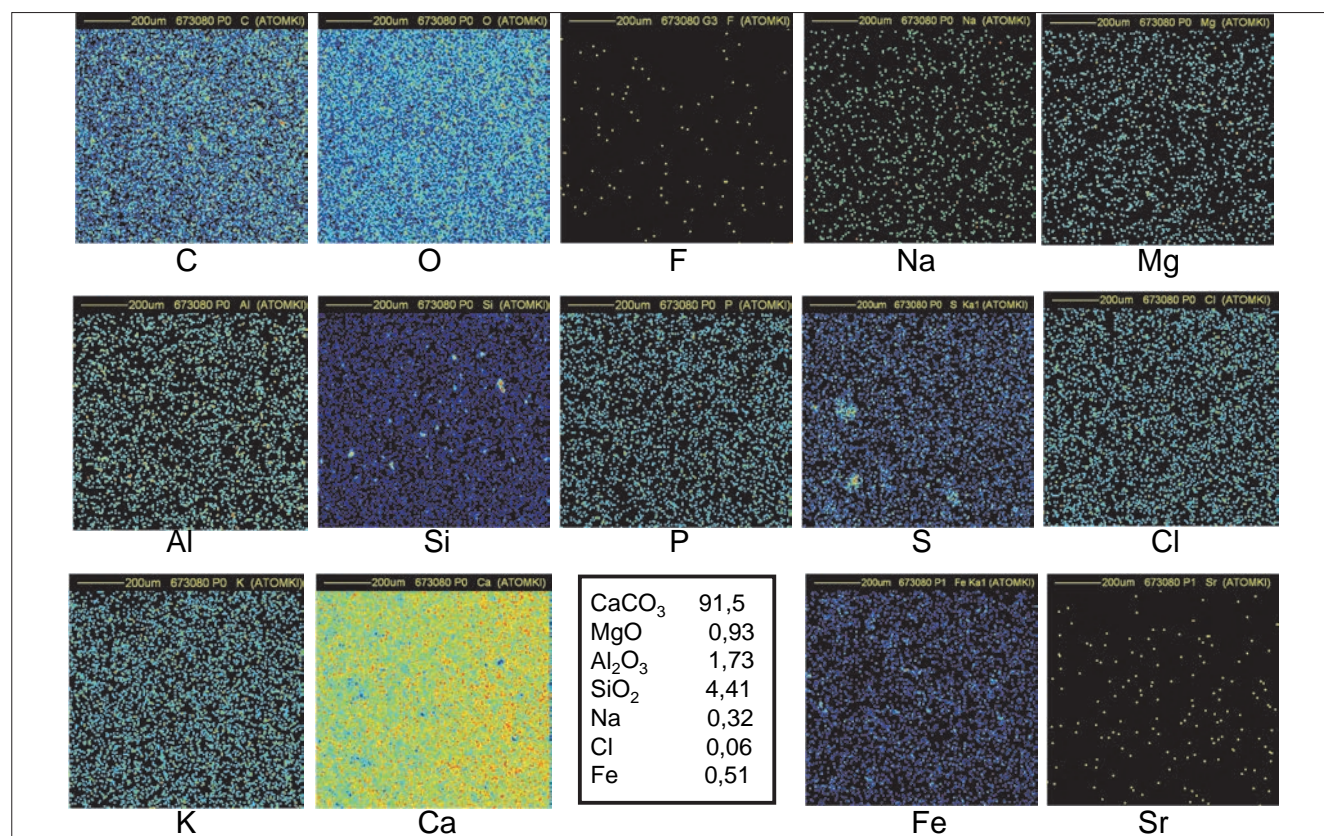


**Figure 10.** Distribution maps of 14 elements in Maadi quarry sample (1 mm × 1 mm).



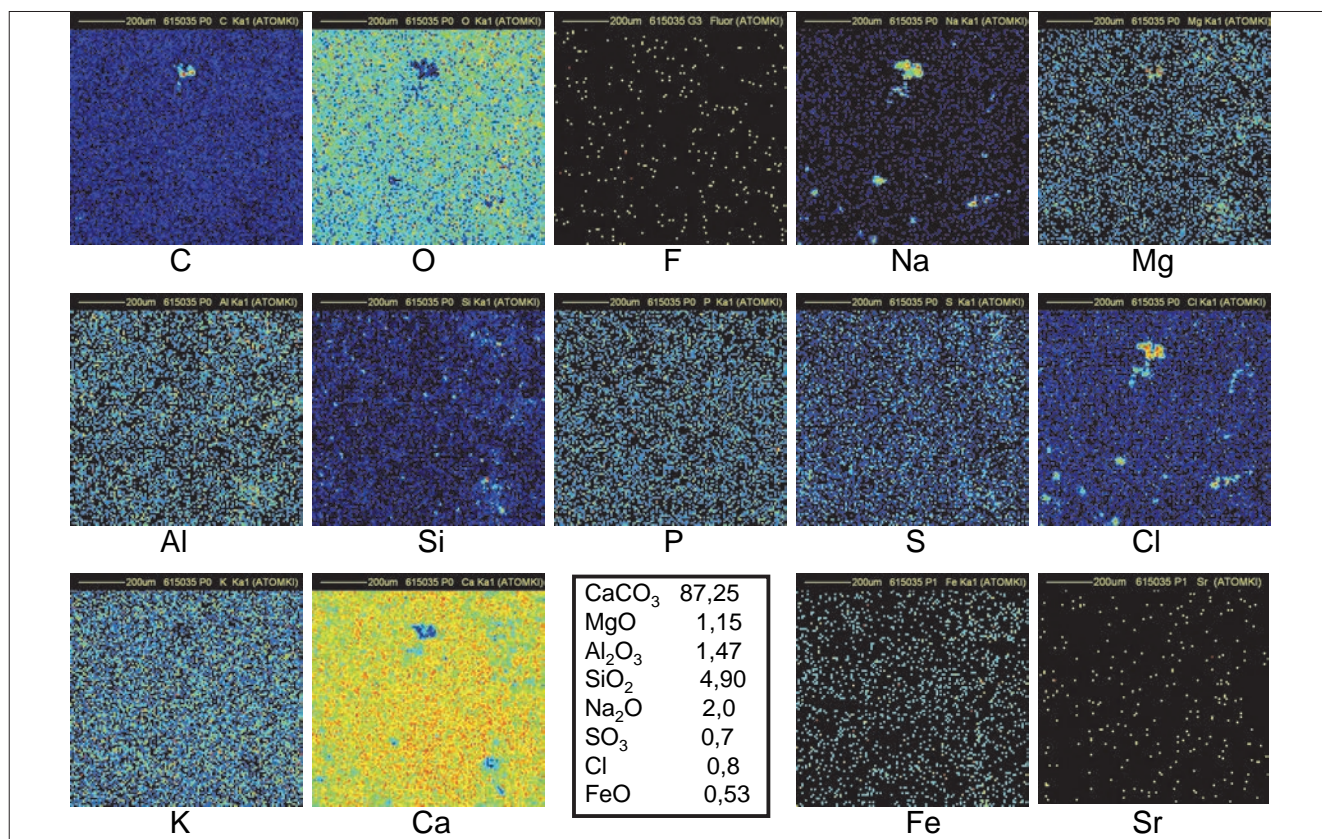


**Figure 11.** Distribution maps of 14 elements in FH123 Khufu Great Gallery sample (1 mm × 1 mm).

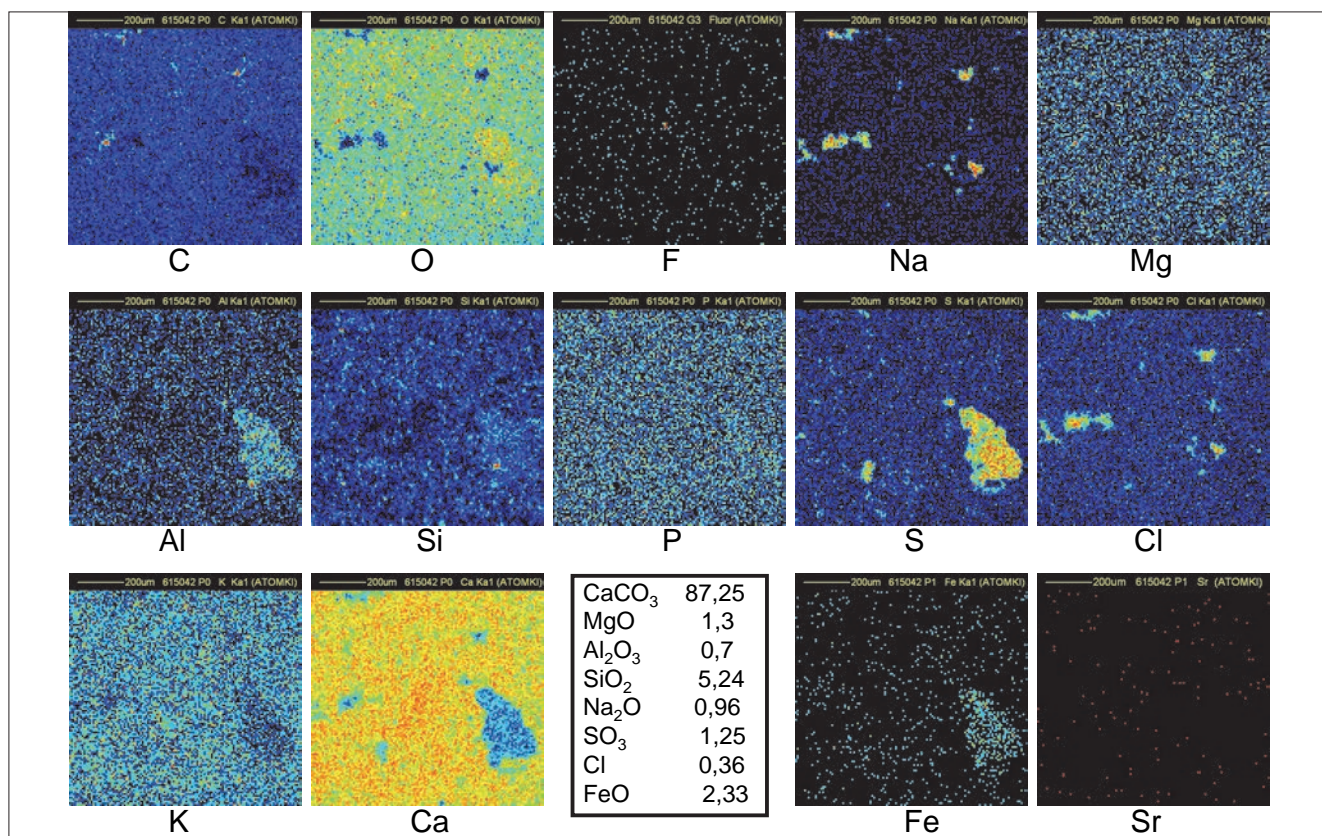


**Figure 12.** Distribution maps of 14 elements in VT3 outside block of Khufu (1 mm × 1 mm).



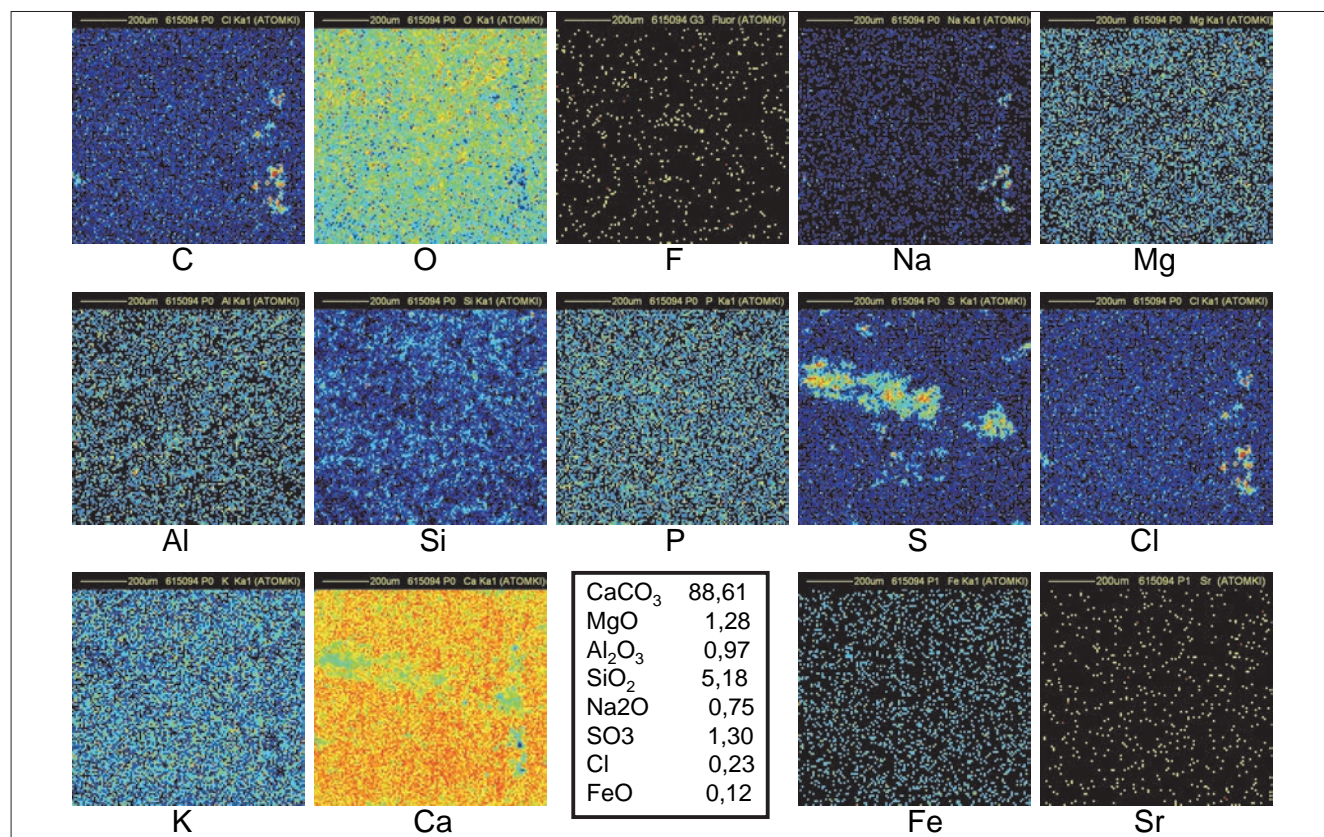


**Figure 13.** Distribution maps of 14 elements in 15a outside block of Khufu (1 mm × 1 mm).

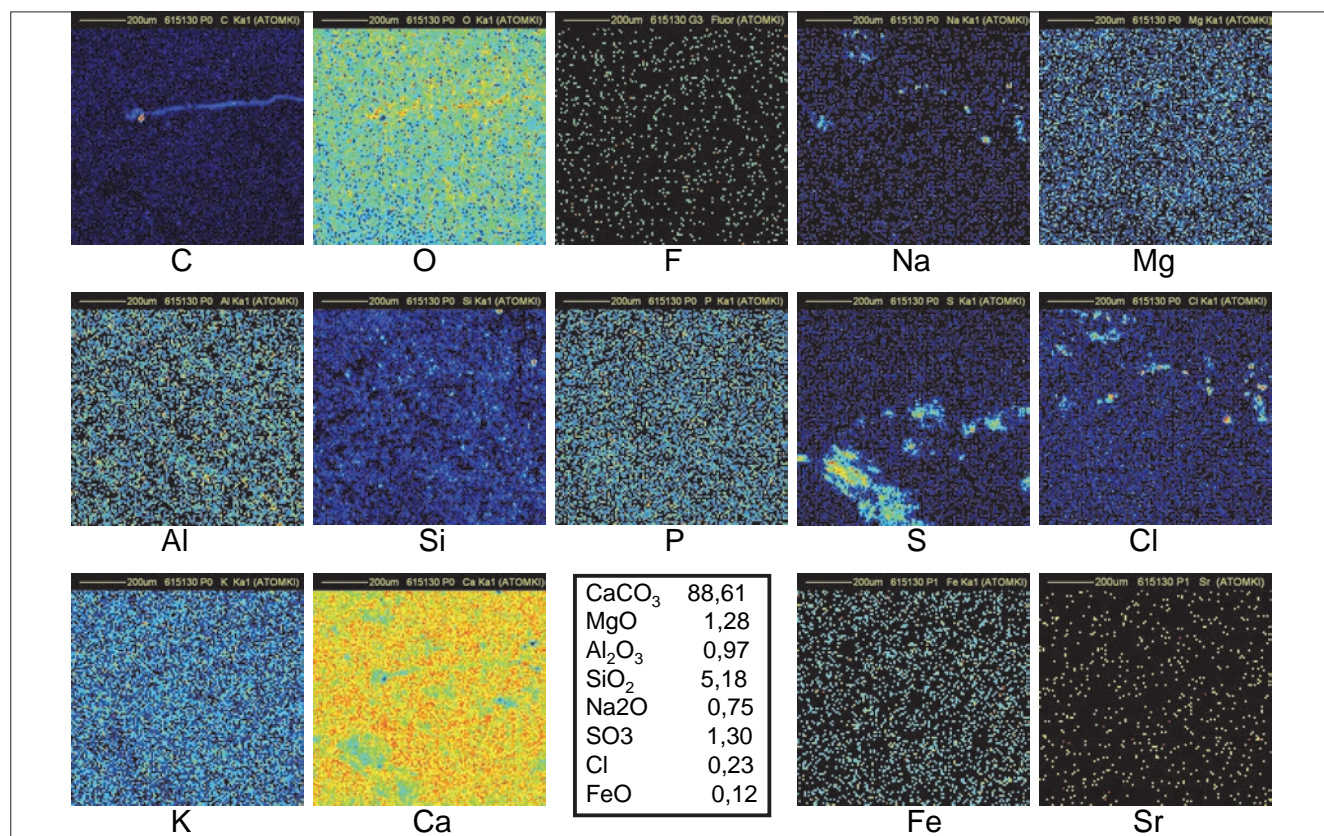


**Figure 14.** Distribution maps of 14 elements in 15b outside block of Khufu (1 mm × 1 mm).



of sodium chloride. Nevertheless, the Na signal is always higher than what is needed to form NaCl (as confirmed by measurements on RMs). At the sites of high concentrations of Na and Cl, the Ca and O concentrations are less than in the surrounding area. Considering that the oxygen content in Na<sub>2</sub>O and H<sub>2</sub>O is lower than in CaCO<sub>3</sub>, it may be concluded that Na<sub>2</sub>O (certainly with some H<sub>2</sub>O) is mixed into the NaCl clusters. Magnesium, phosphorus and potassium are also more abundant in the pyramid samples than in the quarry samples, but they are not distributed in the clusters.<sup>6,7</sup> Their presence may be attributed to ashes used to create the binder with a high chemical pH induced by Na<sub>2</sub>O and H<sub>2</sub>O.<sup>15</sup> Reported concentrations in Figures 10–14 have been computed with the data collected in different regions of several irradiated samples (6–10 different locations) and do not only refer to the specific map. Beside calcium and magnesium oxides, it is known that wood ash contains small quantities of oxides of phosphorus, potassium, manganese and iron.<sup>7</sup>

### Carbon clusters

Carbon clusters have been observed on elemental maps collected on numerous (but not all) pyramid samples, but never on maps from Maadi and Tura quarry samples (see Figures 6 and 7) or in other natural limestone samples from Belgium, Hungary and Saqqarah which were analysed in the complete microprobe runs (more than 150 maps).<sup>6,7,16</sup>

The carbon maps refer to the detection of the low-energy (277 eV) K $\alpha$  line by the SUTW detector. This low-energy CK line, induced in pure CaCO<sub>3</sub> by 2.5 MeV protons, cannot reach the detector if its production is deeper than 1  $\mu$ m below the surface (see Figure 4). However, if the carbon belongs to some organic compound, the information depth may be 5–10 times higher. Therefore, CK could have been produced deeper which would explain the hole in the corresponding Ca map.

The maps in Figure 12 refer to sample FH123 collected in the Great Gallery of the Khufu Pyramid. A bright spot in the C map, correlated to black spots

in both Ca and O maps as shown in the central upper part of maps, indicates that the CK $\alpha$  line is produced deeper than 1  $\mu$ m below the surface. The volume of that C-rich region covering a surface of 25  $\mu$ m  $\times$  25  $\mu$ m could extend down to 10–20  $\mu$ m below the surface. In addition, this region corresponds also to the region of both Na and Cl clusters: a probable signature of the use of natron (a naturally occurring mixture of hydrated sodium carbonate: Na<sub>2</sub>CO<sub>3</sub>  $\cdot$  10H<sub>2</sub>O with some sodium chloride and sodium sulfate). All these observations fit with the model of construction created by Davidovits, who states that the blocks of Khufu pyramid were cast *in situ* using granular limestone aggregates, natron, lime (probably produced by the combustion of wood in domestic fires) and water to produce an alkali alumino-silicate based binder.<sup>15</sup> The black spot in the bottom-left part of the O map coincides with the bright spots in the Na and Cl maps: the O content is indeed lower in Na<sub>2</sub>O than in CaCO<sub>3</sub>. The black spot in the bottom-right of the Ca map corresponds to the bright spot in the Si map: a small amount of SiO<sub>2</sub> is common in natural limestone as is also observed in the distribution maps of Figures 6 and 7.

A similar interpretation may be given for sample VT3 (an outside block from Khufu) for C, O, Na, Cl and Ca maps (Figure 13). Additional large clusters of Al, S and Fe justify the black spots in the Ca map.

Clusters of C in Figure 14 (sample 15B, an outside block from the Khufu pyramid) fully correlated with Na and Cl clusters may be understood as discussed immediately above, but no clear decrease is observed in the corresponding Ca region. The C clusters are thinner than in Figure 12. C, Na and Cl clusters are then concentrated closer to the surface allowing a better transmission of CaK $\alpha$  lines to explain the better uniformity in the Ca map. The holes in the O map are in good correspondence with the clusters in the C, Na and Cl maps. The C map of Figure 14 (same sample 15B but another fragment) shows a filament-shaped distribution suggesting an organic origin.

### Conclusion

Elemental distribution maps of C, O, Na, S, Cl and Ca clearly indicate that the structure of the samples of the Khufu pyramid is not homogeneous and is completely different from samples from the Maadi and Tura quarries. The amount of natural limestone in pyramid samples is about 5–10% less than in samples from the quarries. The other elements, like Na, S and Cl, are mainly distributed in clusters. The mean concentration of Mg is higher in the pyramid samples, but this element is in general homogeneously distributed. Abnormal clusters of C with size varying from 5  $\mu$ m to 30  $\mu$ m are interpreted as from an organic origin. These structural and compositional observations fit with the model of construction involving a moulding procedure.

It would be certainly important to understand why carbon is distributed in clusters. <sup>14</sup>C dating would be the best way to check this. If the C clusters observed by micro-PIXE originate from pollution, their <sup>14</sup>C/<sup>12</sup>C ratio would be the same as that for modern wood. If this ratio is lower by a factor of two ( $T_{1/2}$  of C<sup>14</sup> is indeed very close to the reported age of the Giza pyramids!), the interpretation would suggest the use of some organic material during the construction of the pyramid. A <sup>14</sup>C: <sup>12</sup>C ratio close to zero would mean that carbon is of geological age. As it is difficult to perform <sup>14</sup>C dating on very small samples like those used in the present study, sampling with the agreement of the Egyptian authorities could allow the appropriate quantity of material to be provided to experts in accelerator <sup>14</sup>C dating. The conclusions of <sup>14</sup>C dating would help lift the veil of mystery of the construction of the Egyptian pyramids.

### Acknowledgements

I am indebted to the scientific and technical staff of LARN (Namur, Belgium) and ATOMKI (Debrecen, Hungary) for their important support during the long runs of measurements. My special thanks to Prof. Á.Z. Kiss and Dr I. Uzonyi for fruitful advice and their valuable suggestions concerning the nuclear microprobe equipment.




## References

1. K. Morishima, M. Kuno, A. Nishio, N. Kitagawa, Y. Manabe, M. Moto, F. Takasaki, H. Fujii, K. Satoh, H. Kodama, K. Hayashi, Sh. Odaka, S. Procureur, D. Attié, S. Bouteille, D. Calvet, Chr. Filosa, P. Magnier, I. Mandjavidze, M. Riallot, B. Marini, P. Gable, Y. Date, M. Sigiura, Y. Elshayeb, T. Elnady, M. Ezzy, E. Guerriero, V. Steiger, N. Serikoff, J.-B. Mouret, B. Charlès, H. Heddal and M. Tayoubi, "Discovery of a big void in Khufu's pyramid by observation of cosmic-ray muons", *Nature* **552**, 386 (2017). <https://doi.org/10.1038/nature24647>
2. I. Arnaud, "Pyramide de Khéops: la cavité inconnue s'avère encore plus longue", *Sci. Avenir* 887 (2019).
3. C. Hoare, "Egypt experts set sights on finding lost Pharaoh's remains in Great Pyramid", *Daily Express* 14 November 2019. <https://www.express.co.uk/news/world/1203221/egypt-khufu-found-void-scanpyramid-great-pyramid-giza-zahi-hawass-tutankhamun-saatchi-spt>
4. J. Bertho, *La Pyramide Reconstituée: Les Mystères des Bâtisseurs Égyptiens Révélés*. Editions Unic, Saint-Georges-d'Orques, France (2001).
5. J. Davidovits, "X-ray analysis and X-ray diffraction of casing stones from the pyramids of Egypt, and the limestone of the associated quarries", *Science In Egyptology Symposia*, pp. 511–520 (1984).
6. G. Demortier, "Distribution of sodium and chlorine in samples of Egyptian pyramids", *Geopolym. Archaeol.* **1**, 1–9 (2020). <https://doi.org/10.13140/RG.2.2.33958.75844>
7. G. Demortier, "Scanning micro-PIXE analysis of samples of Egyptian pyramids for a global approach of work involved in their construction", *Curr. Top. Anal. Chem.* **12**, 15–32 (2020). <https://doi.org/10.1111/j.1551-2916.2006.01308.x>
8. M. Barsoum, A. Ganguly and G. Hug, "Microstructural evidence of reconstituted limestone blocks in the Great Pyramids of Egypt", *J. Am. Ceram. Soc.* **89**(12), 3796–3788 (2006).
9. I. Túnyi and I.A. El-hemaly, "Paleomagnetic investigation of the great Egyptian pyramids", *Europhys. News* **43**(6), 28–31 (2012). <https://doi.org/10.1051/eprn/2012604>
10. G. Demortier, "PIXE, PIGE and NMR study of the masonry of the pyramid of Cheops at Giza", *Nucl. Instrum. Meth. B* **226**, 98 (2004). <https://doi.org/10.1016/j.nimb.2004.02.024>
11. G. Demortier, G. Quarta, K. Butalag, M. D'Elia and L. Calcagnile, *X-Ray Spectrom.* **37**, 178 (2008). <https://doi.org/10.1002/xrs.1059>
12. G. Demortier, "Revisiting the construction of Egyptian pyramids", *Europhys. News* **40**(1), 28 (2009). <https://doi.org/10.1051/eprn/2009303>
13. Gy. Szabó and I. Borbély-Kiss, "PIXYKLM computer package for PIXE analyses", *Nucl. Instrum. Meth. B* **75**, 123 (1993). [https://doi.org/10.1016/0168-583X\(93\)95626-G](https://doi.org/10.1016/0168-583X(93)95626-G)
14. I. Uzonyi, Gy. Szabó, "PIXEKLM-TPI—a software package for quantitative elemental imaging with nuclear microprobe", *Nucl. Instrum. Meth. B* **231**, 156–161 (2005). <https://doi.org/10.1016/j.nimb.2005.01.050>
15. J. Davidovits and M. Morris, *The Pyramids, an Enigma Solved*. Hippocrene Books, New York (1988).
16. G. Demortier, "La microsonde à protons pour percer le mystère de la construction de la pyramide de Khéops", *Revue Quest. Sci.* **188**(1), 1–112 (2017). <https://www.rqs.be/app/views/revue.php?id=5>



Guy Demortier has a PhD in nuclear physics, is Emeritus Professor of Physics at University of Namur, Belgium, Co-founder and past director of LARN (Laboratoire d'Analyses par Réactions Nucléaires), Past-president of the Belgian Physical Society, Past-president of COST Action G1 (Ion beam study of art and archaeological objects) and First winner of the EPS-IBA-Europhysics Prize for Applied Nuclear Science and Nuclear Methods in Medicine. His research fields include nuclear properties of light nuclei, neutron physics, accelerator-based methods of elemental analysis (PIXE, PIGE, RBS, RNA, XRF induced by PIXE, nuclear microprobe), and applications in materials science, archaeometry, ancient gold metallurgy, dentistry and superconductors.

 <https://orcid.org/0000-0001-6834-6866>  
[guy.demortier@unamur.be](mailto:guy.demortier@unamur.be)

# Structural, dielectric and Raman spectroscopic study of complex electric and magnetic interactions in multiferroic ionic crystals

Holger Gibhardt,\* Fabian Ziegler and Götz Eckold

Georg-August-University of Göttingen, Tammannstr. 6, D-37077 Göttingen, Germany

## Introduction

While ordinary materials are usually either magnetically or electrically ordered, a relatively new class of materials of so-called multiferroics has been discovered that exhibits magnetic and electrical (and eventually also mechanical) ordering simultaneously. The unique and fascinating feature of these systems is that both phenomena are coupled and that electric forces may be used to control the magnetic structure and vice versa.

Unfortunately, most systems that have been investigated so far exhibit these extraordinary properties only at low temperatures. In view of possible applications in information technology, sensor technology etc., it is, therefore, a crucial task to increase the temperature range of multiferroics. Since the exact mechanism of spin coupling with the movement of ions and the resulting electric dipole moment is still not fully understood, detailed experimental and theoretical studies are needed which require advanced techniques like high-resolution

Raman spectroscopy with suitable laser sources.

One particular interesting system is  $\text{MnWO}_4$ , in which the  $\text{Mn}^{2+}$  is the only magnetic ion. Its magnetic phase diagram is rather complex and exhibits two different antiferromagnetic phases, below  $T_K=6.8\text{ K}$  and between  $T_C=12.3\text{ K}<T<T_N=13.2\text{ K}$ , respectively. In the intermediate multiferroic phase between  $T_K$  and  $T_C$  the spins are no longer antiferromagnetically aligned but form a cycloidal wave along a certain crystallographic direction. The stabilising interactions between different spins are mediated by the diamagnetic oxygen ions by the magnetic super-exchange. Additionally, a force is exerted on the oxygen ions so that they are displaced from their normal position. In consequence, an electric dipole moment is generated and the crystal becomes ferroelectric. The electro-magnetic coupling is usually described by the “inverse Dzyaloshinskii–Moriya” interaction.

Variation of magnetic interaction is a key tool to investigate the electro-magnetic behaviour of such complex systems. This can be done by doping the crystal with other ions. For example, it is possible to replace some manganese ions by non-magnetic ions which leads to a decrease of the magnetic interaction and, hence, to a reduction of the stability region of the multiferroic phase.

On the other hand, the variation of non-magnetic ions can help to increase the ion displacements and the spin-induced electric dipole moments which lead to an enhanced multiferroic regime. In the present study, we replace tungsten by molybdenum and characterise the structural, dielectric and spectroscopic properties of the mixed system  $\text{MnWO}_4\text{--MnMoO}_4$ .

Lattice vibrations reflect details of local interatomic interactions. Hence, Raman spectroscopy is a powerful tool to investigate the effect of ion doping on the spin-oxygen coupling. In a previous publication,<sup>1</sup> we were able to demonstrate that there is an unusual strong temperature dependence of the W–O stretching vibration within the  $\text{WO}_6$  octahedra. Using the green line of an  $\text{Ar}^+$ -ion laser with a wavelength  $\lambda=514.532\text{ nm}$ , a shift of  $0.3\text{ cm}^{-1}$  of this  $884.4\text{ cm}^{-1}$  mode could be detected within the rather small temperature interval of the multiferroic phase (5.5 K). Variations of the magnetic interactions by Mo-doping can, therefore, be monitored by frequency shifts of this particular lattice mode.

The replacement of the tungsten ions by molybdenum ions is rather challenging and needs a multistep chemical solid-state process.<sup>2,3</sup> After mixing the pure components,  $\text{MnWO}_4$  and  $\text{MnMoO}_4$ , several cycles of ball-milling, pellet-pressing, temperature-cycling and

DOI: [10.1255/sew.2021.a22](https://doi.org/10.1255/sew.2021.a22)

© 2021 The Authors

Published under a Creative Commons  
BY licence





final sintering were applied in order to produce well-defined samples of a series of compositions of  $\text{MnW}_{1-x}\text{Mo}_x\text{O}_4$  with  $0 < x < 1$ . Even if both pure compounds belong to the same space group  $P2_1/m$  and exhibit only small differences in their lattice parameters, they differ considerably in the coordination of oxygen ions. While in  $\text{MnWO}_4$  (wolframite), tungsten is six-fold coordinated by oxygen, forming  $\text{WO}_6$ -octahedra, molybdenum in  $\text{MnMoO}_4$  is four-fold coordinated and  $\text{MoO}_4$ -tetrahedra are the corresponding building blocks. As a consequence, there is a limited miscibility with a pronounced gap between  $x=0.3$  and  $x=0.65$ . The exact extension is still under discussion in the literature and seems to depend on the type of preparation. The samples investigated in the present study are, therefore, characterised by X-ray powder diffraction as shown in Figure 1.

There are three concentration regimes which can clearly be distinguished:

- Group I (black):  $0 < x < 0.3$ : the diffraction pattern consists of the reflections of the pure wolframite-phase of  $\text{MnWO}_4$  (except the sample holder reflections indicated by Ta). Hence, in this concentration regime, six-fold coordinated tungsten ions are gradually substituted by molybdenum ions.

- Group III (blue):  $0.65 < x < 1$ : the diffraction pattern consists of the reflections of pure  $\text{MnMoO}_4$  and the four-fold coordinated molybdenum ions are substituted by tungsten.

- Group II (red):  $0.3 < x < 0.65$ : the diffraction pattern resembles that of pure  $\text{MnWO}_4$  but, as indicated by an asterisk, the main reflection of the molybdate-phase is also present at  $26^\circ$  and grows with increasing Mo-content  $x$ . This finding is a clear signature of the miscibility gap even if the reflections of the tungstate-phase are still dominating.

### Raman spectroscopy

More detailed information about the variation of interatomic interactions can be obtained by Raman spectroscopy. Unlike the previous study on pure  $\text{MnWO}_4$ , however, the mixed crystalline system cannot be investigated using the standard argon laser since the molybdenum content makes the sample entirely opaque and strongly absorbs green light.

As a consequence, a green laser is inappropriate for this system and a red one must be preferred. In Raman spectroscopy, fundamental conditions of the exciting light are long-time stability as well as a narrow bandwidth of about  $0.01 \text{ cm}^{-1}$ . Hence, we used a

novel solid-state red laser Solo640 (UNIKLASERS), which meets these requirements very well. This laser has a wavelength of  $\lambda=640 \text{ nm}$  and a maximum power of 500 mW (at the sample, 10 mW are applied).

Figure 2 displays concentration dependent spectra for two ranges of wavenumbers. Again, the three concentration groups can be distinguished well as demonstrated by the colour-coded spectra.

Of particular interest is the concentration dependence of the internal stretching vibration of the oxygen-polyhedron between  $850 \text{ cm}^{-1}$  and  $950 \text{ cm}^{-1}$ . With increasing Mo-content, the well-defined  $\text{WO}_6$ -vibration at  $884.4 \text{ cm}^{-1}$  gets weaker and another mode at  $850 \text{ cm}^{-1}$  is observed with growing intensity which can be attributed to the molybdenum substitution at the centre of the oxygen-octahedra. In the concentration regime of the molybdate-phase (blue spectra), the Raman spectrum is split into several bands which correspond to different types of stretching vibrations in the  $\text{MoO}_4^{2-}$ -tetrahedra. The external vibration at lower wavenumbers shown on the left-hand side of Figure 2 confirm the impression that up to  $x=0.65$ , the features of the tungstate-phase are retained with some modifications due to the Mo-doping. Only beyond  $x=0.7$  the modes of the molybdate-phase dominate and the wolframite modes are strongly reduced in particular.

The effect of molybdenum doping on the multiferroic phase transition is reflected by the temperature dependence of the real part of the dielectric permittivity  $\epsilon'$  shown in Figure 3 as obtained by dielectric impedance spectroscopy. The well-defined peak indicates the Curie-temperatures  $T_C$  where the multiferroic phase is entered on cooling associated with a spontaneous electric polarisation. With increasing molybdenum concentration,  $T_C$  increases significantly and the multiferroic phase is stabilised at higher temperatures. The dielectric loss peak can still be observed for molybdenum concentrations up to  $x=0.5$  even if the intensity decreases gradually. After an almost linear behaviour of  $T_C(x)$  for lower concentrations just as observed by Hardy

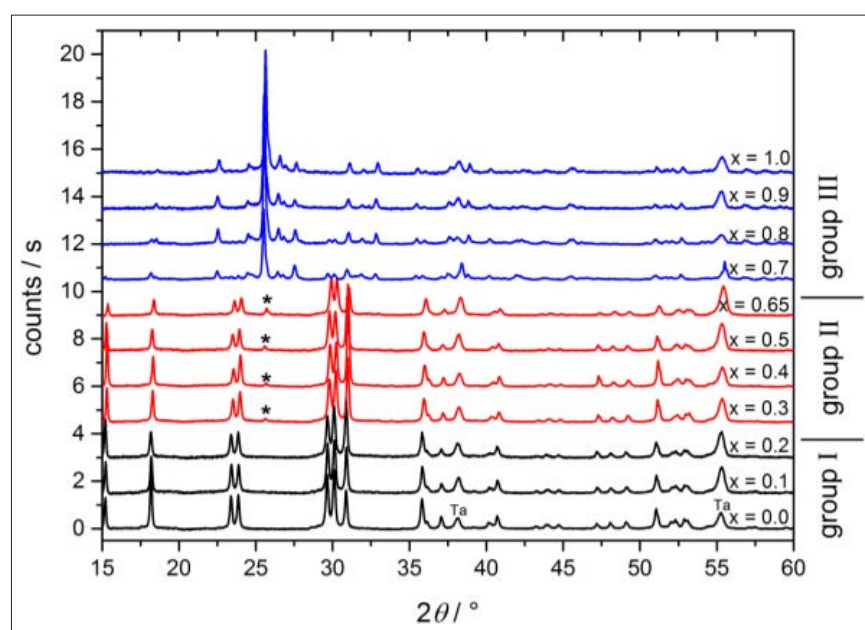


**Figure 1.** X-ray diffraction pattern of sintered  $\text{MnW}_{1-x}\text{Mo}_x\text{O}_4$  samples with different concentrations. Different colours represent concentration regimes with different structural characteristics.

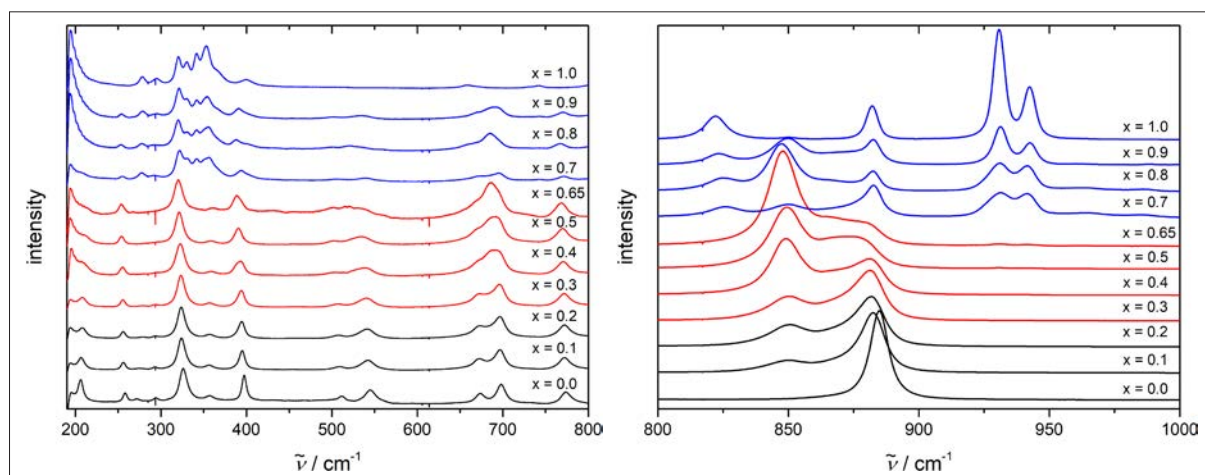


**Figure 2.** Raman spectra of sintered  $\text{MnW}_{1-x}\text{Mo}_x\text{O}_4$  samples with different concentrations. The three concentration regimes are distinguished by different colours. The intensities are normalised with respect to the  $A_g$ -mode at  $327\text{ cm}^{-1}$ .

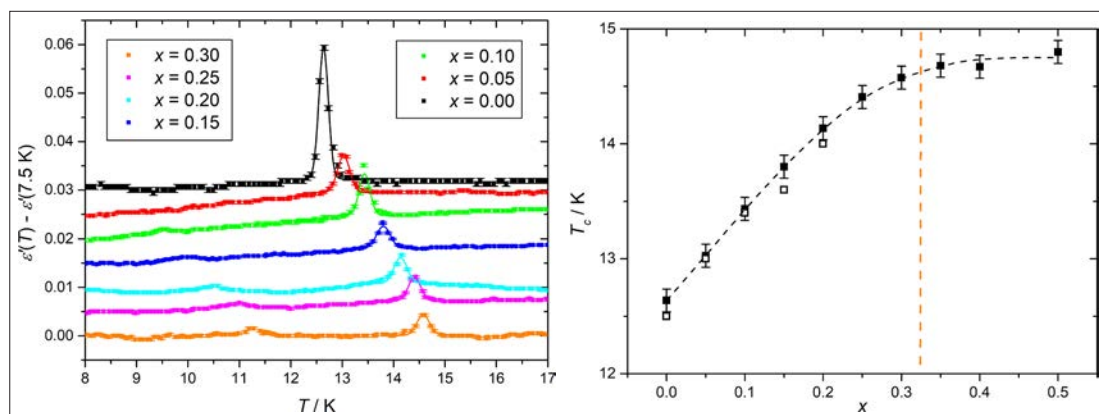


**Figure 3.** Left: temperature dependence of the real part of the dielectric permittivity of  $\text{MnW}_{1-x}\text{Mo}_x\text{O}_4$  for different compositions. Right: concentration dependence of  $T_c$ . Open symbols are datapoints from Reference 4.

*et al.*,<sup>4</sup> there is a saturation near  $x=0.35$  at  $T_c=14.7\text{ K}$  more than  $2\text{ K}$  higher than for pure  $\text{MnWO}_4$ .

The results of the present study indicate, in fact, that partial substitution of ions leads to an extended temperature range of the multiferroic phase. The key feature is the modification and strengthening of the super-exchange interaction between the magnetic ions mediated by oxygen. Understanding the underlying processes on the atomic level is crucial for possible applications and for the development of new materials with exciting properties.

## References

1. F. Ziegler, H. Gibhardt, J. Leist and G. Eckold, "High-resolution polarised Raman scattering study on spin-phonon coupling in multiferroic  $\text{MnWO}_4$ ", *Mater. Res. Express* **2**, 096103 (2015). <https://doi.org/10.1088/2053-1591/2/9/096103>
2. L. Meddar, M. Josse, M. Maglione, A. Guet, C. La, P. Deniard, R. Decourt, C. Lee, C. Tian, S. Jobic, M.-H. Whangbo and C. Payen, "Increasing the phase-transition temperatures in spin-frustrated multiferroic  $\text{MnWO}_4$  by Mo doping", *Chem. Mater.* **24**(2), 353–360 (2012). <https://doi.org/10.1021/cm2031653>
3. L.Y. Chang, "Subsolidus phase relations in the system  $\text{ZnWO}_4$ - $\text{ZnMoO}_4$ - $\text{MnWO}_4$ - $\text{MnMoO}_4$ ", *Mineral. Mag.* **36**(283), 992–996 (1968). <https://doi.org/10.1180/minmag.1968.283.036.11>
4. V. Hardy, C. Payen, F. Damay, L. Meddar, M. Josse and G. Andre, *J. Phys. Condens. Matter* **28**(33), 336003 (2016). <https://doi.org/10.1088/0953-8984/28/33/336003>

Dr Holger Gibhardt studied physics in Heidelberg and Aachen (Germany) and graduated from Aachen in 1994 with the "diploma". In 1998, he finished his PhD thesis at the Institute for Physical Chemistry in Göttingen. His research interests are structural and spectroscopic investigations in different condensed matter systems. Neutron scattering and Raman scattering have been the most important tools. Since, 1999, he is Senior Scientist at the Institute for Physical Chemistry in Göttingen. [hgibhar@gwdg.de](mailto:hgibhar@gwdg.de)



# Surface-enhanced Raman spectroscopy for selected energetic material detection

Mohamed Mokhtar,\* Tamer Wafy and Mahmoud Abdelhafiz

Chemical Engineering Department, Military Technical College, Cairo, Egypt

Raman spectroscopy is an important technique for explosive detection. However, the output spectra are sometimes ambiguous and not strong enough to be analysed. In this work, Surface-Enhanced Raman spectroscopy (SERS) for energetic materials detection was achieved by using *in situ* impregnated silver nanoparticles in the membrane substrate. The substrates used in SERS were characterised by ultraviolet-visible (UV-vis) spectroscopy and scanning electron microscopy (SEM) with energy dispersive spectroscopy (EDS) for elemental analysis. Three substrates were used, all of which were impregnated with silver-nanoparticles. The first substrate (A) received no coating, while the other two substrates (B and C) were coated on one side only with a polymer epoxy layer with a thickness of 0.01 mm and 1 mm, respectively. The three different substrates were used for the detection of an energetic material, TNT, by Raman spectroscopy. The Raman spectrum of TNT using the impregnated substrate without any coating (A) showed an enhancement in the results compared to the epoxy-coated substrates (B and C). Hence, substrate A can be used for energetic materials detection.

## Introduction

Nowadays, with terrorism attacks around the World, researchers are looking at ways to reduce both civilian and military casualties. Early detection of dangerous materials, especially explosives, is one of the main ways in which terrorism operations can be aborted.<sup>1</sup> Fast, practical and accurate detection techniques are in high demand to counter these attacks. Such techniques should produce results that have high sensitivity together with ease and simplicity of use so that they can be deployed in the field. However, it has been found that accurate detection of explosives is challenging. Further, the presence of traces of explosive in water is a serious

problem as it affects directly both living aquatic species and humans.<sup>2</sup> Various analytical techniques have been used to help to identify the explosophorous groups. Chromatographic and spectrometric techniques are the basic methodologies that have been used for what are risky tasks.<sup>3,4</sup> However, relatively expensive techniques such as mass spectrometry and Fourier transform infrared (FT-IR) spectroscopy need special sample preparation and long processing steps to be able to complete the required analysis, which makes them unsuitable for use in the field. In addition, traces of explosive are barely detectable by conventional or even by advanced instruments of these types.

Raman spectroscopy has an advantage over these instruments through on-site detection of sample traces without special sampling treatment.<sup>5,6</sup> In addition, Raman spectroscopy does not need samples to be in solution, which enables it to be utilised in diverse environments. Raman spectroscopy records a unique spectrum that helps to accurately

identify the investigated sample.<sup>7–10</sup> The mechanism of the Raman spectroscopy detection process is that the incident beam from the Raman laser source interacts with the molecules of the investigated sample causing different vibration modes. The reflected radiation from the sample molecules is detected and appears as a characteristic spectrum which is specific to the tested sample.<sup>11</sup> Raman spectroscopy is important in the explosive detection field.<sup>12</sup> However, sometimes, the Raman spectrum of an explosive may be ambiguous due to the absence or weakness of some fundamental peaks used for sample recognition.

Researchers have attempted to improve the Raman spectrum using a variety of techniques to enhance these weak peaks so that they can be easily analysed. It has been found that nanoparticles, especially metallic ones such as silver (Ag) and gold (Au), show a plasmon resonance when subjected to a Raman laser source: the incident beam strikes the metal nanoparticles causing

DOI: [10.1255/sew.2021.a23](https://doi.org/10.1255/sew.2021.a23)

© 2021 The Authors

Published under a Creative Commons  
BY-NC-ND licence



excitation of these particles. When these excited nanoparticles return back to their relaxation mode, the emitted radiation frequency can build a magnetic field within the spot of the incident beam.<sup>13,14</sup> The sample to be tested is placed on these nanoparticles and the reflected beam from the sample molecules is magnified due to the adjacent magnetic field created from the interaction between the incident light beam and the nanoparticles.<sup>15</sup>

2,4,6-Trinitrotoluene (TNT) is a very common explosive which has been involved in the production of land and sea mines, as well as terrorist bombs. TNT is easily absorbed by both skin and soil, and is classified as a carcinogenic material with high toxicity and long-term negative impacts. For these reasons, several researchers have been attracted to investigate the detection of traces of TNT. These attempts were based on the preparation of various substrates impregnated with metallic nanoparticles using the chemical vapour deposition<sup>16</sup> or spin coating techniques.<sup>17</sup> However, all these investigations were based on two-step methodologies involving the preparation of a suspended solution of the explosive traces prior to use of the detection techniques.<sup>18–20</sup>

In this study, a simple, more practical and straightforward one-step method was successfully utilised. The explosive detection technique is based upon the simple preparation of a substrate (commercial filter paper) impregnated with Ag-nanoparticles produced through a one-step *in situ* reduction of silver nitrate using ascorbic acid as a suitable reducing agent. Further treatment after washing and drying to remove unreacted reagents and impurities took place by applying a layer of elastomeric polymer to the substrate surface to improve the capture of sample traces on the substrate.

## Material and methods

### Materials

L-Ascorbic acid from BDH Chemical, Poole, UK, and silver nitrate crystals [general purpose reagent (GPR) A' grade] from Hopkin & Williams were used. Whatman Number 1 filter paper

and diglycidyl ether of bis Phenol A (DGEBA) of EEW 500 epoxy and polyamide as a hardener were purchased from ISPAC. The energetic material, TNT, was prepared in our local laboratory.

### Substrate preparation

3 g of silver nitrate was dissolved in 100 mL distilled water under suitable agitation. The substrate was immersed in this solution for 12 h to guarantee the complete saturation of the filter paper. The ascorbic acid solution, as a reducing agent, was prepared by dissolving 1 g of ascorbic acid in 50 mL distilled water (Figure 1). The prepared reducing agent solution was applied to the saturated filter paper with silver nitrate solution by spraying to ensure *in situ* reduction of the silver nitrate and the production of silver particles. Then, the treated substrate was put in an oven at 60°C for 6 h to evaporate the water solvent. After drying the substrate, the sample was washed with distilled water and dried again.

This cycle of washing and drying the sample was repeated three times to ensure removal of reactant residuals and unattached products. The elastomeric polymer was prepared by mixing the epoxy DGEBA with polyamide in the ratio of 1:0.45 and adding a suitable solvent, such as xylene, to the mixture in the ratio of 0.1:1. Three substrates were used for SERS; all of them were impregnated with

Ag-nanoparticles. Two of them were then coated: substrate B was coated with a 0.01 mm epoxy layer and substrate C was coated with a 1 mm epoxy layer, while the third substrate, A, was left uncoated.

### UV-vis spectroscopy

UV-vis spectroscopy over the range of 200–800 nm was conducted for the prepared Ag-nanoparticles (Figure 2). The previous procedure for Ag-nanoparticle preparation on a substrate was followed except that we did not use a substrate and the reduction reaction took place in a glass test tube. The resulting suspended silver nanoparticles were diluted for analysis using a UV-vis spectrometer (Shimadzu UV-1700).

### Scanning electron microscopy with energy dispersive X-ray spectroscopy

The prepared samples were subjected to scanning electron microscopy (SEM) (Zeiss EVO 10 equipped with a Bruker EDS) to investigate the silver particles' size, size distribution among the substrate, and the surface morphology of the applied epoxy and its homogeneity distribution along the substrate surface. Cross-sectional SEM images were collected to study the silver particles' distribution by substrate depth. Energy dispersive spectroscopy

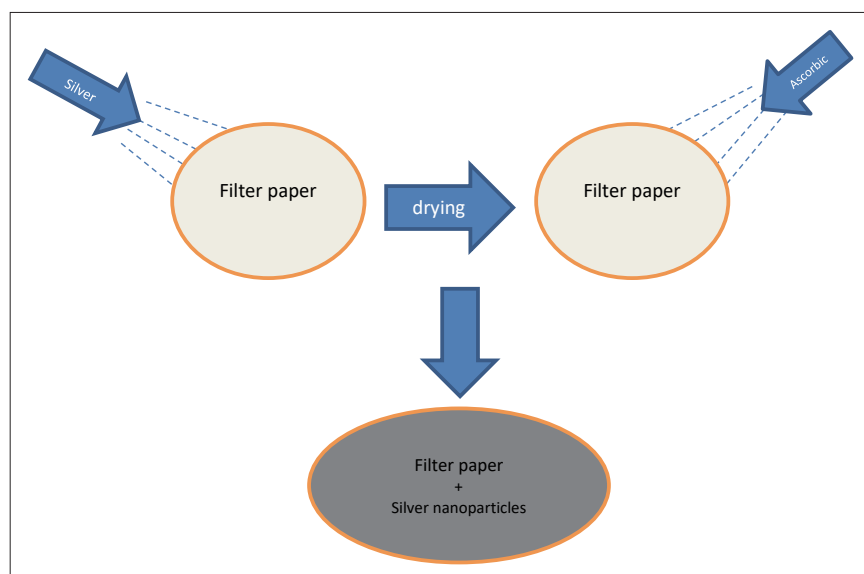


**Figure 1.** Preparation of SERS substrates.



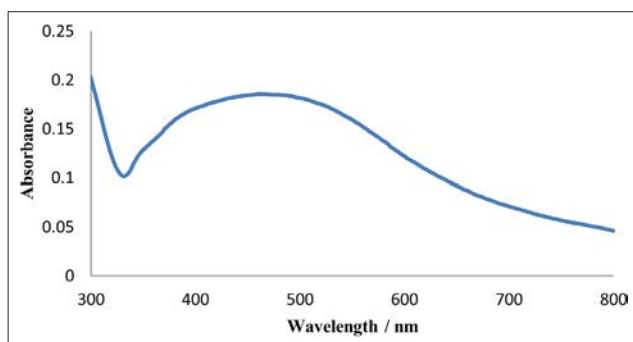


**Figure 2.** UV-vis spectrum of Ag-nanoparticles sample.

(EDS) for elemental analysis was conducted to confirm the nature of the Ag-nanoparticles on the substrate.

### SERS for explosive detection

Raman spectroscopic measurements were carried out on a solid sample of TNT using a dispersive Raman microscope (Senterra II, Bruker, Germany). Raman spectra were collected continuously with spectral resolution of  $4\text{ cm}^{-1}$ . A Nikon 20 $\times$  objective was used to focus the Raman excitation sources (2.5 mW at 532 nm and 100 mW at 785 nm, neodymium-doped yttrium aluminium garnet (Nd:YAG) laser, Bruker, Germany). Spatial resolution was in the order of  $1\text{ }\mu\text{m}$  for the 20 $\times$  objective lens and  $361\text{ }\mu\text{m}$  for the 100 $\times$  objective lens. Several points on the substrates were used in the SERS measurement methodology as shown in Figures 3 and 4. Data collection time was 1000 ms (co-addition of three spectra), the illumination area was  $50 \times 50\text{ }\mu\text{m}$ , fluorescence baseline correction was performed using a third-order polynomial, followed by the application of a three-point moving average filter to eliminate most of the perturbing baseline and improve the signal-to-noise ratio.

First, the explosive sample was placed as solid powder in a quartz cuvette and subjected to Raman spectroscopy to collect the Raman spectrum of the explosive sample as a reference. Then we measured the prepared membrane substrate by Raman spectroscopy without any explosive samples to produce a Raman zero background (so we could subtract the Raman spectrum of

the substrate from the analysis of the real samples). 0.01 mg of the explosive powder was put on the membrane substrate and then subjected to Raman spectroscopy for detection.

## Results and discussion

### UV-vis spectroscopy

UV-vis spectra of the prepared Ag-nanoparticles in the spectral range 200–800 nm showed a peak at 484 nm. The peak is broad and according to Mie's observations, could be attributed to the irregular shape and polydispersity of the sample.<sup>21</sup>

### SERS for explosive detection

TNT on substrate A showed no results when using the laser source at 532 nm with different powers. Figure 5 shows the Raman spectrum of TNT explosive alone and the enhanced Raman spectrum of TNT + substrate A using a laser source of 785 nm and a power of 100 mW. Several experiments were conducted to reach this power as the minimum required to

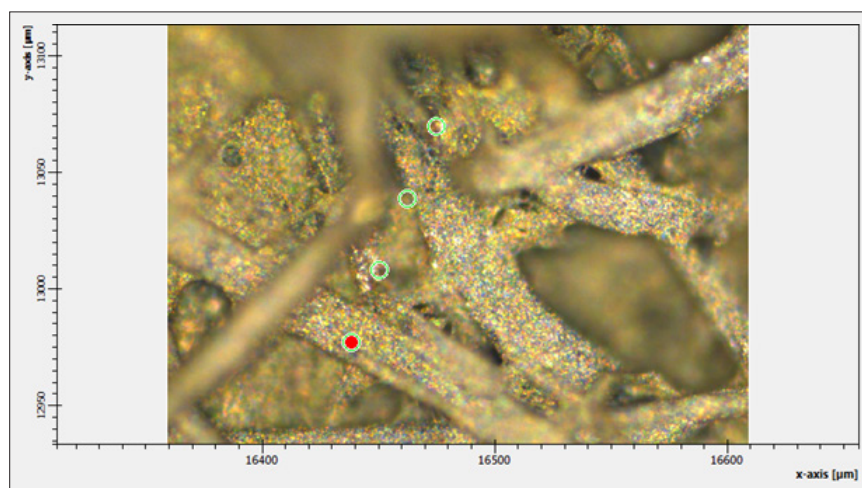


**Figure 3.** Several selected points for Raman analysis of pure Ag-nanoparticles on substrate.

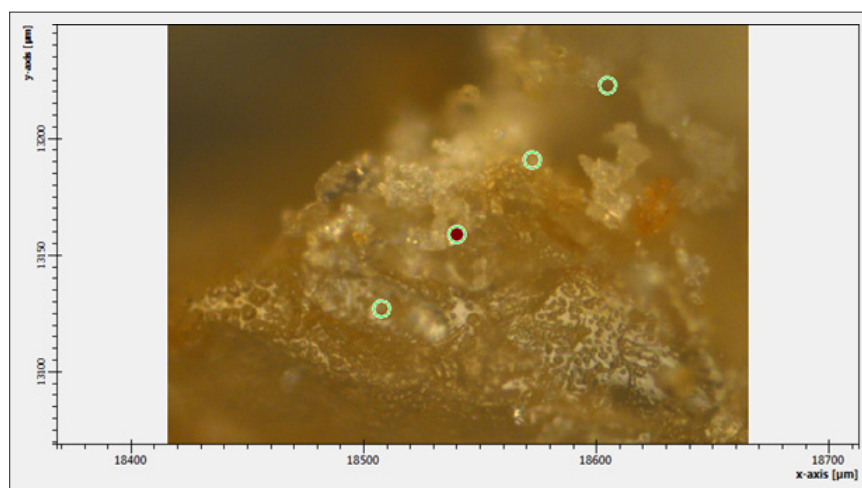


**Figure 4.** Several selected points for Raman analysis of Raman spectrum of TNT + Ag-nanoparticles on substrate at 785 nm.

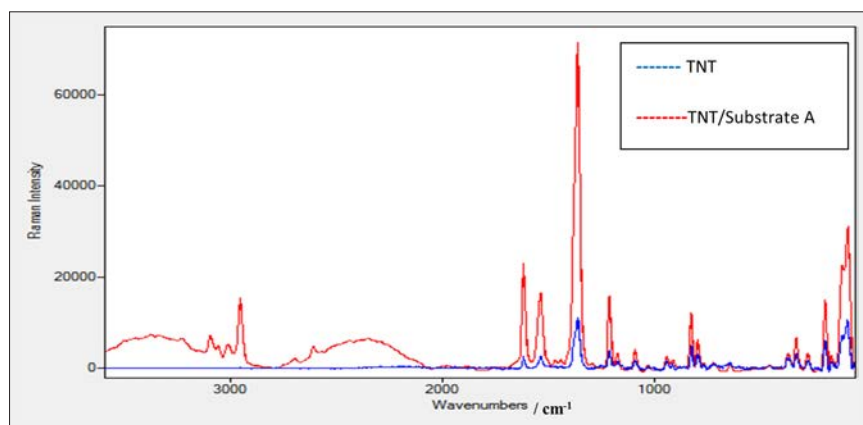


**Figure 5.** Raman spectrum for TNT sample alone and TNT sample on the prepared substrate A using a laser source at 785nm and power of 100mW.

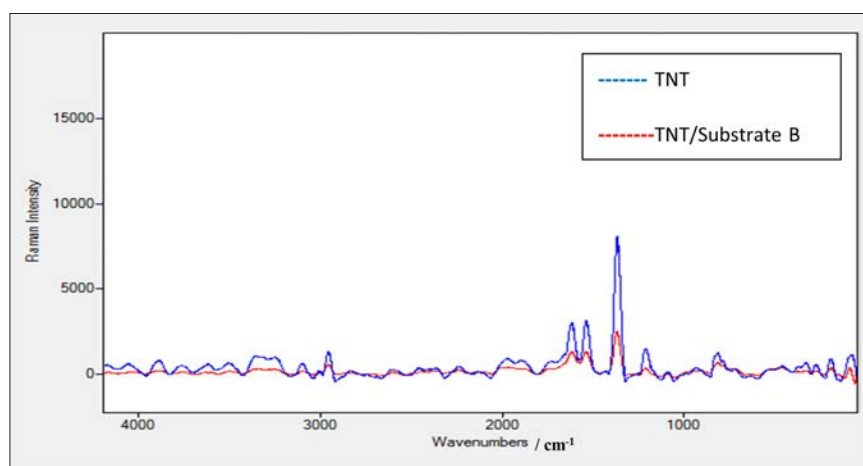


**Figure 6.** Raman spectrum for TNT sample alone and Raman spectrum for TNT sample on the prepared substrate B using a laser source at 532nm and power of 2.5mW.

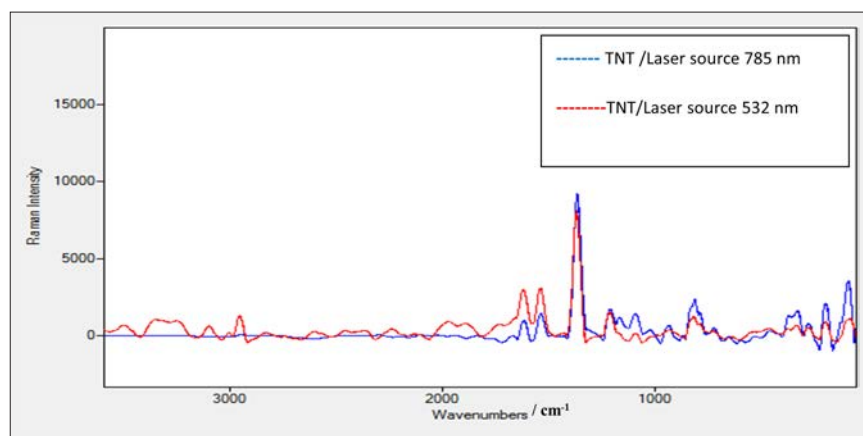


**Figure 7.** Raman spectrum for TNT sample alone using a laser source of 532nm and power of 2.5mW and TNT sample alone using laser source 785nm and power 100mW.

get a good spectrum for TNT. Different peaks were seen in the range between  $1700\text{ cm}^{-1}$  and  $100\text{ cm}^{-1}$ . Peaks at  $1616\text{ cm}^{-1}$  and  $1532\text{ cm}^{-1}$  are attributed to strong vibration of the C=C  $\pi$  bond in an aromatic ring chain—the benzene ring in the case of TNT<sup>22</sup>—or are attributed to an asymmetric vibration of the 2,6-NO<sub>2</sub> bond and an asymmetric vibration of the -NO<sub>2</sub> bond in the benzene ring.<sup>23</sup> The peak at  $1358\text{ cm}^{-1}$  is due to a strong symmetric vibration of the C-NO<sub>2</sub> bond as the nitrate groups attached to the benzene ring in the TNT structure.<sup>24</sup> Peaks at  $823\text{ cm}^{-1}$  and  $792\text{ cm}^{-1}$  are due to the scissoring vibration mode of the C-NO<sub>2</sub> bond and the stretching vibration mode for C-CH<sub>3</sub>. For the SERS of TNT using substrate A, it was noticed that new, interesting peaks appeared for the first time in the Raman spectrum; such as the peak at  $2956\text{ cm}^{-1}$ , which is related to the strong vibration of the C-H bond, and the peak at  $3098\text{ cm}^{-1}$ , due to the strong vibration of the =C-H bond in an aromatic structure such as a benzene ring. Moreover, the intensity of the peaks, from comparing the half-height width of the peaks, increased by approximately seven times. This enhancement effect could be attributed to the plasmon resonance of the distributed Ag-nanoparticles on the substrate.

Figure 6 shows the Raman spectrum of TNT using the laser source at 532 nm with power of 2.5 mW. The same peak positions appeared as in the TNT Raman spectrum using the 785 nm laser source. In addition, a new peak at  $2956\text{ cm}^{-1}$  appeared which is attributed to the strong vibration of the C-H bond in the TNT structure. A further peak at  $3098\text{ cm}^{-1}$  is due to the strong vibration of the =C-H bond. An observation to note is that when comparing the Raman spectra of TNT using 532 nm and 785 nm lasers and the enhanced Raman spectrum of TNT using substrate A as shown in Figure 7, the methods all share the same peak positions except those at  $2956.50\text{ cm}^{-1}$  and at  $3098\text{ cm}^{-1}$  with the 532 nm laser which do not appear with the 785 nm laser. This means that these peaks are characteristic of TNT and only appear using a high-energy laser source such



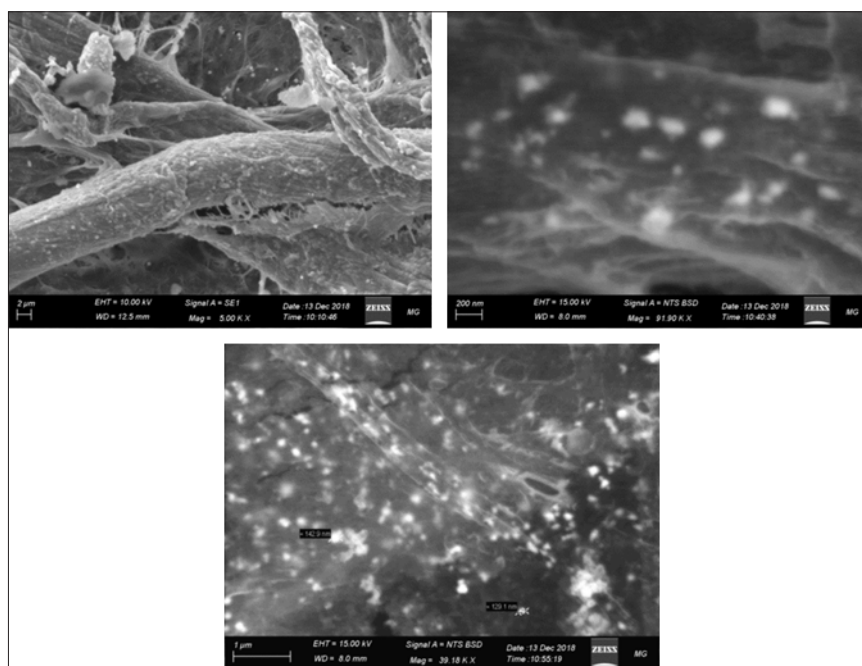


**Figure 8.** SEM spectroscopy of substrate A (Ag-nanoparticles on filter paper substrate).

as 532nm. This is a good verification that substrate A significantly enhances the peak at  $2956\text{ cm}^{-1}$  when we use a Raman spectrometer with a low-energy laser source at 785nm. The same procedure was conducted for TNT on the coated substrates B and C. Substrate C, with a thick film of elastomer, was excluded as it gives a poor signal-to-noise ratio. On the other hand, no results were seen when using the 785nm laser with different powers for TNT on substrate B. However, substrate B—TNT coated with a thin film of

elastomer—gave clear results when the 532nm laser source with 2.5mW power was used. The decrease in the intensity of the scattered light is due to the presence of this thin elastomer film which absorbs some of the scattered light which consequentially affects its intensity.

### SEM-EDS

Figure 8 shows that substrate A is doped with well-distributed Ag-nanoparticles of different nano sizes. At high magnification (39 kx), it is observed that the

Ag-nanoparticles are in the size range 130–250nm and are distributed evenly through the substrate.

From the EDS analysis, as shown in the elemental analysis graph in Figure 9 and the element distribution pattern in Figure 10, it can be seen that the sample had 17.03% mass of C, 6.48% mass of O, 0.22% mass of Si, 1.15% mass of S and 38.71% mass of Ag. This indicates that the Ag-nanoparticles are present in greater mass in substrate A, which we propose is suitable as a substrate for Raman enhancement proposes.

### Conclusions

In this study, a simple, more practical and straightforward one-step method was successfully utilised for the detection of TNT explosive traces in their naturally solid form. Herein, *in situ* deposition of Ag solid nanoparticles upon a commercial filter paper, as the substrate, occurred directly instead of the preparation of a suspended solution as in most of the previous works in the literature. Interestingly, new characteristic peaks for TNT appeared either at high-energy (583nm) or at low-energy laser source (785nm). This could be considered as an improvement in the detection technique of solid particles of TNT using a simple one-step method. Adding a polymeric layer on the substrate by coating it with the elastomer DGEBA made the substrate more flexible and sticky for sample capture purposes. However, applying the polymer to the impregnated substrate destroys its capability for Raman enhancement. Substrate A shows a good Raman enhancement of the tested sample TNT. Substrate C showed unexpected failure in Raman spectrum enhancement due to the thick layer of the polymer coat. Substrate B with the applied thin layer of the elastomer is sticky enough to hold the traces of the tested sample. However, it showed no difference in Raman enhancement for the tested explosive sample of TNT, so it is not suitable for explosive detection. Substrate A is suitable for explosive detection using the Raman enhancement technique, and in the future work on different explosives will be carried out with this substrate.

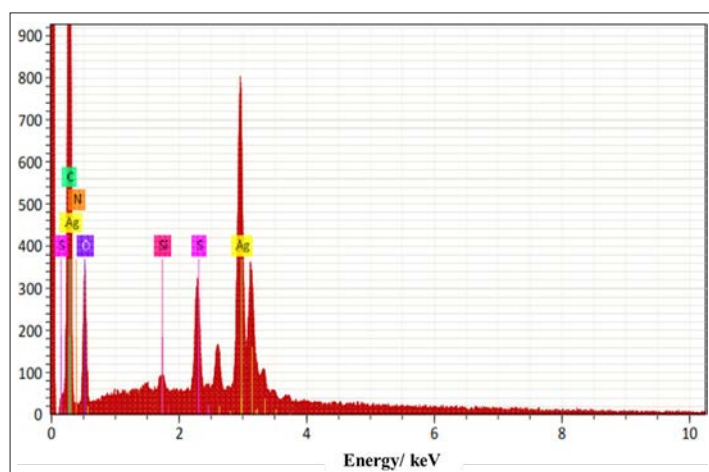


**Figure 9.** EDS elemental analysis for substrate A.

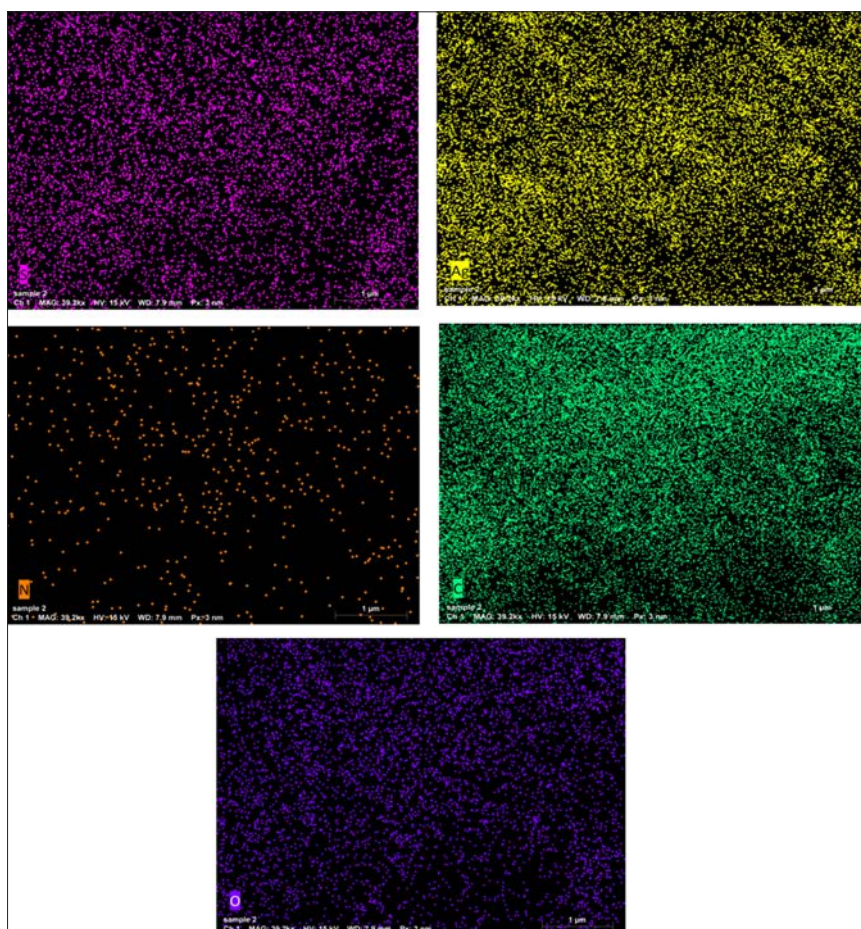


**Figure 10.** EDS elemental distribution pattern of substrate A.

### Author contributions

The manuscript was written through contributions of all authors. All authors have given approval to the final version of the manuscript.

### CRediT authorship contribution statement

Mohamed Mokhtar, Tamer Wafy and Mahmoud Abdelhafiz supervised/co-ordinated the whole work and were involved in funding acquisition, project administration, experimental work, measurement and data treatment, writing/reviewing the text and conceptualisation and proposing the main idea.

### Declaration of competing interests

The authors declare that they have no known competing financial interests or personal relationships that could have appeared to influence the work reported in this paper.

### References

1. W.O. Rivera, *Standoff Raman Spectroscopy System for Detection of Explosives, Chemical Warfare Agents Simulants and Toxic Industrial Compounds*. University of Puerto Rico, Mayaguez, Puerto Rico (2008). <https://hdl.handle.net/20.500.11801/444>
2. O.A. Sadik, A.K. Wanekaya and S. Andreescu, "Advances in analytical technologies for environmental protection and public safety", *J. Environ. Monitor.* **6**, 513–522 (2004). <https://doi.org/10.1039/b401794n>
3. A. Eshkeiti, B. Narakathu and A. Reddy, "A novel fully gravure printed flexible surface enhanced Raman spectroscopy (SERS) substrate for the detection of toxic heavy metals", *14<sup>th</sup> International Meeting on Chemical Sensors - IMCS 2012*, Ch. P2.3 Sensors Based on Optical

Techniques (2012). <https://doi.org/10.5162/IMCS2012/P2.3.11>

4. N. Zhang, L. Tong and J. Zhang, "Graphene-based enhanced Raman scattering toward analytical applications", *Chem. Mater.* **28**(18), 6426–6435 (2016). <https://doi.org/10.1021/acs.chemmater.6b02925>
5. S.N. Chen, X. Li, S. Han, J.H. Liu and Y.Y. Zhao, "Synthesis of surface-imprinted Ag nanoplates for detecting organic pollutants in water environments based on surface enhanced Raman scattering", *RSC Adv.* **5**, 99914–99919 (2015). <https://doi.org/10.1039/C5RA19528D>
6. S. Sadate, C.F. Iii, A. Kassu and A. Sharma, "Standoff Raman spectroscopy of explosive nitrates using 785 nm laser", *Am. J. Remote Sens.* **3**(1), 1–5 (2015). <https://doi.org/10.11648/j.ajrs.20150301.11>
7. R.S. Das and Y.K. Agrawal, "Raman spectroscopy: recent advancements, techniques and applications", *Vibr. Spectrosc.* **57**(2), 163–176 (2011). <https://doi.org/10.1016/j.vibspec.2011.08.003>
8. E.L. Izake, "Forensic and homeland security applications of modern portable Raman spectroscopy", *Forensic Sci. Int.* **202**(1–3), 1–8 (2010). <https://doi.org/10.1016/j.forsci-int.2010.03.020>
9. J.R. Baena and B. Lendl, "Raman spectroscopy in chemical bioanalysis", *Curr. Opin. Chem. Biol.* **8**(5), 534–539 (2004). <https://doi.org/10.1016/j.cbpa.2004.08.014>
10. J.Jehlička, P. Vítka, H.G.M. Edwards, M. Heagraves and T. Čapoun, "Application of portable Raman instruments for fast and non-destructive detection of minerals on outcrops", *Spectrochim. Acta A* **73**(3), 410–419 (2009). <https://doi.org/10.1016/j.saa.2008.09.004>
11. A. Eshkeiti, *Fabrication of Printed Substrate for Surface Enhanced Raman Spectroscopy*. Master's Thesis, Western Michigan University (2012). [https://scholarworks.wmich.edu/masters\\_theses/25/](https://scholarworks.wmich.edu/masters_theses/25/)
12. C.M. Wynn, S. Palmacci, R.R. Kunz and M. Rothschild, "A novel method




- for remotely detecting trace explosives", *Lincoln Lab. J.* **17**(2), 1 (2008). <https://www.ll.mit.edu/about/lincoln-laboratory-publications/lincoln-laboratory-journal/lincoln-laboratory-journal-8>
13. L. Dolgov, D. Pidhirnyi, G. Dovbeshko, T. Lebedieva, V. Kiisk, S. Heinsalu, S. Lange, R. Jaaniso and I. Sildos, "Graphene-enhanced Raman scattering from the adenine molecules", *Nanoscale Res. Lett.* **11**, 197 (2016). <https://doi.org/10.1186/s11671-016-1418-5>
  14. Y. Song, "Molecular selectivity of graphene-enhanced Raman scattering", *Nano Lett.* **15**(5), 2892–2901 (2015). <https://doi.org/10.1021/nl5045988>
  15. G. Herrera, A. Padilla and S. Hernandez-Rivera, "Surface enhanced Raman scattering (SERS) studies of gold and silver nanoparticles prepared by laser ablation", *Nanomaterials* **3**(1), 158–172 (2013). <https://doi.org/10.3390/nano3010158>
  16. W. Xu, X. Ling, J. Xiao, M.S. Dresselhaus, J. Kong, H. Xu, Z. Liu and J. Zhang, "Surface enhanced Raman spectroscopy on a flat graphene surface", *Proc. Natl. Acad. Sci. USA* **109**(24), 9281–9286 (2012). <https://doi.org/10.1073/pnas.1205478109>
  17. K. Mondal, J. Kumar and A. Sharma, "TiO<sub>2</sub>-nanoparticles-impregnated photocatalytic macroporous carbon films by spin coating", *Nanomater. Energ.* **2**(3), 121–133 (2013). <https://doi.org/10.1680/nme.12.00034>
  18. E.L. Holthoff, D.N. Stratis-Cullum and M.E. Hankus, "A nanosensor for TNT detection based on molecularly imprinted polymers and surface enhanced Raman scattering", *Sensors* **11**(3), 2700–2714 (2011). <https://doi.org/10.3390/s110302700>
  19. J.R. Lombardi and R.L. Birke, "A unified approach to surface-enhanced Raman spectroscopy", *J. Phys. Chem. C* **112**(14), 5605–5617 (2008). <https://doi.org/10.1021/jp800167v>
  20. L. Yang, L. Ma, G. Chen, J. Liu and Z.-Q. Tian, "Ultrasensitive SERS detection of TNT by imprinting molecular recognition using a new type of stable substrate", *Chem. Eur. J.* **16**(42), 12,683–12,693 (2010). <https://doi.org/10.1002/chem.201001053>
  21. K.-A. Kim, J.-R. Cha, S.-W. Yun and M.-S. Gong, *Bull. Korean Chem. Soc.* **36**(5), 1426–1432 (2015). <https://doi.org/10.1002/bkcs.10281>
  22. Y. Liu, R. Perkins, Y. Liu and N. Tzeng, "Normal mode and experimental analysis of TNT Raman spectrum", *J. Mol. Struct.* **1133**, 217–225 (2017). <https://doi.org/10.1016/j.molstruc.2016.12.015>
  23. K. Andersson, *Masters Thesis*. Umea University (2010).
  24. R. Chirico, S. Almagia, F. Colao, L. Fiorani, M. Nuvoli, W. Schweikert, F. Schnürer, L. Cassioli, S. Grossi, D. Murra, I. Menicucci, F. Angelini and A. Palucci, "Proximal detection of traces of energetic materials with an eye-safe UV Raman prototype developed for civil applications", *Sensors* **16**(1), 8 (2015). <https://doi.org/10.3390/s16010008>

## ARTICLE



Mohamed Mokhtar had obtained his BSc and MSc (Chemical Engineering) from the Military Technical College, Cairo, Egypt in 2001 and 2008, respectively, and a PhD in ion selective membranes from McMaster University, Canada. He currently works as a lecturer in the Chemical Engineering department of the Military Technical College. His main areas of research include synthesis, characterisation and applications of nano-sized particles, MOFs, synthesis and characterisation of selective membranes, water and wastewater treatment, developing of energetic materials, analysis and detection of energetic materials.

 <https://orcid.org/0000-0003-3138-5460>  
[m.mokhtar@mtc.edu.eg](mailto:m.mokhtar@mtc.edu.eg)




Tamer Z. Wafy graduated from the Chemical Engineering branch of the Military Technical College (MTC), Egypt in 1997, and obtained a Master of Science (MSc.Eng) in composite propellants there in 2003. He received his doctor of philosophy (PhD) in nanostructured materials from The University of Manchester in 2013. He joined the Chemical Engineering Branch of the MTC in 1998 initially as Teaching Assistant, then Assistant Lecturer, Lecturer and Associate Professor.

His research is mainly in nanostructured materials specialising in nanocarbons and their applications. His interests are in aspects of the relationships between structure and mechanical properties of polymers and energetic composites, and he has published more than 15 papers in the field. This is now the main activity of his research which investigates the application of Raman spectroscopy to monitor deformation processes in carbon nanotubes and composites and in explosives detection, and standoff detection of explosives. Also he is focusing on developing scalable processes to synthesise a variety of nanomaterials with well-defined atomic structures, assemble these nanomaterials into functional macroscale structures, and use these novel materials for explosives detection, ballistic protection and environmental applications.

[Tamer.z.wafy@mtc.edu.eg](mailto:Tamer.z.wafy@mtc.edu.eg)



Mahmoud Abdelhafiz obtained his BSc and MSc (Chemical Engineering) from the Military Technical College, Cairo, Egypt in 1997 and 2003, respectively. He was granted The Egyptian State Award in 2003 for being in first place among my whole patch. He obtained a PhD degree in nanotechnology applications from the Chemical and Biological Engineering Department, University of Sheffield, UK. He is currently working as a Teacher Assistant in the Explosives and Rocket Propellants department, Chemical Engineering Branch, Military Technical College. His main areas of research include synthesis, characterisation and applications of nano-sized particles, electrospinning technology, synthesis and characterisation of high-energy materials, development of insensitive ammunition and high-performance plastic explosives, Investigation of modern gun and rocket propellants, ageing and life extension of propellants.

 <https://orcid.org/0000-0001-7482-5695>  
[hafiz\\_theone@hotmail.com](mailto:hafiz_theone@hotmail.com)



# Four generations of quality: “measuring up”

**New ISO committee for reference materials committed to excellence in accurate measurement results**

**John P. Hammond**

Technical Manager, Starna Scientific Limited, 52–54 Fowler Road, Hainault, Essex IG6 3UT, UK

## Introduction

This article, the fourth in the series, details the ISO technical committee that is responsible for reference materials (RMs) etc.<sup>1</sup> This Reference Material committee, formally ISO/REMCO, has now been reorganised by ISO as TC 334. The history of ISO/REMCO is discussed, together with the probable changes in this technical committee brought about by its conversion to TC 334.

There has always been, and will continue to be, collaboration between individual producers of RMs, and in many countries around the World, you will find national “mirror” committees reflecting and inputting regional decisions into their appropriate ISO representatives. However, many years ago, RM producers recognised that the growing need by the analytical community for a number and variety of RMs as well as a need for the assurance of the quality of RMs called for collaboration at the international level. This has been achieved through REMCO, the Council Committee on Reference Materials of the International Organization for Standardization (ISO), which celebrated its 40<sup>th</sup> anniversary in 2016. The evolution of this organisation and its conversion into the formal ISO

TC 334—Reference Material continues in 2021 and beyond, and the key likely changes are detailed here.

## 1<sup>st</sup> Generation: the years between 1940 and 1975

The first serious effort towards international cooperation in the field of RMs was the Symposium on an International Reference Materials Program held in May 1969 at the then National Bureau of Standards (NBS), in Washington, DC, under joint sponsorship by the International Committee on Weights and Measures (CIPM) and NBS. It was recognised that the need for RMs was greater than ever before in history and that cooperation on an international scale was needed to meet the World's future needs. The Symposium recommended that the International Bureau of Weights and Measures (BIPM) be asked to establish an organisational mechanism to gather and disseminate information on the availability of RMs, their characteristics and prices, coordinate information on the needs for standard reference materials (SRMs), identify potential suppliers of RMs, and coordinate information on potential RM certifying facilities. Subsequent to the symposium, CIPM had to decline this role because the limitations of its charter and available resources allowed it to assume only the responsibility for SI base unit metrological SRMs.

Given the lack of progress on this important topic, in November 1973 an *ad hoc* International Meeting on RMs, under the sponsorship of the International Organization of Legal

Metrology (OIML) was held at NBS in Washington, DC. Six international organisations and 12 countries were represented. It was recommended that an independent International Commission on Reference Materials (REMPA) be formed to define and gather and disseminate information on RMs as to their availability, ordering information, properties certified etc. and recommend a plan of action to increase their availability on an international scale.

## 2<sup>nd</sup> Generation: the years 1975 to 2000

REMPA met first in April 1975 at which time it established two working groups.

In September 1975, the ISO Council transformed REMPA into the Council Committee on Reference Materials (REMCO) with the following six terms of reference. It is interesting to compare the evolution of these terms with the final versions of ISO/REMCO from 2020 shown in [blue](#).

- 1) To establish definitions, categories, levels and classification of RMs for use by ISO.  
[To establish concepts, terms and definitions related to RMs.](#)
- 2) To determine the structure of related forms of RMs.  
[To specify the basic characteristics of RMs as required by their intended use.](#)
- 3) To formulate criteria to be applied for choice of sources for mention in ISO documents (covering also legal aspects).  
[To propose actions on RMs required to support other ISO activities.](#)

DOI: [10.1255/sew.2021.a24](https://doi.org/10.1255/sew.2021.a24)

© 2021 The Author

Published under a Creative Commons BY-NC-ND licence



# QUALITY MATTERS

- 4) To prepare guidelines for technical committees for making reference to RMs in ISO documents.

To prepare guidelines for ISO Technical Committees when dealing with reference material issues.

- 5) To propose, as far as necessary, action to be taken on RMs required for ISO work.

To communicate with other international organisations on reference material matters.

- 6) To deal with matters within its competence arising in relation with other international organizations and to advise Council on action to be taken.

To advise the ISO Technical Management Board (TMB) on reference material issues.

The first meeting of REMCO took place in January 1976, just prior to the International Round Table on Reference Materials.

The mandate of REMCO was to carry out and encourage a broad international effort for the harmonisation, production and application of certified reference materials (CRMs), and during this period REMCO developed a broad series of ISO Guides on RMs:

## ISO Guide 6. "Mention of reference materials in International Standards"

This Guide was incorporated into the ISO Directives for technical work as Annex 2c in February 1980 and is, therefore, not recognised today as a separate entity.

**ISO Guide 30 "Terms and definitions used in connection with reference materials": harmonises the vocabulary used in connection with RMs**

**ISO Guide 31 "Reference materials—Contents of certificates and labels": ensures that users have sufficient information on a CRM**

**ISO Guide 32 "Calibration of chemical analysis and uses of certified reference materials" was intended for users of RM in calibration for chemical analysis**

This Guide was incorporated into a scheduled revision of ISO Guide 33 in the 3<sup>rd</sup> Generation.

**ISO Guide 33 "Uses of certified reference materials": describes how to use CRMs in widely diverse fields"**

**ISO Guide 34 "General requirements for the competence of reference material producers": was developed to give users increased confidence in the "quality" of CRMs**

**ISO Guide 35 "Certification of reference materials—General and statistical principles": was intended mainly for producers of CRMs**

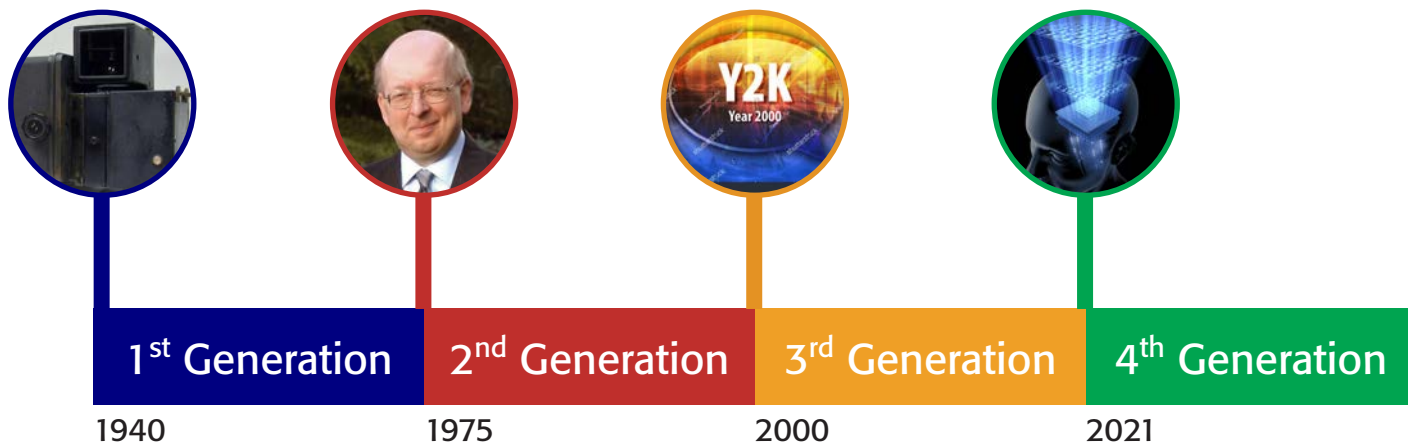
At the 14<sup>th</sup> meeting in May 1989, REMCO decided that the subjects of traceability and levels of RMs were very complicated and reduced its terms of reference to revising ISO Guide 30—"Terms and definitions of reference materials" and harmonising it with the terminology in metrology.

The 15<sup>th</sup> meeting of REMCO in May 1991 saw Mr S. Rasberry (ANSI, NIST) take the Chair of REMCO. A revised work programme was set out for 1991–1996, and a specific Task Group "Accreditation" was added, tasked as follows:

- To assess the need for the accreditation of RM producers.
- To collect, assess and analyse viewpoints and documentation concerning the accreditation of RM producers.
- To provide liaison with appropriate national and international organisations concerned with accreditation of RM producers.
- To produce a draft ISO guide on the requirements for accrediting RM producers.
- To coordinate future revisions of the resultant ISO guide.

The 17<sup>th</sup> meeting of REMCO in April 1994 was given strong support for its activities in accreditation by the ISO Central Secretariat. The latter foresaw the need for the international accreditation of RM producers under ISO 9002 or compatible quality system and believed that REMCO had the potential to be recognised as the authoritative body to register RM producers.

The 18<sup>th</sup> meeting of REMCO in April 1995 led to an initiative to prepare a position paper to examine possible options, including their pros and cons, for establishing some form of international recognition for RM producers.





# QUALITY MATTERS

The 20<sup>th</sup> meeting of REMCO was strongly focused on draft revised Guide 34 based on the ILAC document. The ILAC representative to REMCO agreed to take the draft revised Guide 34 to ILAC for collaboration to produce a mutually agreed-to document.

The Accreditation Task Group also agreed to produce a draft document on establishing a "Register" of CRM producers that also included "quality" statements about each producer. The intent was to put this Register of CRM producers on the Internet via the ISO server.

REMCO undertook a new work initiative to compile a list of problems faced by CRM producers due to differences in legal and other requirements for labelling, packaging and shipping these materials to different countries in the World. This resulted in the associated Technical Report, ISO/TR 11773:2013—Global distribution of reference materials.

The 21<sup>st</sup> meeting of REMCO was held in April 1998 and saw the beginning of collaboration with the Pharmacopoeial Discussion Group (PDG). This Group has prepared reference substances for over 70 years and the use of most of these reference substances is mandated by legislation in the member countries. However, these materials do not strictly comply with the VIM definition

for "certified reference material", and to this day the vast majority are certified for specific applications within the pharmacopoeial requirements, and do not contain an associated Expanded Uncertainty budget for the assigned value. In 1998, the PDG wanted to develop a mechanism to have their RMs accepted as "CRMs" since the term "reference materials" gives the perception of lower quality. REMCO members were divided on this issue but agreed to collaborate with PDG to harmonise the concepts and principles related to the certification of RMs. Over 20 years later, this debate still rumbles on; the pros and cons of which will be expanded upon in the next article in this series, when the history/development of the Quality requirements of the whole GxP pharmaceutical environment will be reviewed.

At the 22<sup>nd</sup> meeting of REMCO in April 1999, REMCO approved the final draft of ISO Guide 34 for submission to the ISO TMB for acceptance by its national member bodies, and also requested its ILAC representative to ask ILAC to accept and to use the revised Guide 34 instead of the corresponding ILAC document.

After its publication in 2000, some national standards bodies selected ISO Guide 34 "General requirements for the competence of reference material

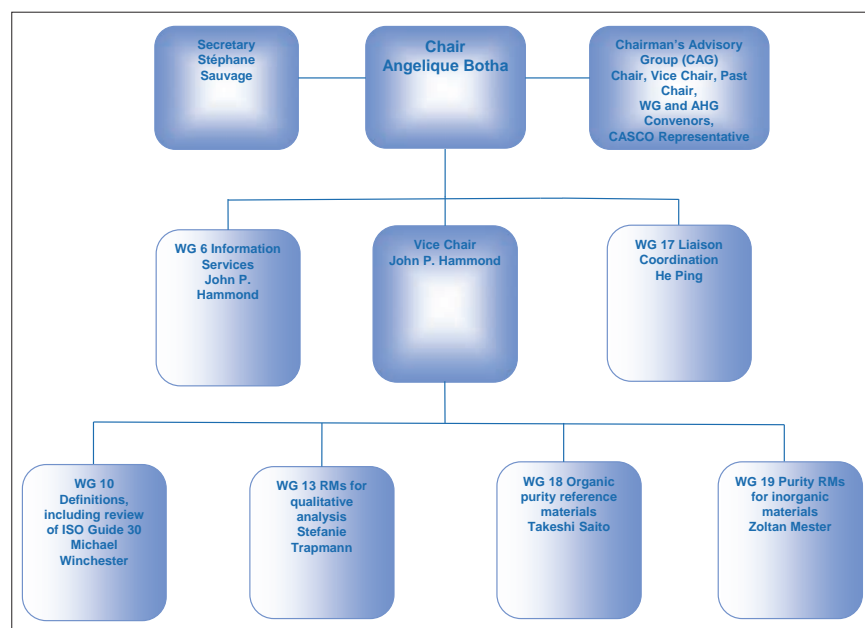


Figure 1. ISO/REMCO Committee structure (2020).



**The first company worldwide to achieve ISO/IEC 17025 accreditation for liquid and glass CRMs**  
 ...and the preferred supplier to leading pharmaceutical companies, instrument manufacturers and accredited laboratories globally.

2000

**2001**

2002

2003

2004

2005

**2006** — accreditation to ISO 17034 (formerly Guide 34)

2007

2008

2009

2010

2011

2012

2013

2014

2015

2016

2017

2018

2019

2020

**2021**







**Starna**  
 Starna Scientific Ltd  
[www.starna.com](http://www.starna.com)





# QUALITY MATTERS

producers" as the basis for the accreditation of RM producers instead of the corresponding ILAC Guide 12, and so began the process of converting a "Guide" into a "Standard", i.e. ISO Guide 34 into ISO 17034, a project previously documented in this publication.<sup>2</sup> As we shall see later this conversion did set a precedent, that could be seen as the process that initiated the formation of TC 334, but more of that later.

It was during this period (in 1995) that, from a personal perspective, I was invited by Dr Michael Parkany from ISO to present a paper at an International symposium in Melbourne on "Quality Assurance and TQM for Analytical laboratories".<sup>3</sup> It was also at this symposium that I met key personal active in REMCO, and as a consequence was invited on to the Cooperation on International Traceability in Analytical Chemistry (CITAC), and ultimately on to the REMCO committee as a UK Industrial representative, in a role that continues to this day.

## 3<sup>rd</sup> Generation: the years 2000 to 2020

The 23<sup>rd</sup> meeting of REMCO was held in May 2000, and a completely new structure, which was essentially maintained

until its disbandment in 2021, was approved. The "Executive Committee" was renamed the "Chairman's Advisory Group" and was composed of the ISO Secretary, the Chair and Chair-elect and the Convenors of the Task Groups, which were renamed Steering Groups.

During this period, this structure was maintained and adjusted to reflect the current work programme, but the format shown in a graphical format in Figure 1, provides a valuable reference for the 4<sup>th</sup> Generation discussions detailed below.

During this period the committee continued to produce both new and revised guidance documents as follows:

- ISO Guide 30:2015 Reference materials—Selected terms and definitions
- ISO Guide 31:2015 Reference materials—Contents of certificates, labels and accompanying documentation
- ISO Guide 33:2015 Reference materials—Good practice in using reference materials
- ISO Guide 35:2017 Reference materials—Guidance for characterization and assessment of homogeneity and stability
- ISO Guide 80:2014 Guidance for the in-house preparation of quality control materials (QCMs)

## Guide(s) under development

- ISO Guide 85:202x RMs for qualitative property values
- ISO Guide 86:202x Purity RMs for small organic molecules
- ISO Guide 87:202x Purity RMs for metals and metalloids
- ISO/TR 79:2015 Reference materials—Examples of reference materials for qualitative properties
- ISO/TR 10989:2009 Reference materials—Guidance on, and keywords used for RM categorization
- ISO/TR 11773:2013 Global distribution of reference materials
- ISO/TR 16476:2016 Reference materials—Establishing and expressing metrological traceability of quantity values assigned to reference materials

The interrelationship of these documents is shown graphically in Figure 2, in which one should note the following structural aspects:

- At the centre is the standard for Reference Material producers, namely ISO 17034.<sup>4</sup>
- The adjacent ring provides the associated Guide documents, which are either normative references to ISO 17034, or at the very least should be used for additional guidance associated with ISO 17034.
- The outer ring details other published/pending documents from the TC.

## 4<sup>th</sup> Generation: from 2021 forward

This essential role of supporting ISO 17034 continues as the primary mandate of TC 334, but here is the first significant change in this TC.

By definition, an ISO Technical Committee's main role is to write standards, appropriate to its defined area of expertise.

Also, in the language of ISO, a "Guide", is defined as an informative document which assists an ISO TC in the construction of standards, appropriate to the TC.

However, as you can see from the above list the ISO/REMCO Guides, in some cases, are not designed for this purpose, but are informative documents for RM producers *per se*. So, the first

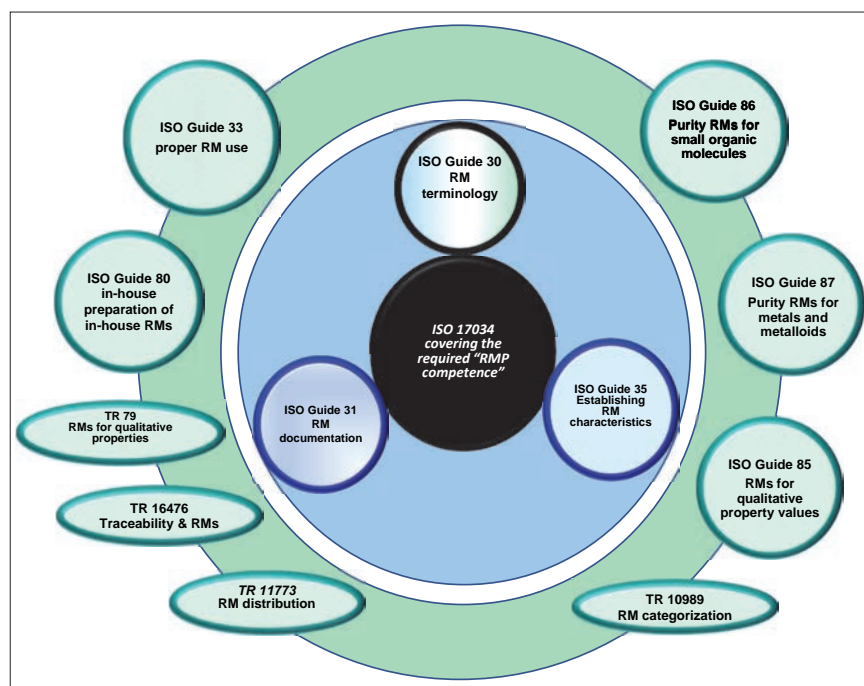


**Figure 2.** ISO/REMCO Guides and TRs (2020).



# QUALITY MATTERS

task that the new TC 334 has to consider is how to meet this requirement and convert these Guides into the appropriate standards.

In addition, in a TC structure a Working Group is tasked with a specific project plan, and associated timeframe to investigate (and produce if appropriate) a related standard; and as one can see from the final ISO/REMCO structure there are a couple of currently defined Working Groups (WG6 and WG17) that do not meet this requirement. Therefore, a structural rearrangement with respect to these essential requirements will be required.

These changes, together with other inter-related communication/liaison requirements will be discussed at the upcoming inaugural virtual TC 334 meeting in early September 2021; and we will

keep you updated in the Quality Matters column, as these details are released.

So, on reflection, and given the historical evolution of "Guides" into "Standards", c.f. ISO Guides 25, and 34 into ISO 17025<sup>5</sup> and ISO 17034,<sup>4</sup> respectively, ISO/REMCO to ISO TC/334 is not really an unexpected transition, is it?

The next (and future) article(s) will discuss similar and evolving Quality environments.

*"Will their paths converge ... only time will tell?"*

## References

1. ISO Press Release, <https://www.spectroscopyeurope.com/news/new-iso-committee-reference-materials>
2. J. Hammond, "Into the future (Part 2): changes to ISO 17025 and ISO

Guide 34", *Spectrosc. Europe* **29(4)**, 11 (2017). <https://www.spectroscopyeurope.com/quality/future-part-2-changes-iso-17025-and-iso-guide-34>

3. M. Parkany (Ed.), *Quality Assurance and TQM for Analytical Laboratories*. The Royal Society of Chemistry, Special Publication No. 169 (1995). ISBN 0-85404-760-3
4. ISO 17034, *General Requirements for the Competence of Reference Material Producers*. International Organization for Standardization (ISO), Geneva, Switzerland (2016).
5. ISO/IEC 17025, *General Requirements for the Competence of Testing and Calibration Laboratories*. International Organization for Standardization (ISO), Geneva, Switzerland (2017).



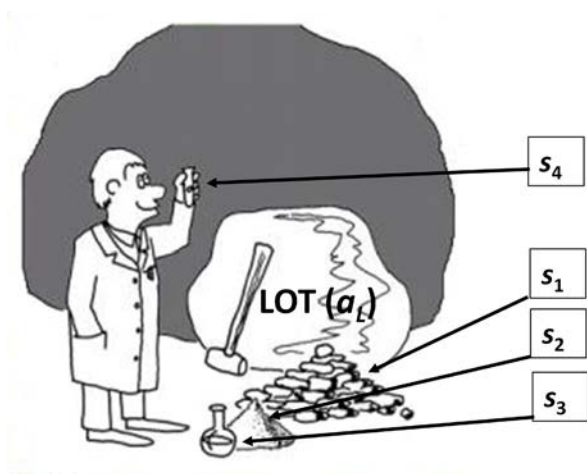
John Hammond is an experienced analytical scientist, spectroscopist and technical marketing professional, skilled in the development, production and marketing of analytical systems into highly regulated and controlled industries. A Fellow of the Royal Society of Chemistry (FRSC), executive member of ISO/TC334 and an Expert Advisor to the United States Pharmacopeia, General Chapters, Chemical Analysis committee.

[j.p.hammond@starna.com](mailto:j.p.hammond@starna.com)

# “Sampling vs analytical error: where the money is ...”

**Pentti Minkinen**

Professor emeritus, Lappeenranta Lahti University of technology (LUT), Finland and President, Senior Consultant, Sirpeka Oy, Finland



Sampling for analysis is a multi-stage operation, from extracting a primary sample ( $s_1$ ) via sub-sampling ( $s_2$ ) ... ( $s_3$ ) towards the final analytical aliquot ( $s_4$ ). At each stage, a sampling error is incurred if not properly reduced or eliminated, collectively adding to the error budget. Nobody wants the total measurement error to be larger than absolutely necessary, lest important decisions based thereupon are seriously compromised. However, it is in the interregnum between sampling and analysis where one finds plenty of usually unknown hidden costs, lost opportunities and a bonanza of bold, red figures below the bottom line. We have asked one of the peers of sampling, with extensive industrial and technological experience, to focus on the economic consequences of not engaging in proper sampling. Enjoy these “horror stories” from which we can all learn, not least at management level.

## Along the full lot-to-analysis pathway

Analytical measurements comprise at least two error generating steps: delineating and extracting the primary sample, and analysis of the analytical aliquot. There may be several sub-sampling steps before having a sufficiently small aliquot (analytical sample) of the original material ready for proper analysis. In this chain of operations, the weakest link determines how reliable the analytical result is. The reason is that variances (squared standard deviations) are *additive*.

If only one primary sample is processed through  $i$  stages, the error variance of the analytical result,  $\sigma_L$  is:

$$s_{\sigma_L}^2 = \sum_{i=1}^I s_i^2 \quad (1)$$

This variance can be *reduced* (always popular for those who worry about the **total** sampling-plus-analysis error) by taking replicate samples at different stages. Consider a three-level process:  $n_1$  primary samples are extracted from the lot, with each primary sample processed and divided into  $n_2$  secondary samples—of which  $n_{lab}$  analytical samples are finally analysed. In this case Equation 2 shows how the complement of stage error variance components propagate to the analytical result.

$$s_{\sigma_L}^2 = \frac{s_1^2}{n_1} + \frac{s_2^2}{n_1 \cdot n_2} + \frac{s_{lab}^2}{n_1 \cdot n_2 \cdot n_{lab}} \quad (2)$$

The total number of samples analysed is  $n_{tot} = n_1 \cdot n_2 \cdot n_{lab}$ .

From a replication design, the variance components  $s_i^2$  can be estimated by using the statistical facility of analysis of variance (ANOVA), or analysis of relative variances (RELANOVA).<sup>1</sup>

## Master example: the effectiveness of replication

The following example will help gain insight into where efforts to reduce and control the total accumulated error is best spent. Let us consider three *schemes* where, for each scheme, the relative standard deviation error estimates are:  $s_{r1}=10\%$ ,  $s_{r2}=4\%$  and  $s_{r3}=2\%$ .

A) **No replicates**,  $n_1=n_2=n_{lab}=1$ . Total number of samples analysed is 1.

$$s_{\sigma_L}^2 = (10\%)^2 + (4\%)^2 + (2\%)^2 = 120(\%)^2 \text{ and } s_{\sigma_L} = 11.0\%$$

B) **Primary samples replicated**,  $n_1=10$ ;  $n_2=n_{lab}=1$ . Total number of samples analysed is 10.

$$s_{\sigma_L}^2 = \frac{(10\%)^2}{10} + \frac{(4\%)^2}{10} + \frac{(2\%)^2}{10} = 12.0(\%)^2 \text{ and } s_{\sigma_L} = 3.5\%$$

C) **Primary samples and duplicated analytical samples**,  $n_1=5$ ;  $n_2=1$ ;  $n_{lab}=2$ . Total number of samples analysed is again 10.

DOI: [10.1255/sew.2021.a25](https://doi.org/10.1255/sew.2021.a25)

© 2021 The Author

Published under a Creative Commons BY licence





# SAMPLING COLUMN

$$s_{a_L}^2 = \frac{(10\%)^2}{5} + \frac{(4\%)^2}{5 \cdot 1} + \frac{(2\%)^2}{5 \cdot 1 \cdot 2}$$

$$= 23.6(\%)^2 \text{ and } s_{a_L} = 4.9\%$$

This example demonstrates that even if the best and most expensive analytical technology available is used in the laboratory, this does not by itself guarantee a reliable result with minimised total uncertainty. **Still, some laboratories routinely run analyses in duplicates or even in triplicates to be sure that their results are "correct". While analytical costs have doubled or tripled, nothing is gained!** It is also common that the uncertainty estimates which laboratories assign to their results are based on the results of the laboratory replicates only; in reality hiding the full pathway uncertainty.

## Selection of optimal sampling mode

Most current standards and guidelines *assume* glibly—although very rarely expressed explicitly—that sampling errors can be estimated using standard statistics. This is based on another assumption, that of a random spatial analyte distribution within the sampling target. When primary samples are extracted from large lots like process streams, environmental targets, shipment of raw materials or commodities or from manufactured products, the same *assumption* of "normality" may in fact lead to sampling plans that are more expensive than the optimised plan and, more importantly, do not provide reliable results. When the purpose of sampling is to estimate the mean value of the lot, the first issue to address is which sampling mode to use: *random, stratified or systematic*. Figure 1 shows and compares the principle of these modes. Very few guidelines refer to the sampling modes at all. Very often in monitoring programmes samples are collected systematically (all good), but the resulting analytical results are then treated as so-called random data sets. As the following example shows this actually results in a *massive loss of information*.

Figure 1 presents a comparison of these three fundamental sampling modes as applied to a process stream.

First, there is no significant difference between them if the process standard deviation is estimated from all nine samples taken in each mode, i.e. the nine samples are treated as one data set. But their difference becomes clear when the mean of the whole process range is calculated. The bias of the mean is decreased from 4.49 % (random) to 3.92 % (stratified) and to -0.48 % (systematic) and the relative standard deviation of the mean from 11.3 % (random) to 8.28 % and to 2.26 %. The difference is even more clear if, based on these data, a sampling plan is requested, for example, with a target that the relative standard deviation of the mean shall not exceed 1%. The "expert" who recommends *random sampling* gives a plan that requires extraction of no less than 385 samples. However, a *stratified sampling plan* will only require 186 samples—whereas if the *systematic mode* is selected, only 12 samples are needed to reach the relative standard deviation target. To summarise, in cost-benefit analysis of an analytical sampling plan the selection mode is crucial.

To select the *optimal* sampling mode and number of replicates, the unit costs

are needed. Operators usually can estimate the cost structure, but the variance estimates can seldom be estimated theoretically. Sometimes they can be estimated from the existing data, but very often pilot studies are needed. Combining specific variance estimates with unit costs of the various operations in the full analytical measurement pathway will allow drastic improvements in the efforts needed; some examples are given below. Further examples of the informed use of the Theory of Sampling (TOS)' principles in the context of total expenditure estimation are given in Reference 2.

## The value of engaging in proper sampling

### Case 1

A pulp mill was extracting a valuable side product ( $\beta$ -sitosterol) which is used in the cosmetic and medical industries, and which has high quality requirement. Customers requested a report on the quality control system from the company in question. I was asked to audit the sampling and analytical procedures and to give recommendations, if needed. I proposed some pilot studies to be carried out and based on these

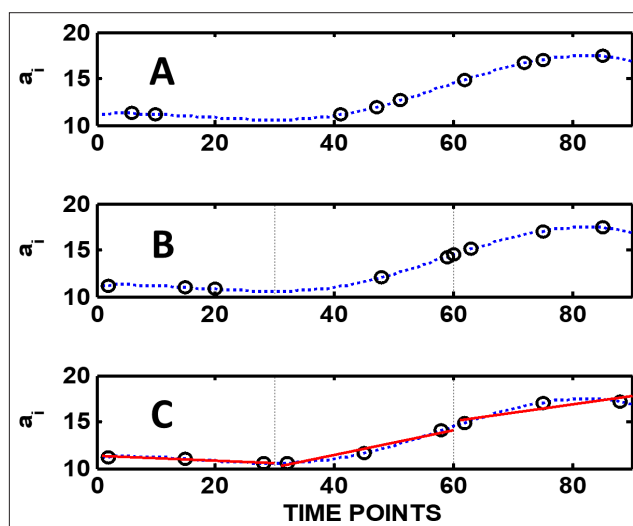


**Figure 1.** A: Random sampling: sampling times or locations are selected randomly. B: In stratified (random) sampling the process lot is divided into individual strata (three strata in this example) and within each stratum the sampling points are selected randomly. C: In systematic sampling the within-stratum samples are all taken at fixed intervals. The continuous line is based on process analyser measurements at short time intervals. For all three cases the lot average  $a_L = 13.193$ , the relative sampling and analysis variance  $s_{r2} = 6.962$  and relative standard deviation  $s_r = 0.20$  (=20%).

# SAMPLING COLUMN

empirical results recommended a new sampling system to be implemented—this was accepted.

**In comparison to the old, the new sampling system annually saved the equivalent of one laboratory technician's salary.**

## Case 2

An undisclosed pulp mill was feeding a paper mill through a pipeline pumping the pulp at about 2% “consistency” (industry term for “solids content”). The total mass of the delivered pulp was estimated based on the measurements with a process analyser installed in the pipeline immediately after the slurry pump at the pulp factory. The receiving paper mill claimed that it could not produce the expected tonnage of paper from the tonnage of pulp they had been charged for by the pulp factory. An expert panel was asked to check and evaluate the measurement system involved. A careful audit, complemented with TOS-compatible experiments, revealed that the consistency measurements were biased, in fact giving up to 10% too high results. The bias was found to originate from two main sources. 1) The process analyser was placed in the wrong location and suffered from a serious increment delimitation error; this is an often-met weakness of process analysers installed on or in pipelines. 2) The other error source was traced to the process analyser calibration. It turned out that the calibration was dependent on the quality of the pulp: softwood and hardwood pulps needed different calibrations. By a determined effort to make the process sampling system fully TOS-compatible, and by updating the analyser calibration models, it was possible to fully eliminate the 10% bias detected.

It is interesting to consider the payback time for the efforts involved to focus on proper TOS in this case. The pulp production rate was about  $100,000 \text{ ton y}^{-1}$ , or  $12 \text{ ton h}^{-1}$ . The contemporary price of pulp could be set as an average of  $\$700 \text{ ton}^{-1}$ , so the value produced per hour was approximately  $\$8400 \text{ h}^{-1}$ . The value of the 10% bias would thus be  $\$840 \text{ h}^{-1}$  ( $\$7 \text{ million y}^{-1}$ ). As the cost of the evaluation study was about  $\$10,000$

**the payback time of the audit and the panel investigations was about 12h.**

It does not have to be expensive to invoke proper TOS competency—it is often possible to get a better quality at lower cost.

## Are our current sampling standards and guides adequate?

In most current standards, the findings of the TOS have often been ignored, or at best only partially recommended. Statistical considerations assume that sampling errors can be estimated using classical statistics which are based on the ubiquitous assumption of random spatial analyte distributions within the sampling targets. **The basic three sampling modes, random, stratified or systematic, are seldom even mentioned as options.** As shown above, when primary samples are taken from large lots like process streams, environmental targets, shipment of raw materials or products, ill-informed or wrong assumptions simply lead to wrong conclusions, and usually too expensive or inefficient solutions. More examples are given below.

## Case 3: Estimation of the concentration genetically modified (GMO) soybeans

In the European Union, the limit of acceptable GMO content in soybeans is 1% (or 1 GMO bean/100 beans). If the content exceeds this limit, the lot must be labelled as containing GMO material. To allow for the sampling and analytical error, in practice 0.09% is used as the effective threshold limit for deciding on labelling the material as containing GMO or not. Theoretically, this seems a simple sampling and analysis problem. GMO soybeans and their natural counterparts are identical with no tendency to segregate. So, theoretically the required sample size can be estimated from considerations assuming a binomial distribution. The reality is **very** different, however.

In References 3–5 experimental analytical data from the KeLDA project were re-analysed, with a special focus on the inherent sampling issues involved. In the KeLDA project, 100 shiploads arriving

at different EU ports were sampled by collecting 100 primary 0.5-kg samples (each containing approximately 3000 beans) using systematic sampling. At the 1% concentration level, the relative standard deviation of the total analytical error ( $S_{TAE}$ ) was found to be 11.4%. For an ideal binomial mixture, conventional statistical calculations showed that the minimum number of 0.5-kg samples to be analysed in order to guarantee that the probability (risk) is less than 5% that the mean 0.09% could be from a lot having mean concentration above 1%—is 10 samples. The official number of samples recommended by many organisations vary between 4 and 12. So far, so good... **if** the conventional assumptions hold up to reality... alas!

A shipload often consists of products from many different *sources* having different GMO concentrations. In such cases the lot can be seriously segregated in the distributional sense w.r.t. domains having different GMO contents, making the assumption of spatial randomness grossly erroneous. Instead of the theoretical 10 samples, the thorough study reported in Reference 4 (lots of statistics in there, but they are not necessary for the present purpose) ended up with a much higher required number of samples needed, 42 to be precise (a famous number, if the reader is fan of Douglas Adams' *Hitchhiker's Guide to the Galaxy*). It is this number of samples which **must** be collected using the *systematic sampling mode* to make a correct decision regarding the labelling issue.

From enclosed stationary lots, such as the cargo hold(s) of grain shipments, or truckloads, railroad cars, silos, storage containers... it is in general impossible to collect representative samples without a TOS intervention. Samples must be taken either during *loading* or during *unloading* of the cargo, i.e. when the cargo lot is in a moving lot configuration on a conveyor belt. Otherwise, the average concentration simply cannot be reliably estimated. References 3–5 tell the full story, the conclusion of which is: conventional statistics based on the assumption of spatial random analyte distributions always runs a significant risk of underestimating the

# SAMPLING COLUMN

number of samples needed to reach a specified quality specification—compared to informed TOS-competent understanding of heterogeneity, spatial heterogeneity in this case. **Proper TOS-competence is a must.**

## Case 4: Sampling for aflatoxins in peanut kernels

Mycotoxins, e.g. aflatoxins and ochratoxins, are poisonous and are also regarded as potent carcinogens. Their contents in foodstuff must, therefore, be carefully monitored and controlled and the levels regarded safety are extremely low, down to  $5\mu\text{g kg}^{-1}$  (ppm), or even lower. But detection and quantification even of these very low concentration levels is usually not a challenge for modern analytical techniques in dedicated analytical laboratories. The real challenge is **how to** provide a *guaranteed representative* analytical aliquot (of the order of *grams* only) from the type of *large* commercial lots used in the international trade of such commodities (of the order of magnitude of *thousands of tons*). Effective sampling ratios are staggering, e.g.  $1:10^6$  to  $1:10^9$ , or even higher. It is *somebody's* responsibility that the overwhelming  $1/10^6$  to  $1/10^9$  mass reduction is scrupulously representative at/over all sampling and sub-sampling stages. It is fair to say, that this setup is not always known, recognised, far less honoured in a proper way, sadly (because this is where the money is lost, big time) with the unavoidable result that nobody (nor any guideline or standard) can guarantee representativity.

Campbell *et al.*<sup>6</sup> carried out an extensive sampling study in connection with analysing peanuts for aflatoxins. It is interesting to study their findings using the principles of TOS: they sampled a lot having an average aflatoxin content  $0.02\text{mg kg}^{-1}$  by taking 21.8 kg primary samples. The average aflatoxin content of individual “mouldy” peanut kernels was  $112\text{mg kg}^{-1}$ . The average mass of one peanut kernel is about 0.6 g. In Reference 6 it was found that the experimental relative standard deviation of the 21.8-kg primary samples  $s_r(\text{exp})$  was  $0.55=55\%$ . This empirical result exceeds the theoretically expected value, however, indicating

that “something” is not right ... A TOS rationale follows below.

## Involving TOS

The mass of aflatoxin in a single mould contaminated kernel:  $m_a=112\text{mg kg}^{-1} \times 0.6 \times 10^{-3}\text{ kg}=0.0672\text{ mg}$ . If the acceptable average aflatoxin level is  $0.02\text{mg kg}^{-1}$ , this result means that just **one** mouldy peanut is enough to contaminate a whole sample of 3.36 kg. On the other hand, if the maximum tolerable level is only  $0.005\text{mg kg}^{-1}$ , one kernel will contaminate a 13.44-kg sample. If the kernels are crushed to 50 mg fragments, average samples containing one contaminated fragment are now 0.28 kg and 1.12 kg at average aflatoxin concentrations  $0.02\text{mg kg}^{-1}$  and  $0.005\text{mg kg}^{-1}$ , respectively. The relative standard deviation of a sample containing one contaminated peanut taken from a random distribution is  $1=100\%$ .

The theoretical relative standard deviation of a 21.8-kg sample from a random mixture is  $s_r=39.3\%$  whereas the experimental value was 55%. The difference between these variance estimates [ $0.55^2-0.393^2=0.148$ , or 38.5% as RSD%] is a strong indication of *spatial segregation*. Such segregation of mycotoxins in large lots is a natural phenomenon, since moulds, which are producing the toxins, tend to grow in localised “pockets” where mould growth conditions are favourable. As an unavoidable consequence, the distribution of contaminated individual nuts within the full lot volume is in reality **far** from random. Because large lots, almost exclusively found in restricted and confined containers, cannot be well mixed (randomised), segregation has a drastic adverse effect on sampling uncertainty at the primary sampling stage—whereas at all later sample preparation stages, when only small masses are handled, it is possible to randomise various sized sub-samples by careful mixing, and here the theoretical values can be used to estimate the uncertainty of the sub-sampling steps involved.

For the ideal case of truly random mixtures, it is easy to estimate the sample size that gives the required relative standard deviation of the lot as a function

of the primary sample size. For the two lot averages used here as examples,  $a_L$  is  $0.02\text{mg kg}^{-1}$  and  $0.005\text{mg kg}^{-1}$ , and targeting to 10% relative standard deviation of the lot mean, the *realistic minimum sample sizes* are:

$$m_s = \frac{(100\%)^2}{(10\%)^2} \cdot 3.36\text{ kg} = \mathbf{336\text{ kg}}$$

$$m_s = \frac{(100\%)^2}{(10\%)^2} \cdot 13.44\text{ kg} = \mathbf{1344\text{ kg}}$$

If the distribution is indeed random, the  $m_s$  can be a composite sample or single increment, the expected RSD of the mean is the same, 10%, independent of the sampling mode. But the situation is radically different if there is indeed segregation, e.g. clustering of the contaminated peanuts. Then the required primary sample size and number will depend on the spatial distribution pattern and this can only be estimated empirically, either by a *variographic experiment* or by involving an ANOVA design, see References 3–6.

The only result that can be estimated from the reported data in the Campbell *et al.* study, is **how many** 21.8-kg samples,  $n_{\text{req}}$ , are needed if random sampling is used. If the target threshold is 10% RSD of the mean at  $a_L=0.02\text{mg kg}^{-1}$ :

$$n_{s(\text{req})} = \frac{s_r^2(\text{exp})}{(10\%)^2} = \frac{(55\%)^2}{(10\%)^2} = 30.3$$

and the total mass of the samples  $30.3 \cdot 21.8\text{ kg} \approx \mathbf{660\text{ kg}}$ .

## Implications for commodity trade a.o.

In international trade agreements regarding foodstuffs, the tight limits set by regulators must be met at the entry port before the cargo materials can be released to the markets. As the examples above show, sampling and sample preparation for analysis are extremely difficult when the unwanted contaminants are present at their usual low, or very low ppm (or even ppb) levels. In the case of the present peanut example, at an average concentration  $5\mu\text{g kg}^{-1}$  in an ideal case (i.e., assuming randomness), the weight of the total number of primary samples should be about 1350 kg if the 10% relative standard deviation is



# SAMPLING COLUMN

the target. In sample preparation, if the secondary samples are each 10 kg and the analytical sample from which the toxins are extracted, are, say, 200 g, the peanuts must be ground to 0.45 mm and 0.09 mg particle sizes corresponding to approximately 0.96 mm and 0.56 mm particle diameters. But these are the results of an ideal case, very rarely found. Segregation makes the theoretical considerations much more complicated.

## *The simple moral from underlying complexities*

The above technical intricacies notwithstanding, it is abundantly clear, that the quality of sensitive foodstuffs must be adequately monitored—and it is equally clear that at the inherent trace and ultra-trace levels of the analytes involved, the primary sampling and sample preparation are extremely difficult operations, but absolutely necessary! If the uncertainties of the analytical results are too high, this means that a high number of shipments containing excess amount of the contaminants may enter the market essentially undetected and, vice versa, shipments containing acceptable material may be stopped—but both types of misclassification are **not** caused by analytical difficulties. The resulting economic losses are **huge**, for each shipment that is wrongly stopped and returned due to “erroneous” analytical results. **The lesson from the somewhat technical story above is clear: primary sampling, and subsequent sub-sampling and sample preparation errors, are very nearly always the real culprits—perpetrators are not to be found in analytical laboratories.**

## What to do?

When decision limits are set, the capability of modern analytical instruments alone cannot be used as the guide for reliability. The capability of the **whole** measurement chain must be evaluated. If it turns out that the proposed decision limit is so low that it cannot be achieved at acceptable costs, even when the best methods of the TOS are applied in designing the sampling and measurement plan, then it must be decided what are the *maximum allowable costs* of the

control measurements. First, then is it possible to set realistic decision limits so that they can be reached with methods optimised to minimise the uncertainty of the full lot-to-aliquot measurement pathway within a given budget which is regarded as acceptable; a more fully developed treatment of these interlinked technical and economic factors can be found in References 1 and 2.

## References

1. P. Minkkinen, “Cost-effective estimation and monitoring of the uncertainty of chemical measurements”, *Proceedings of the Ninth World Conference on Sampling and Blending*, Beijing, China, pp. 672–685 (2019).
2. P. Minkkinen, “Practical applications of sampling theory”, *Chemometr. Intell. Lab. Syst.* **74**, 85–94 (2004). <https://doi.org/10.1016/j.chemo-lab.2004.03.013>
3. K.H. Esbensen, C. Paoletti and P. Minkkinen, “Representative sampling of large kernel lots I. Application to soybean sampling for GMO control”, *Trends Anal. Chem.* **32**, 154–164 (2012). <https://doi.org/10.1016/j.trac.2011.09.008>
4. P. Minkkinen, K.H. Esbensen and C. Paoletti, “Representative sampling of large kernel lots II. Theory of sampling and variographic analysis”, *Trends Anal. Chem.* **32**, 165–177 (2012). <https://doi.org/10.1016/j.trac.2011.12.001>
5. K.H. Esbensen, C. Paoletti and P. Minkkinen, “Representative sampling of large kernel lots III. General considerations on sampling heterogeneous foods”, *Trends Anal. Chem.* **32**, 178–184 (2012). <https://doi.org/10.1016/j.trac.2011.12.002>
6. A.D. Campbell, T.B. Whitaker, A.E. Pohland, J.W. Dickens and D.L. Park, “Sampling, sample preparation, and sampling plans for foodstuffs for mycotoxin analysis”, *Pure Appl. Chem.* **58**(2), 305–314 (1986). <https://doi.org/10.1351/pac198658020305>

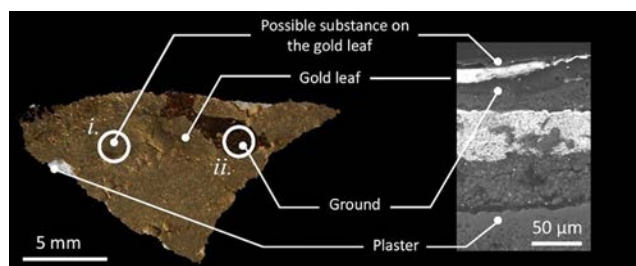


Pentti Minkkinen received his MSc (eng.) from Helsinki University of Technology in 1969. He then worked as an Associate Expert in two UN Development Program mineral exploration projects in Turkey and in Egypt before completing his graduate studies at Helsinki. In 1976, he started as Associate Professor (Inorganic and Analytical Chemistry) at a newly founded University, Lappeenranta University of Technology, from which retired as full professor by the end of 2007, after a 40+ year tenure. Here he started teaching the theory and applications of sampling in 1978, soon also chemometrics, as an important part of process analytical chemistry. He has been lecturing sampling at undergraduate and graduate courses at several universities, at professional continuing education courses, and at numerous conferences and at industry courses. After retirement, he worked three periods as Visiting Professor at Aalborg University, Campus Esbjerg, Denmark in Prof. Esbensen's research group (2007, 2008 and 2009). In 2012, he founded Sirpeka Oy from which he offers consulting services on sampling, analytical quality control and in chemometrics. At his old university, now amalgamated and named Lappeenranta Lahti University of Technology (LUT), he continues his scientific career as Professor emeritus. Prof. Minkkinen was the founding chairman of the continuing biannual conference series, Scandinavian Symposium of Chemometrics. He was also co-chairman for the first World Conference on Sampling and Blending. He is the founding chairman of the Discussion Group of Chemometrics in the Finnish Chemical Society. He has published ~80 papers on chemometrics and sampling in refereed journals and conference proceedings; his invited and contributed lectures in various conferences and symposia contributions is close to 200. He has received three international awards: The Kowalski Prize in Chemometrics (2002), the Herman Wold Gold Medal in Chemometrics (2007) and the Pierre Gy Sampling Gold Medal (2007); he is the only recipient of all three distinguished awards.

<https://orcid.org/0000-0002-0918-0234>

[Pentti.Minkkinen@lut.fi](mailto:Pentti.Minkkinen@lut.fi); [pentti.minkkinen@sirpeka.fi](mailto:pentti.minkkinen@sirpeka.fi)

# APPLICATIONS

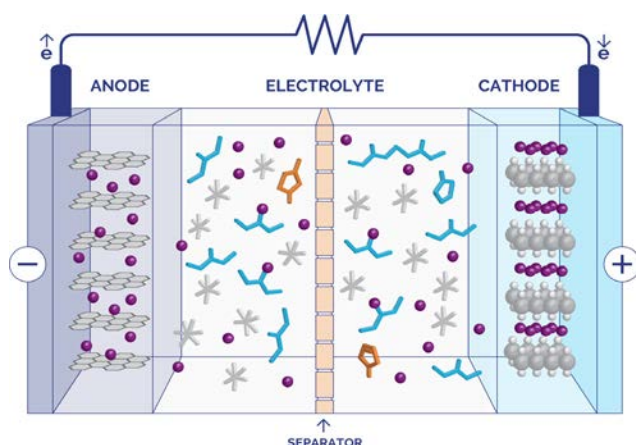


## SurveyIR and cultural heritage

Gildings are commonly found highlighting details of ornamental or iconographic value such as halos. They are documented on a variety of artefacts including statues, stuccos, wall paintings as well as paintings on canvas, wood panels and illuminated manuscripts. Gildings consist of  $\mu\text{m}$ -thick leaves of different metals (e.g., gold, silver, metal alloys) applied to the substrate by a thin adhesive ground layer. Depending on the gilding technique, the composition of the ground may vary from mainly inorganic to mainly organic, and may be coloured with pigments (e.g., lead pigments, ochres). Over time, such materials undergo unavoidable decay due to oxidation of metal leaves and loss of adhesive properties of the ground, hence conservation treatments can be applied to restore the mechanical–optical properties of the original materials, or to protect the gilding from further interaction with the environment. This note investigates the gilding technique.

*Specac*

► [Download Application Note](#)



## Observing and monitoring electrolyte decomposition by benchtop NMR

Lithium-ion (Li-ion) batteries have become ubiquitous in daily life, providing power for a diverse range of applications, ranging from mobile phones, computers, power tools and medical devices, to the power storage behind emerging green technologies such as electric cars and solar panels, among many others. As our usage of lithium-ion batteries has grown, so has the need to optimise their performance and to ensure reliability over a long lifetime. Benchtop NMR has many potential lithium-ion

battery QA/QC applications, as the well-resolved spectra of the small organic molecules and ions are ideally suited for quick, convenient analysis.

*Oxford Instruments*

► [Download Application Note](#)



## ATR analysis of the relative concentrations of active pharmaceutical ingredients

Infrared quantitative analyses are an everyday requirement in the analytical laboratory. While liquid solutions are commonly analysed, mixtures of powdered components also exist and often require quantitative analysis without dissolution into a solvent. The traditional infrared analysis method for powdered samples is the collection of a KBr pellet spectrum of an aliquot of the powdered sample. However, preparation of KBr pellets requires skill and precise weighing of every component for each sample. The Golden Gate™ single reflection diamond ATR provides a simple and effective alternative, suitable for the infrared analysis of powders. ATR analysis is less complicated than using KBr pellets, is fast and only requires a very small amount of the sample.

*Specac*

► [Download Application Note](#)



## Compact mass spectrometers: controlled substance detection

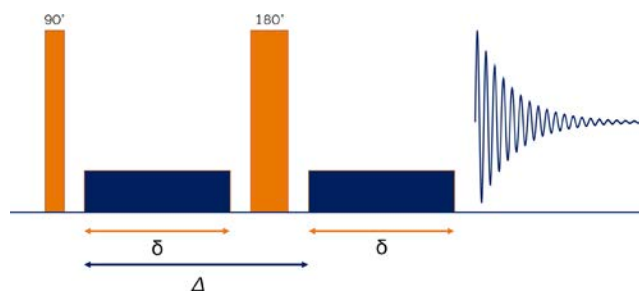
Controlled substance analysis is changing with compact mass spectrometers. BaySpec's Portability™ and Continuity™ mass spectrometer series offers a new way to approach controlled substance analysis. No longer do the samples need to go to the lab, but now the lab can go to the samples. With the growing

# APPLICATIONS

risk of exposure to fentanyl and its analogues, there is a need in law enforcement and decontamination services for analysis that is fast, dependable and can be operated with little to no training.

*Bayspec*

► [Download Application Note](#)



Pulse sequence diagram of the PFGSE experiment. Rectangular hard pulses are shown in orange, and pulsed field gradients are in blue.  $\Delta$  is the diffusion delay, while  $\delta$  denotes the duration of the gradient pulses.

## Measuring diffusion at different temperatures using NMR with pulsed field gradients

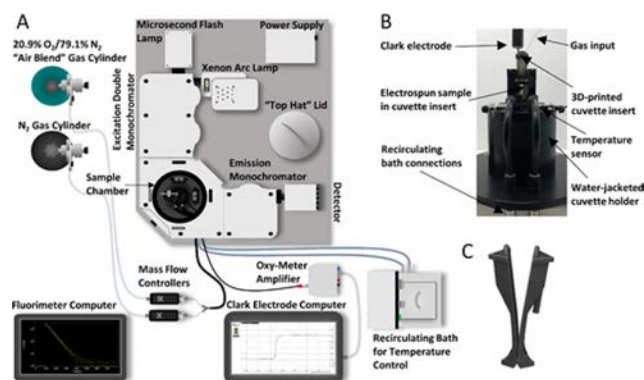
Benchtop NMR instruments have brought convenient, fast sample analysis into many research and industrial chemistry laboratories, but while early applications largely focused on basic 1D  $^1\text{H}$  NMR spectra, modern spectrometers offer many additional capabilities. One important example is the ability to measure self-diffusion coefficients, which can be used to extract physical information about a sample.

A benchtop NMR spectrometer equipped with Pulsed Field Gradient (PFG) hardware can use techniques such as the Pulsed Field Gradient Spin Echo experiment to determine diffusion coefficients of sample components by measuring change in NMR signal as a function of the PFG strength. Adding variable

temperature capability allows the study of sample thermal behaviour under a range of expected working conditions. Finally, a single broadband benchtop NMR system can analyse the behaviour of multiple components in the given sample, a crucial aspect in understanding physical and chemical properties.

*Oxford Instruments*

► [Download Application Note](#)



## Time-resolved spectroscopy of phosphorescent oxygen sensors in a relevant *in vitro* environment for biomedical applications

This note describes how candidate materials for optical *in vivo* oxygen sensing were evaluated in a relevant *in vitro* environment through careful control and monitoring of the solution temperature and dissolved oxygen concentration. Sensor performance was characterised via changes in phosphorescence lifetime; these long lifetime materials were assessed using Multi-Channel Scaling (MCS) and a microsecond flash lamp.

*Edinburgh Instruments*

► [Download Application Note](#)



# PRODUCT FOCUS

## Product Focus on Luminescence

Edinburgh  
Instruments

Tel: 01506425300  
[sales@edinst.com](mailto:sales@edinst.com)  
<https://www.edinst.com/>



**PRODUCT:** FLS1000 Photoluminescence Spectrometer

**APPLICATIONS:** Life sciences • Forensic science & security • Environmental services • Material sciences • Geology

**KEY FEATURES:** Industry leading sensitivity specification <35,000:1 (SQRT Method) • Unrivalled spectral coverage from the deep UV to the MIR, 185 nm up to 5500 nm • Modular construction • Unmatched monochromator performance with "plug and play" triple-grating turrets, integrated filter wheel, 325 mm focal length



**PRODUCT:** FS5 Spectrofluorometer

**APPLICATIONS:** Bioscience • Materials research • Analytical science • Nano-technology • Environmental science

**KEY FEATURES:** Live signal monitoring • Load/save measurement settings • Batch measurements • Correction and higher order removal • Plug-and-play sample holders/accessories



**PRODUCT:** LifeSpec II Lifetime Spectrometer

**APPLICATIONS:** Materials science • Analytical research • Environmental science • Life sciences • BioScience

**KEY FEATURES:** Fastest TCSPC instrument on the market due to zero temporal dispersion • Subtractive double-monochromators result in zero temporal dispersion • 5 ps–50  $\mu$ s lifetimes (detector and laser dependent) • Extended NIR range • Multi-laser integration



**PRODUCT:** Mini-tau Lifetime Spectrometer

**APPLICATIONS:** Research • Q.A. • Teaching

**KEY FEATURES:** Sample chamber with source and detector • PC and TCSPC plug-in board • Sub nano-second pulsed LED or picosecond diode laser (with choice of wavelength) • Integrated electronics with repetition rate up to 20 MHz • Ultra-fast, blue or red sensitive single photon counting PMT



Shimadzu  
Europa GmbH

Tel: +49-203-76870  
[shimadzu@shimadzu.eu](mailto:shimadzu@shimadzu.eu)  
[www.shimadzu.eu](http://www.shimadzu.eu)



**PRODUCT:** RF-6000

**APPLICATIONS:** Environmental; Food • Life science • Pharma • Chemicals

**KEY FEATURES:** Outstanding sensitivity • High-speed 3D measurement • Easy operation • Trace amounts analyses • "Best in class" signal to noise ratio



Starna  
Scientific Ltd

Tel: + 44 (0) 20 8500 1264  
[sales@starna.com](mailto:sales@starna.com)  
<https://www.starna.com>



**PRODUCT:** Certified Fluorescent Reference Materials

**APPLICATIONS:** Instrumental verification and monitoring • Spectral correction • Detector linearity validation • Process quality control • Medical diagnostic compliance

**KEY FEATURES:** Highly stable and solid-state • Certified emission spectra • Calibrated intensity series • Customisable formats and intensity levels for OEM • NIST Tracible & UKAS accredited



TOPTICA  
Photonics AG

Tel: +498985837-0  
[info@toptica.com](mailto:info@toptica.com)  
<https://www.toptica.com>



**PRODUCT:** FemtoFiber ultra 920 – Femtosecond Fibre Laser for 2-Photon Microscopy and Neuroscience

**APPLICATIONS:** 2P-Microscopy • Neuroscience • SHG microscopy • Advanced microscopy techniques

**KEY FEATURES:** Centre wavelength 920 nm • Pulse duration <100 fs • Average output power >1.5 W • Repetition rate 80 MHz



Wasatch  
Photonics

Tel: +1 919-544-7785  
[info@wasatchphotonics.com](mailto:info@wasatchphotonics.com)  
[www.wasatchphotonics.com](http://www.wasatchphotonics.com)



**PRODUCT:** WP 785 ER Raman Spectroscopy Research Bundle

**APPLICATIONS:** Spectroscopy • Raman

**KEY FEATURES:** High level of measurement sensitivity • 100–3600  $\text{cm}^{-1}$  spectral range • Integrated 785 nm integrated laser • High NA (f/1.3) optical bench with patented high-efficiency transmission grating • User-configurable Raman probe with replaceable optics



# FEATURED PRODUCT

## Compact, affordable Raman spectrometer



Ocean Insight has introduced the Ocean HDX Raman spectrometer, a compact, high-performance spectrometer for 785 nm Raman excitation applications. The spectrometer has a spectral range of 150–3400  $\text{cm}^{-1}$ , is available with a 25  $\mu\text{m}$  or 50  $\mu\text{m}$  entrance slit and can be combined with a 785 nm laser, general-purpose probe and sample holder to create a modular Raman system. Applications range from authentication of spirits and analysis of cannabinoids, to identification of polymers and characterisation of pharmaceutical ingredients. The Ocean HDX Raman is available in high-throughput and high-resolution models. The Raman Wizard in the OceanView spectroscopy software simplifies startup. The Ocean HDX Raman is suitable for university teaching and research labs, and budget-limited start-ups. In addition, the Ocean HDX Raman can be integrated into other products, offering the advantages of small size and light weight, plus thermal stability and Ethernet connectivity.

*Ocean Insight*

► <https://link.spectroscopyeurope.com/689-P1-2021>

# NEW PRODUCTS

## INFRARED

### Greenhouse gas analyser

The Gasera One GHG greenhouse gas analyser is based on the Gasera One platform combining cantilever-enhanced photo-acoustic detection technology with a quantum cascade laser source operating at a mid-IR fundamental spectral absorption line of the target greenhouse gases: methane ( $\text{CH}_4$ ) and nitrous oxide ( $\text{N}_2\text{O}$ ). This provides ppb sensitivity to measure ambient background levels of methane and nitrous oxide. It also gives an exceptionally high level of stability with a recommended recalibration period of 12 months. The analyser can measure  $\text{CH}_4$  and  $\text{N}_2\text{O}$  simultaneously, its short optical path provides a wide dynamic range and only a few mL of sample are required.

Gasera

► <https://link.spectroscopyeurope.com/5395-P1-2021>



### Testing optical fingerprint sensors

Instrument Systems has developed a modular IR test solution that meets the requirements of optical under-display fingerprint sensors with wavelengths above 1100 nm. In smartphones, under-display fingerprint scanning is widely used to unlock a device comfortably and safely. The light output used for this application was previously at a wavelength of around 940 nm. Unfortunately, at this specific wavelength burn-in phenomena occur in OLED displays. A solution for this disadvantage is to use radiation at 1380 nm. As the application stays the same for the user, the shift from lower to higher wavelengths in the NIR requires other high-resolution and calibrated test equipment for the precise measurement of radiometric quantities, pulse measurement in the  $\mu\text{s}$  range and temperature control.

The core of the system is the model IR1 spectroradiometer, which is optimised for wavelength measurement in the near infrared range. With a cooled InGaAs line sensor, the instrument has a wavelength range from 780 nm to 1650 nm and features thermoelectric cooling of the sensors down to a temperature of  $-10^\circ\text{C}$ . The high-gain option enables the sensitivity range to be significantly extended to include low power applications. A high-resolution model with a wavelength range from 1300 nm to 1440 nm additionally enables detailed investigation of narrow-band radiation sources with an optical resolution  $<1\text{ nm}$ .

Instrument Systems

► <https://link.spectroscopyeurope.com/2184-P1-2021>



## ION MOBILITY

### SLIM-based ion mobility system

MOBILion Systems has launched its first commercial High-Resolution Ion Mobility (HRIM) product, MOBIE, which is aimed at biopharmaceutical drug development and quality monitoring. The technology behind MOBIE is the SLIM (Structures for Lossless Ion Manipulation) technology originally invented by Dr



# NEW PRODUCTS



Richard D. Smith at Pacific Northwest National Laboratory. It can separate and identify molecular structures that can either be too time-consuming or even impossible to detect with established methods such as liquid chromatography (LC).

In 2018, MOBILion announced its partnership with Agilent Technologies to integrate its first HRIM system with Agilent's 6500 line of Q-TOF mass spectrometers and earlier this year, MOBILion announced that it had joined forces with Protein Metrics to integrate with the BYOS biopharma software suite, providing a full workflow solution including data processing.

*MOBILion Systems*

► <https://link.spectroscopyeurope.com/5657-P1-2021>

## LUMINESCENCE

### PicoQuant improves the MultiHarp 150's temporal resolution

PicoQuant is releasing a free firmware update for several models of its MultiHarp 150 high-throughput multichannel event timers. A major feature of this update is the improvement of the temporal resolution from 10 ps to 5 ps for the MultiHarp 150 4P, 8P and 16P, without affecting other parameters like the data throughput or the system's dead time. Another new feature the update provides is a programmable input hysteresis for noise suppression in difficult environments. These MultiHarp 150 models are suitable as TCSPC electronics for fast and precise fluorescence lifetime imaging (rapidFLIM) and high throughput multichannel photon correlation.

*PicoQuant*

► <https://link.spectroscopyeurope.com/1096-P2-2021>



## MASS SPECTROMETRY

### timsTOF trueSCP

The timsTOF trueSCP is the culmination of Bruker's collaboration with the laboratory of Professor Matthias Mann at the Max Planck Institute of Biochemistry in Martinsried, Germany, and with Evosep on new Whisper methods at ultra-low flow rates of  $\sim 100 \text{ nL min}^{-1}$ . The timsTOF trueSCP achieves five times higher ion transmission for data-independent (dia)-PASEF or parallel reaction monitoring (prm)-PASEF methods. The dia-PASEF2 method has demonstrated true, unbiased 4D-proteomics from single cells with quantitation of  $\sim 1500$  proteins/cell, in hundreds of isolated single cells *ex situ*, in combination with the Evosep One LC with Whisper. The timsTOF trueSCP is a dedicated ultra-high sensitivity instrument for unbiased single cell proteomics, after laser capture microdissection of one or a few cells, as well as for ultra-sensitive neoantigen discovery in immunopeptidomics in the field of immuno-oncology research. With the timsTOF trueSCP, a system is now available to expand the single-cell biology horizons beyond genomics and transcriptomics to unbiased, quantitative 4D-proteomics. Quantitative biology can now be



# NEW PRODUCTS

done also with unbiased single cell proteomics, as cells at different stages in the growth cycle have a protein core with sufficient copy numbers to observe statistically relevant changes in abundance, when compared to sparse mRNA copy numbers.

*Bruker*

► <https://link.spectroscopyeurope.com/2428-P1-2021>

## Next-generation timsTOF Pro 2

The timsTOF Pro 2 is a new proteomics workhorse for robust, unbiased, deep and quantitative 4D-proteomics and 4D-epiproteomics for plasma, tissue samples and from cell cultures. Further design advances combined with enhanced dda-PASEF, dia-PASEF and prm-PASEF methods deliver industry-leading performance, with unparalleled robustness and throughput. The timsTOF Pro 2 allows the detection of >6000 proteins and >60,000 peptides by dda-PASEF with 60 min gradients on 200 ng of digest. It also has new high sensitivity methods that enable very good proteome coverage with 10× less digest, down to 20 ng, for >3500 protein groups and >25,000 unique peptides using a 30 min gradient. dia-PASEF workflows on timsTOF Pro 2 include an improved interface for designing experiments, and can now identify ~8000 protein groups and 70,000 peptides in 60 min on 200 ng of digests.

*Bruker*

► <https://link.spectroscopyeurope.com/2428-P2-2021>



## New PaSER capabilities

The mass spectrometry search platform, PaSER, now has a MOMA (mobility offset mass aligned) viewer to characterise co-eluting isomeric or isobaric ions by large-scale CCS. The GPU-based search has been extended into immunoproteomics. Working with Professor Tony Purcell and Bioinformatics Solutions Inc., the ability to perform real-time *de novo* sequence assignment delivers new capabilities for novel neoantigen discovery. PaSER 2022 incorporates a new CCS-enabled database search algorithm, called TIMScore™, developed together with Professor John Yates, and driven by machine learning. TIMScore becomes the first fundamentally CCS-enabled database search algorithm, increasing the number of protein and peptides identified, while maintaining FDR control and real-time search speeds.

*Bruker*

► <https://link.spectroscopyeurope.com/2428-P3-2021>



## SCIEX presents new accurate mass instrument

SCIEX has introduced the ZenoTOF 7600 system, a new accurate mass LC-MS/MS instrument. It includes the proprietary Zeno trap and electron activated dissociation (EAD) fragmentation for the first time in a commercial instrument. Zeno trap pulsing overcomes the traditional duty cycle challenges of orthogonal TOF technology, delivering up to 20× the sensitivity and enabling the routine detection of important low-abundant molecules. In combination, tuneable EAD fragmentation ensures novel



# NEW PRODUCTS

structural information can be extracted and quantified from diverse compound types. Compared to previous systems, the ZenoTOF 7600 system can quantify up to 40% more proteins and analyse samples 5× faster for large biobank studies. In addition, EAD fragmentation brings new capabilities to understand how the proteins are post-translationally modified. The ZenoTOF 7600 can fully characterise an individual lipid from a single spectrum using EAD fragmentation.

SCIEX

► <https://link.spectroscopyeurope.com/5073-P1-2021>

## SCIEX OS introduces OneOmics suite and Molecule Profiler app

SCIEX has introduced the OneOmics suite for big data, multi-omics research through collaborative cloud computing on SCIEX Cloud. OneOmics suite enables life science researchers to process large-scale proteomics and metabolomics data sets up to 10× faster than desktop computing. Data are securely stored in the SCIEX Cloud, allowing researchers to process their data from anywhere, anytime and collaborate globally.

The Molecule Profiler enables biotransformations and impurities to be identified and quantified across a wide range of molecular classes, including therapeutic oligonucleotides, small molecule drugs, peptide therapeutics and antibody-drug conjugates.

SCIEX

► <https://link.spectroscopyeurope.com/5073-P2-2021>



## Waters introduces the SARS-CoV-2 LC-MS kit

Waters has introduced a new research use only LC-MS, the SARS-CoV-2 LC-MS Kit, which uses an orthogonal analytical method that directly detects and quantifies SARS-CoV-2 Nucleocapsid (NCAP) peptides that initial studies have shown to yield highly accurate, quantitative results. Waters developed the kit in support of a coalition of academic, commercial and government research scientists. This coalition worked to develop an alternative test method on LC-MS platforms in support of the United Kingdom's National Health Service (NHS) Test & Trace programme. Their goal was to create a complementary, high-throughput screening method that would also use different reagents to help relieve strain on the PCR reagent supply chain.

Waters

► <https://link.spectroscopyeurope.com/103-P2-2021>

## New Waters Multi Reflecting Time-of-Flight platform

Waters has introduced the Waters™ SELECT SERIES™ MRT, a high-resolution mass spectrometer that combines Multi Reflecting Time-of-Flight (MRT) technology with enhanced DESI and new MALDI imaging sources. The SELECT SERIES MRT platform is the basis for the next generation of Waters' high-resolution mass spectrometers. It is capable of attaining 200,000 Full Width Half



# NEW PRODUCTS

Maximum (FWHM) resolution and part-per-billion mass accuracy independent of scan speed. The MRT technology features an extended flight path of almost 50 m to give a clearer picture of structural information, including fine isotope structure.

The first application of the SELECT SERIES MRT is for MS imaging using DESI and MALDI ionisation. DESI is a direct-from-sample, soft ionisation technique performed under ambient environmental conditions, requiring no prior sample preparation. It provides imaging information about the biochemical distribution of small molecule drugs, lipids and naturally occurring metabolites within a slice of tissue or on other sample surfaces. The DESI XS source has a new high-performance sprayer and a heated transfer line.

The SELECT SERIES MRT is also available with a newly designed MALDI source. MALDI is an ideal complementary technique for the imaging of biological molecules such as peptides and can visualise tissue sections at spatial resolutions of less than 10  $\mu\text{m}$ .

*Waters*

► <https://link.spectroscopyeurope.com/103-P3-2021>



## New Orbitrap-based mass spectrometer

The Thermo Scientific Orbitrap IQ-X Tribrid mass spectrometer has been designed for small-molecule structural elucidation of metabolites and unknown compounds. The instrument utilises Thermo Scientific AcquireX workflows for increased sample throughput and ease-of-use. It provides improved fragmentation for small-molecule analysis with options to add to the platform's experimental flexibility. An ultraviolet photodissociation option provides insights on the lipid double-bond localisation, site-specific glucuronidation and complementary fragmentation for structure assignment while the 1,000,000 resolution option improves unknown analysis and fine isotope detection.

*Thermo Fisher Scientific*

► <https://link.spectroscopyeurope.com/106-P4-2021>



## New differential ion mobility interface

The Thermo Scientific FAIMS Pro Duo interface enhances signal-to-noise ratios and expands sample coverage, allowing users to explore complex samples with reduced matrix interference. Additionally, optimal performance across a wide range of chromatographic flow rates (100 nLmin<sup>-1</sup> to 1 mLmin<sup>-1</sup>) has benefits in areas such as proteome coverage, quantitative analysis, and more recently, glycoproteomics, single-cell proteomics and structural biology. The FAIMS Pro Duo interface easily integrates with Thermo Fisher's mass spectrometers, including the Thermo Scientific Orbitrap Tribrid, Thermo Scientific Orbitrap Exploris, Thermo Scientific TSQ Altis and Thermo Scientific TSQ Quantis.

*Thermo Fisher Scientific*

► <https://link.spectroscopyeurope.com/106-P5-2021>



# NEW PRODUCTS



## Mass spectrometer for the semiconductor industry

Atonarp has announced the launch of Aston, an *in situ* mass spectrometer with an integrated plasma ionisation source for semiconductor metrology. Aston has been built for semiconductor production, and can replace multiple legacy tools and provide control across a number of applications, including lithography, dielectric and conductive etch and deposition, chamber clean, chamber matching, and abatement. Endpoint detection (EPD) is the most efficient way to run a semiconductor tool and FAB. EPD has not been able to be deployed in many process steps because the required *in situ* sensor would not survive the harsh process or chamber cleaning chemicals, or would alternatively suffer clogging from condensate deposits. FABs have had to use a fixed time to ensure that a process was complete. Aston optimises production by detecting exactly when a process has finished, including chamber cleaning, which can reduce the required clean-time by up to 80%. Aston is resistant to corrosive gases and gaseous contaminant condensates. It has independent dual ionisation sources, a classic electron impact ionisation source and a filament-less plasma ioniser, that work reliably in the harsh conditions encountered in semiconductor production. This enables Aston to be used in environments where traditional electron ionisers would corrode and fail very rapidly.

Aston offers an interval between service events that is up to 100× longer than legacy mass analysers. It includes self-cleaning capability that eliminates the build-up resulting from the deposition of condensates present in certain processes. Since Aston generates its own plasma, it works with or without process plasma present. This provides an advantage over optical emission spectroscopy techniques, which require a plasma source to operate, making Aston ideal for ALD and certain metal deposition processes that may use a weak, pulsed or no plasma for processing.

Atonarp

► <https://link.spectroscopyeurope.com/6476-P1-2021>

## RAMAN

### Process development Raman

B&W Tek have introduced the PTRam, a 19" rack-mountable Raman analyser designed for product and process development in the lab or in pilot plant settings. It uses a 785nm laser producing 340mW at the sample at full power. Power is adjustable by software in 1% increments. It has a spectral range of 150–2800  $\text{cm}^{-1}$  with resolution of  $<6.0 \text{ cm}^{-1}$  at 912nm. It is supplied with a lab-grade fibre optic probe, an ASTM polystyrene validation standard and Vision software. Vision acquires data and allows the development of methods; it also runs the self-calibration and system monitoring to ensure data validity. The system can also be operated with the BWSpec software, providing full



# NEW PRODUCTS

acquisition control, continuous measurements, additional data processing capabilities and viewing options.

*B&W Tek*

► <https://link.spectroscopyeurope.com/1783-P2-2021>

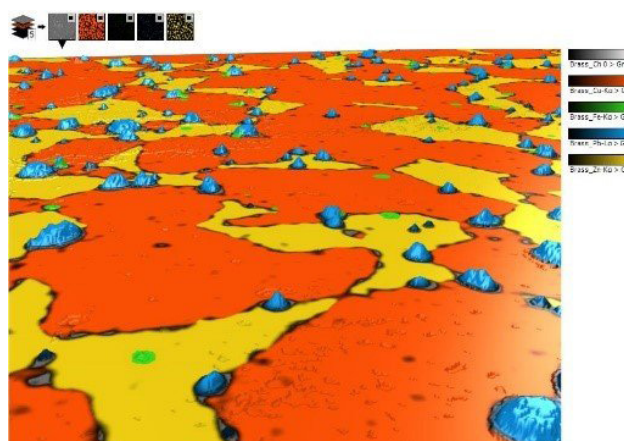
## SOFTWARE

### Image analysis software now has spectroscopy support

Digital Surf has released Mountains® 9, a major new version of the company's software platform for image and surface analysis in microscopy and metrology. Version 9 also includes a new branch of Mountains® software, MountainsSpectral®, for correlation and spectroscopy analysis. There are also three new modules version 9. Shell Topography provides surface texture analysis to freeform surfaces (shells). Chemical cubes is for the visualisation and analysis of multi-channel cubes of compositional data. IV Spectroscopy provides SPM investigation of electrical surface properties including 3D visualisation of datacubes and individual IV curve analysis (including CITS). New data types supported include point cloud data, allowing users to visualise and analyse data from 3D scanners etc. and multi-channel cubes for studying the composition of materials in full 3D. Data from different sources (SEM, AFM, EDS/EDX etc.) can be brought together to form single multi-layer datasets. A new colour mixing tool allows users to choose which layers of data they wish to bring to the fore. So, scanning electron microscope users can generate spectacular 3D renderings associating EDS/EDX maps or other spectral/compositional data with SEM images or reconstructed topography when available.

*Digital Surf*

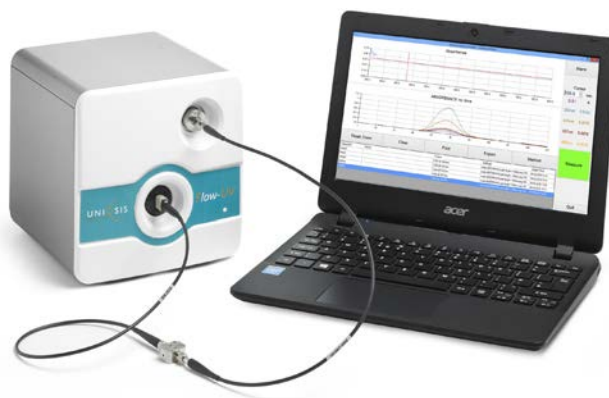
► <https://link.spectroscopyeurope.com/6436-P1-2021>



## UV/VIS

### Universal UV-Visible accessory for flow chemistry

The Flow-UV™ UV-Visible spectrophotometric detector from Uniqsis has been designed for use with almost any commercial flow chemistry system and fits into even crowded fume cupboards. The Flow-UV™ is an affordable solid state, full spectrum UV-Visible spectrophotometer that may be used for batch analysis as well as continuous flow applications. The standard flow cell has a pathlength of 1 mm. Other pathlengths are available and the instrument is compatible with a wide range of Z-configuration flow cells that may be more suitable for high-throughput process applications. At room temperature, the standard flow cell can withstand pressures of up to 35 bar and may be positioned anywhere in the flow path. Dispersion and steady state may be monitored at five user-selected wavelengths in real time to assist with product collection and quality control. In conjunction with Uniqsis FlowControl II system control software,





# NEW PRODUCTS

the Flow-UV is used to automate reaction product collection in either "Collect All", "Steady State" or "Balanced" collection modes. The spectrometer control software allows saved methods to be recalled and will automatically record a background spectrum at the start of each experiment.

*Uniqsis*

► <https://link.spectroscopyeurope.com/6413-P1-2021>

## X-RAY

### New Epsilon 1 ED-XRF spectrometer

Malvern Panalytical has launched the Epsilon 1, which is pre-calibrated in the factory and is an out-of-the-box solution for the analysis of low sulphur content in fuels. The Epsilon 1 does not require helium, which makes it easy to operate with low cost per analysis, and complies with ISO 13032 and similar test methods. The Epsilon 1 is a fully integrated energy dispersive XRF analyser consisting of a spectrometer, built-in computer and analysis software. It has a well-designed optical path, a wide range of excitation capabilities ranging from 7kV to 30kV for light and heavier elements and a sensitive SDD detector system. Epsilon 1 can be used for the characterisation and analysis of any type of sample in industry segments such as cement, cosmetics, environmental, food, forensics, metals and coatings, mining and minerals, nanomaterials, petrochemicals, pharmaceuticals, polymers and RoHS-2.

*Malvern Panalytical*

► <https://link.spectroscopyeurope.com/690-P2-2021>



## Conferences 2021

1–6 August, Freiberg (Sachsen), Germany. **Geoanalysis 2021**. ✉ [geoanalysis2021@hzdr.de](mailto:geoanalysis2021@hzdr.de), 🌐 <https://geoanalysis2021.de>

23–26 August, Online. **11<sup>th</sup> International Conference on Advanced Vibrational Spectroscopy (ICAVS 11)**. ✉ [icavs2021@targi.krakow.pl](mailto:icavs2021@targi.krakow.pl), 🌐 <http://www.icavs.org/gb/>

1–3 September 2021, Online. **15<sup>th</sup> International Conference on Mid-Infrared Optoelectronic Materials and Devices (MIOMD)**. 🌐 <https://www.surrey.ac.uk/miomd2021>

6–9 September 2021, Aalborg, Denmark. **17<sup>th</sup> Scandinavian Symposium on Chemometrics**. 🌐 <https://www.ssc17.org>

8–9 September, Sheffield, UK. 🌐 **41<sup>st</sup> BMSS Annual Meeting**. <https://www.bmss.org.uk/41st-bmss-annual-meeting/>

20–24 September, Online. **11<sup>th</sup> International Workshop on Infrared Microscopy and Spectroscopy with Accelerator Based Sources**. ✉ [WIRMS2021@spring8.or.jp](mailto:WIRMS2021@spring8.or.jp), 🌐 <http://www.spring8.or.jp/en/WIRMS2021/>

29 September–1 October, Berlin, Germany. **26<sup>th</sup> International Workshop on Single Molecule Spectroscopy and Super-Resolution Microscopy**. ✉ [workshop@picoquant.com](mailto:workshop@picoquant.com), 🌐 <http://www.single-molecules.org>

30 September–1 October, Online and Porto, Portugal. **SensorFINT Workshop**. 🌐 <https://www.sensorfint.eu/events/first-sensorfint-international-workshop-smart-spectral-sensors-for-agri-food-quality-and-process-control/>

18–21 October, Online. **20<sup>th</sup> Biennial Meeting of the International Council for NIR Spectroscopy (ICNIRS2021)**. ✉ [nir2021@nir2021.com](mailto:nir2021@nir2021.com), 🌐 <https://www.nir2021.com>

31 October–4 November, Philadelphia, PA, United States. **69<sup>th</sup> ASMS Conference**. 🌐 <https://www.asms.org/conferences/annual-conference/future-annual-conferences>

16–20 December, Honolulu, Hawaii, United States. **The International Chemical Congress of Pacific Basin Societies 2021**. 🌐 <https://pacificchem.org>

## 2022

28 February–4 March, Moscow, Russia. **13<sup>th</sup> Winter Symposium on Chemometrics (WSC-13)**. ✉ [wsc13@chemometrics.ru](mailto:wsc13@chemometrics.ru), 🌐 <https://wsc.chemometrics.ru>

31 May–2 June, Kristiansand, Norway. **10<sup>th</sup> World Conference on Sampling and Blending (WCSB10)**. ✉ [contact@wcsb10.com](mailto:contact@wcsb10.com), 🌐 <https://wcsb10.com>

5–9 June, Minneapolis, Minnesota, United States. **70<sup>th</sup> ASMS Conference**. 🌐 <https://www.asms.org/conferences/annual-conference/future-annual-conferences>

4–7 July, Skagen, Denmark. **International Association for Spectral Imaging (IASIM)**. ✉ [2020@iasim.net](mailto:2020@iasim.net), 🌐 <https://2020.iasim.net>

5–9 September, Heraklion, Crete, Greece. **NanoBio Conference 2021**. ✉ [info@nanobioconf.com](mailto:info@nanobioconf.com), 🌐 <https://nanobioconf.com>

## 2023

29 January–3 February, Ljubljana, Slovenia. **2023 European Winter Conference on Plasma Spectrochemistry**. Johannes T. VanElteren, 🌐 <http://www.ewcps2021.ki.si>

## Exhibitions 2021

23–25 September, Hyderabad, India. **analytica Anacon India and India Lab Expo**. ✉ [sheron.david@mm-india.in](mailto:sheron.david@mm-india.in), 🌐 <https://www.analyticaindia.com/>

30 November–2 December, São Paulo, Brazil. **Analítica Latin America**. 🌐 <https://www.analiticanet.com.br/>

3–4 November, Birmingham, UK. Lab Innovations. 🌐 <https://www.lab-innovations.com>

3–4 November, Madrid, Spain. **Farmaforum 2021**. 🌐 <https://farmaforum.es/>

15–17 November, Dubai, United Arab Emirates. **ARABLAB 2021**. ✉ [info@arablab.com](mailto:info@arablab.com), 🌐 <https://www.arablab.com>

## 2022

5–9 March, Atlanta, GA, USA. **Pittcon 2022**. 🌐 <https://www.pittcon.org>

4–8 April, Munich, Germany. **ACHEMA**. 🌐 <https://www.achema.de/>

27–28 April, Basel, Switzerland. Lab Vision. 🌐 <https://www.spectaris.de/analysen-bio-und-labortechnik/labvision>

24–26 November, Istanbul, Turkey. **Turkchem**. 🌐 <http://www.chemshoweurasia.com/>

# DIRECTORY

## ATOMIC

Bruker AXS GmbH	<a href="mailto:info.BAXS@bruker.com">info.BAXS@bruker.com</a> <a href="http://www.bruker.com/about-us.html">www.bruker.com/about-us.html</a>
Oxford Instruments NanoScience	<a href="mailto:nanoscience@oxinst.com">nanoscience@oxinst.com</a> <a href="http://nanoscience.oxinst.com">nanoscience.oxinst.com</a>


## Atomic Emission

Bruker AXS GmbH	<a href="mailto:info.BAXS@bruker.com">info.BAXS@bruker.com</a> <a href="http://www.bruker.com/about-us.html">www.bruker.com/about-us.html</a>
-----------------	--

## Atomic Fluorescence

Oxford Instruments NanoScience	<a href="mailto:nanoscience@oxinst.com">nanoscience@oxinst.com</a> <a href="http://nanoscience.oxinst.com">nanoscience.oxinst.com</a>
--------------------------------	--

## CHEMICALS AND RMS

Bureau of Analysed Samples Ltd	<a href="mailto:enquiries@basrid.co.uk">enquiries@basrid.co.uk</a> <a href="http://www.basrid.co.uk">www.basrid.co.uk</a>
	Starna Scientific Limited <a href="mailto:sales@starna.com">sales@starna.com</a> <a href="http://www.starna.com">www.starna.com</a>

## DATA HANDLING

	ACD/Labs <a href="mailto:info@acdlabs.com">info@acdlabs.com</a> <a href="http://www.acdlabs.com">www.acdlabs.com</a>
	Linkam Scientific Instruments <a href="mailto:info@linkam.co.uk">info@linkam.co.uk</a> <a href="http://www.linkam.co.uk">www.linkam.co.uk</a>
	Renishaw Ltd <a href="mailto:raman@renishaw.com">raman@renishaw.com</a> <a href="http://www.renishaw.com/raman">www.renishaw.com/raman</a>
	SepSolve Analytical Ltd <a href="mailto:hello@sepsolve.com">hello@sepsolve.com</a> <a href="http://www.sepsolve.com">www.sepsolve.com</a>
	S.T.Japan-Europe GmbH <a href="mailto:contact@stjapan.de">contact@stjapan.de</a> <a href="http://www.stjapan.de">www.stjapan.de</a>

## GAMMA-RAY

 Instruments That Advance The Art	XIA LLC <a href="mailto:sales@xia.com">sales@xia.com</a> <a href="http://www.xia.com">www.xia.com</a>
--	---

## IMAGING

 BaySpec, Inc.	ABB Measurement & Analytics <a href="mailto:ftir@ca.abb.com">ftir@ca.abb.com</a> <a href="http://abb.com/analytical">abb.com/analytical</a> <a href="mailto:info@bayspec.com">info@bayspec.com</a> <a href="http://www.bayspec.com">www.bayspec.com</a>
	Bruker Optik GmbH <a href="mailto:info.bopt.de@bruker.com">info.bopt.de@bruker.com</a> <a href="http://www.bruker.com/optics">www.bruker.com/optics</a>
	Delta Optical Thin Film A/S <a href="mailto:info@deltaopticalthinfilm.com">info@deltaopticalthinfilm.com</a> <a href="http://www.deltaopticalthinfilm.com">www.deltaopticalthinfilm.com</a>
	IM Publications Open LLP <a href="mailto:info@impopen.com">info@impopen.com</a> <a href="http://www.impopen.com">www.impopen.com</a>
	Linkam Scientific Instruments <a href="mailto:info@linkam.co.uk">info@linkam.co.uk</a> <a href="http://www.linkam.co.uk">www.linkam.co.uk</a>
 MEDWAY OPTICS LTD	Medway Optics Ltd <a href="mailto:medwayoptics@aol.com">medwayoptics@aol.com</a> <a href="http://www.medwayoptics.com">www.medwayoptics.com</a>
Oxford Instruments NanoScience	<a href="mailto:nanoscience@oxinst.com">nanoscience@oxinst.com</a> <a href="http://nanoscience.oxinst.com">nanoscience.oxinst.com</a>
Pro-Lite Technology Ltd	<a href="mailto:info@pro-lite.co.uk">info@pro-lite.co.uk</a> <a href="http://www.pro-lite.co.uk">www.pro-lite.co.uk</a>
	Quantum Design UK and Ireland Ltd <a href="mailto:info@qd-uki.co.uk">info@qd-uki.co.uk</a> <a href="http://www.qd-uki.co.uk">www.qd-uki.co.uk</a>
	WITec GmbH <a href="mailto:info@witec.de">info@witec.de</a> <a href="http://www.witec.de">www.witec.de</a>

## Want To Be Seen Here?

You can be part of the 2021 Directory from £145/€160/\$190 and reach a global audience of over 26,000

[spectroscopyeurope.com/advertise](http://spectroscopyeurope.com/advertise)



# DIRECTORY

## INFRARED



ABB Measurement & Analytics  
[ftir@ca.abb.com](mailto:ftir@ca.abb.com)  
[abb.com/analytical](http://abb.com/analytical)



AP Technologies Ltd  
[info@aptechnologies.co.uk](mailto:info@aptechnologies.co.uk)  
[www.aptechnologies.co.uk](http://www.aptechnologies.co.uk)

BaySpec, Inc.

[info@bayspec.com](mailto:info@bayspec.com)  
[www.bayspec.com](http://www.bayspec.com)



Bruker Optik GmbH  
[info.bopt.de@bruker.com](mailto:info.bopt.de@bruker.com)  
[www.bruker.com/optics](http://www.bruker.com/optics)



Edinburgh Instruments Ltd  
[alison.winn@edinst.com](mailto:alison.winn@edinst.com)  
[www.edinst.com](http://www.edinst.com)



Gigahertz Optik GmbH  
[info@gigahertz-optik.de](mailto:info@gigahertz-optik.de)  
[www.gigahertz-optik.de](http://www.gigahertz-optik.de)



IM Publications Open LLP  
[info@impopen.com](mailto:info@impopen.com)  
[www.impopen.com](http://www.impopen.com)



Linkam Scientific Instruments  
[info@linkam.co.uk](mailto:info@linkam.co.uk)  
[www.linkam.co.uk](http://www.linkam.co.uk)



Medway Optics Ltd  
[medwayoptics@aol.com](mailto:medwayoptics@aol.com)  
[www.medwayoptics.com](http://www.medwayoptics.com)



Ocean Insight  
[info@oceaninsight.com](mailto:info@oceaninsight.com)  
[oceaninsight.com](http://oceaninsight.com)

Oxford Instruments  
 NanoScience

[nanoscience@oxinst.com](mailto:nanoscience@oxinst.com)  
[nanoscience.oxinst.com](http://nanoscience.oxinst.com)

Pro-Lite Technology  
 Ltd

[info@pro-lite.co.uk](mailto:info@pro-lite.co.uk)  
[www.pro-lite.co.uk](http://www.pro-lite.co.uk)



Specac Ltd  
[sales@specac.co.uk](mailto:sales@specac.co.uk)  
[www.specac.com](http://www.specac.com)



Starna Scientific Limited  
[sales@starna.com](mailto:sales@starna.com)  
[www.starna.com](http://www.starna.com)



S.T.Japan-Europe GmbH  
[contact@stjapan.de](mailto:contact@stjapan.de)  
[www.stjapan.de](http://www.stjapan.de)



Viavi Solutions Inc.  
[steve.saxe@viavisolutions.com](mailto:steve.saxe@viavisolutions.com)  
[www.micronir.com](http://www.micronir.com)



Wasatch Photonics  
[info@wasatchphotonics.com](mailto:info@wasatchphotonics.com)  
[www.wasatchphotonics.com](http://www.wasatchphotonics.com)

## LASER



Edinburgh Instruments Ltd  
[alison.winn@edinst.com](mailto:alison.winn@edinst.com)  
[www.edinst.com](http://www.edinst.com)



Gigahertz Optik GmbH  
[info@gigahertz-optik.de](mailto:info@gigahertz-optik.de)  
[www.gigahertz-optik.de](http://www.gigahertz-optik.de)

LTB Lasertechnik Berlin  
 GmbH

[info@ltb-berlin.de](mailto:info@ltb-berlin.de)  
[www.ltb-berlin.de/en/homepage/](http://www.ltb-berlin.de/en/homepage/)



Linkam Scientific Instruments  
[info@linkam.co.uk](mailto:info@linkam.co.uk)  
[www.linkam.co.uk](http://www.linkam.co.uk)



Ocean Insight  
[info@oceaninsight.com](mailto:info@oceaninsight.com)  
[oceaninsight.com](http://oceaninsight.com)

Oxford Instruments  
 NanoScience

[nanoscience@oxinst.com](mailto:nanoscience@oxinst.com)  
[nanoscience.oxinst.com](http://nanoscience.oxinst.com)

## LUMINESCENCE

Applied Photophysics  
 Ltd

[info@photophysics.com](mailto:info@photophysics.com)  
[www.photophysics.com](http://www.photophysics.com)



AP Technologies Ltd  
[info@aptechnologies.co.uk](mailto:info@aptechnologies.co.uk)  
[www.aptechnologies.co.uk](http://www.aptechnologies.co.uk)



Delta Optical Thin Film A/S  
[info@deltaopticalthinfilm.com](mailto:info@deltaopticalthinfilm.com)  
[www.deltaopticalthinfilm.com](http://www.deltaopticalthinfilm.com)



Edinburgh Instruments Ltd  
[alison.winn@edinst.com](mailto:alison.winn@edinst.com)  
[www.edinst.com](http://www.edinst.com)



Linkam Scientific Instruments  
[info@linkam.co.uk](mailto:info@linkam.co.uk)  
[www.linkam.co.uk](http://www.linkam.co.uk)

LTB Lasertechnik Berlin  
 GmbH

[info@ltb-berlin.de](mailto:info@ltb-berlin.de)  
[www.ltb-berlin.de/en/homepage/](http://www.ltb-berlin.de/en/homepage/)



Medway Optics Ltd  
[medwayoptics@aol.com](mailto:medwayoptics@aol.com)  
[www.medwayoptics.com](http://www.medwayoptics.com)



Ocean Insight  
[info@oceaninsight.com](mailto:info@oceaninsight.com)  
[oceaninsight.com](http://oceaninsight.com)

Oxford Instruments  
 NanoScience

[nanoscience@oxinst.com](mailto:nanoscience@oxinst.com)  
[nanoscience.oxinst.com](http://nanoscience.oxinst.com)

Pro-Lite Technology  
 Ltd

[info@pro-lite.co.uk](mailto:info@pro-lite.co.uk)  
[www.pro-lite.co.uk](http://www.pro-lite.co.uk)



Quantum Design UK and Ireland Ltd  
[info@qd-uki.co.uk](mailto:info@qd-uki.co.uk)  
[www.qd-uki.co.uk](http://www.qd-uki.co.uk)

# DIRECTORY



Wasatch Photonics  
[info@wasatchphotonics.com](mailto:info@wasatchphotonics.com)  
[www.wasatchphotonics.com](http://www.wasatchphotonics.com)



WITec GmbH  
[info@witec.de](mailto:info@witec.de)  
[www.witec.de](http://www.witec.de)



XIA LLC  
[sales@xia.com](mailto:sales@xia.com)  
[www.xia.com](http://www.xia.com)

## MAGNETIC RESONANCE



IM Publications Open LLP  
[info@impopen.com](mailto:info@impopen.com)  
[www.impopen.com](http://www.impopen.com)



Magritek GmbH  
[sales@magritek.com](mailto:sales@magritek.com)  
[www.magritek.com](http://www.magritek.com)



Oxford Instruments  
[magres@oxinst.com](mailto:magres@oxinst.com)  
[www.oxinst.com/nmr](http://www.oxinst.com/nmr)

## MASS SPECTROMETRY

BaySpec, Inc.

[info@bayspec.com](mailto:info@bayspec.com)  
[www.bayspec.com](http://www.bayspec.com)



Hidden Analytical Ltd  
[info@hidden.co.uk](mailto:info@hidden.co.uk)  
[www.hiddenanalytical.com](http://www.hiddenanalytical.com)



IM Publications Open LLP  
[info@impopen.com](mailto:info@impopen.com)  
[www.impopen.com](http://www.impopen.com)



SepSolve Analytical Ltd  
[hello@sepsolve.com](mailto:hello@sepsolve.com)  
[www.sepsolve.com](http://www.sepsolve.com)

## MOBILE SPECTROMETERS



AP Technologies Ltd  
[info@aptechnologies.co.uk](mailto:info@aptechnologies.co.uk)  
[www.aptechnologies.co.uk](http://www.aptechnologies.co.uk)

BaySpec, Inc.

[info@bayspec.com](mailto:info@bayspec.com)  
[www.bayspec.com](http://www.bayspec.com)

Bruker AXS GmbH

[info.BAXS@bruker.com](mailto:info.BAXS@bruker.com)  
[www.bruker.com/about-us.html](http://www.bruker.com/about-us.html)



Bruker Optik GmbH  
[info.bopt.de@bruker.com](mailto:info.bopt.de@bruker.com)  
[www.bruker.com/optics](http://www.bruker.com/optics)



Gigahertz Optik GmbH  
[info@gigahertz-optik.de](mailto:info@gigahertz-optik.de)  
[www.gigahertz-optik.de](http://www.gigahertz-optik.de)



Magritek GmbH  
[sales@magritek.com](mailto:sales@magritek.com)  
[www.magritek.com](http://www.magritek.com)



Ocean Insight  
[info@oceaninsight.com](mailto:info@oceaninsight.com)  
[oceaninsight.com](http://oceaninsight.com)

Pro-Lite Technology Ltd

[info@pro-lite.co.uk](mailto:info@pro-lite.co.uk)  
[www.pro-lite.co.uk](http://www.pro-lite.co.uk)



VIAVI Solutions

ViaVi Solutions Inc.  
[steve.saxe@viavisolutions.com](mailto:steve.saxe@viavisolutions.com)  
[www.micronir.com](http://www.micronir.com)



Wasatch Photonics  
[info@wasatchphotonics.com](mailto:info@wasatchphotonics.com)  
[www.wasatchphotonics.com](http://www.wasatchphotonics.com)



XIA LLC  
[sales@xia.com](mailto:sales@xia.com)  
[www.xia.com](http://www.xia.com)

## PLASMA SPECTROSCOPY



Linkam Scientific Instruments  
[info@linkam.co.uk](mailto:info@linkam.co.uk)  
[www.linkam.co.uk](http://www.linkam.co.uk)

LTB Lasertechnik Berlin GmbH

[info@ltb-berlin.de](mailto:info@ltb-berlin.de)  
[www.ltb-berlin.de/en/homepage/](http://www.ltb-berlin.de/en/homepage/)

Pro-Lite Technology Ltd

[info@pro-lite.co.uk](mailto:info@pro-lite.co.uk)  
[www.pro-lite.co.uk](http://www.pro-lite.co.uk)

## POLARIMETRY

Applied Photophysics Ltd

[info@photophysics.com](mailto:info@photophysics.com)  
[www.photophysics.com](http://www.photophysics.com)



Linkam Scientific Instruments  
[info@linkam.co.uk](mailto:info@linkam.co.uk)  
[www.linkam.co.uk](http://www.linkam.co.uk)



Starna Scientific Limited  
[sales@starna.com](mailto:sales@starna.com)  
[www.starna.com](http://www.starna.com)

## PROCESS



ABB Measurement & Analytics  
[ftir@ca.abb.com](mailto:ftir@ca.abb.com)  
[abb.com/analytical](http://abb.com/analytical)



Bruker Optik GmbH  
[info.bopt.de@bruker.com](mailto:info.bopt.de@bruker.com)  
[www.bruker.com/optics](http://www.bruker.com/optics)



Hidden Analytical Ltd  
[info@hidden.co.uk](mailto:info@hidden.co.uk)  
[www.hiddenanalytical.com](http://www.hiddenanalytical.com)



Linkam Scientific Instruments  
[info@linkam.co.uk](mailto:info@linkam.co.uk)  
[www.linkam.co.uk](http://www.linkam.co.uk)

# DIRECTORY

LTB Lasertechnik Berlin  
GmbH



## PHOTONICS & OPTICS



LTB Lasertechnik Berlin  
GmbH



MEDWAY OPTICS LTD

Oxford Instruments  
NanoScience



[info@ltb-berlin.de](mailto:info@ltb-berlin.de)  
[www.ltb-berlin.de/en/homepage/](http://www.ltb-berlin.de/en/homepage/)

Magritek GmbH  
[sales@magritek.com](mailto:sales@magritek.com)  
[www.magritek.com](http://www.magritek.com)

Ocean Insight  
[info@oceaninsight.com](mailto:info@oceaninsight.com)  
[oceaninsight.com](http://oceaninsight.com)

Renishaw Ltd  
[raman@renishaw.com](mailto:raman@renishaw.com)  
[www.renishaw.com/raman](http://www.renishaw.com/raman)

Starna Scientific Limited  
[sales@starna.com](mailto:sales@starna.com)  
[www.starna.com](http://www.starna.com)

Viavi Solutions Inc.  
[steve.saxe@viavisolutions.com](mailto:steve.saxe@viavisolutions.com)  
[www.micronir.com](http://www.micronir.com)

AP Technologies Ltd  
[info@aptechnologies.co.uk](mailto:info@aptechnologies.co.uk)  
[www.aptechnologies.co.uk](http://www.aptechnologies.co.uk)

Bruker Optik GmbH  
[info.bopt.de@bruker.com](mailto:info.bopt.de@bruker.com)  
[www.bruker.com/optics](http://www.bruker.com/optics)

Delta Optical Thin Film A/S  
[info@deltaopticalthinfilm.com](mailto:info@deltaopticalthinfilm.com)  
[www.deltaopticalthinfilm.com](http://www.deltaopticalthinfilm.com)

Edinburgh Instruments Ltd  
[alison.winn@edinst.com](mailto:alison.winn@edinst.com)  
[www.edinst.com](http://www.edinst.com)

Gigahertz Optik GmbH  
[info@gigahertz-optik.de](mailto:info@gigahertz-optik.de)  
[www.gigahertz-optik.de](http://www.gigahertz-optik.de)

Linkam Scientific Instruments  
[info@linkam.co.uk](mailto:info@linkam.co.uk)  
[www.linkam.co.uk](http://www.linkam.co.uk)

[info@ltb-berlin.de](mailto:info@ltb-berlin.de)  
[www.ltb-berlin.de/en/homepage/](http://www.ltb-berlin.de/en/homepage/)

Medway Optics Ltd  
[medwayoptics@aol.com](mailto:medwayoptics@aol.com)  
[www.medwayoptics.com](http://www.medwayoptics.com)

[nanoscience@oxinst.com](mailto:nanoscience@oxinst.com)  
[nanoscience.oxinst.com](http://nanoscience.oxinst.com)

Quantum Design UK and Ireland Ltd  
[info@qd-uki.co.uk](mailto:info@qd-uki.co.uk)  
[www.qd-uki.co.uk](http://www.qd-uki.co.uk)

Specac Ltd  
[sales@specac.co.uk](mailto:sales@specac.co.uk)  
[www.specac.com](http://www.specac.com)



Starna Scientific Limited

[sales@starna.com](mailto:sales@starna.com)  
[www.starna.com](http://www.starna.com)



Wasatch Photonics  
[info@wasatchphotonics.com](mailto:info@wasatchphotonics.com)  
[www.wasatchphotonics.com](http://www.wasatchphotonics.com)

## RAMAN



LTB Lasertechnik Berlin  
GmbH



Oxford Instruments  
NanoScience

Pro-Lite Technology  
Ltd



Bruker Optik GmbH  
[info.bopt.de@bruker.com](mailto:info.bopt.de@bruker.com)  
[www.bruker.com/optics](http://www.bruker.com/optics)

Edinburgh Instruments Ltd  
[alison.winn@edinst.com](mailto:alison.winn@edinst.com)  
[www.edinst.com](http://www.edinst.com)

IM Publications Open LLP  
[info@impopen.com](mailto:info@impopen.com)  
[www.impopen.com](http://www.impopen.com)

Linkam Scientific Instruments  
[info@linkam.co.uk](mailto:info@linkam.co.uk)  
[www.linkam.co.uk](http://www.linkam.co.uk)

[info@ltb-berlin.de](mailto:info@ltb-berlin.de)  
[www.ltb-berlin.de/en/homepage/](http://www.ltb-berlin.de/en/homepage/)

Ocean Insight  
[info@oceaninsight.com](mailto:info@oceaninsight.com)  
[oceaninsight.com](http://oceaninsight.com)

[nanoscience@oxinst.com](mailto:nanoscience@oxinst.com)  
[nanoscience.oxinst.com](http://nanoscience.oxinst.com)

[info@pro-lite.co.uk](mailto:info@pro-lite.co.uk)  
[www.pro-lite.co.uk](http://www.pro-lite.co.uk)

Renishaw Ltd  
[raman@renishaw.com](mailto:raman@renishaw.com)  
[www.renishaw.com/raman](http://www.renishaw.com/raman)

Rigaku Europe SE  
[rese@rigaku.com](mailto:rese@rigaku.com)  
[www.rigaku.com](http://www.rigaku.com)

S.T.Japan-Europe GmbH  
[contact@stjapan.de](mailto:contact@stjapan.de)  
[www.stjapan.de](http://www.stjapan.de)

Starna Scientific Limited  
[sales@starna.com](mailto:sales@starna.com)  
[www.starna.com](http://www.starna.com)

Wasatch Photonics  
[info@wasatchphotonics.com](mailto:info@wasatchphotonics.com)  
[www.wasatchphotonics.com](http://www.wasatchphotonics.com)

WITec GmbH  
[info@witec.de](mailto:info@witec.de)  
[www.witec.de](http://www.witec.de)



# DIRECTORY

## RELATED EQUIPMENT



Bruker Optik GmbH  
[info.bopt.de@bruker.com](mailto:info.bopt.de@bruker.com)  
[www.bruker.com/optics](http://www.bruker.com/optics)



Linkam Scientific Instruments  
[info@linkam.co.uk](mailto:info@linkam.co.uk)  
[www.linkam.co.uk](http://www.linkam.co.uk)

LTB Lasertechnik Berlin GmbH

[info@ltb-berlin.de](mailto:info@ltb-berlin.de)  
[www.ltb-berlin.de/en/homepage/](http://www.ltb-berlin.de/en/homepage/)



Magritek GmbH  
[sales@magritek.com](mailto:sales@magritek.com)  
[www.magritek.com](http://www.magritek.com)



Quantum Design UK and Ireland Ltd  
[info@qd-uki.co.uk](mailto:info@qd-uki.co.uk)  
[www.qd-uki.co.uk](http://www.qd-uki.co.uk)



Renishaw Ltd  
[raman@renishaw.com](mailto:raman@renishaw.com)  
[www.renishaw.com/raman](http://www.renishaw.com/raman)



Starna Scientific Limited  
[sales@starna.com](mailto:sales@starna.com)  
[www.starna.com](http://www.starna.com)



Viavi Solutions Inc.  
[steve.saxe@viavisolutions.com](mailto:steve.saxe@viavisolutions.com)  
[www.micronir.com](http://www.micronir.com)



Instruments That Advance The Art

XIA LLC  
[sales@xia.com](mailto:sales@xia.com)  
[www.xia.com](http://www.xia.com)

## SAMPLE PREPARATION



Medway Optics Ltd  
[medwayoptics@aol.com](mailto:medwayoptics@aol.com)  
[www.medwayoptics.com](http://www.medwayoptics.com)



SepSolve Analytical Ltd  
[hello@sepsolve.com](mailto:hello@sepsolve.com)  
[www.sepsolve.com](http://www.sepsolve.com)



Specac Ltd  
[sales@specac.co.uk](mailto:sales@specac.co.uk)  
[www.specac.com](http://www.specac.com)



S.T. Japan-Europe GmbH  
[contact@stjapan.de](mailto:contact@stjapan.de)  
[www.stjapan.de](http://www.stjapan.de)

## SEPARATION SCIENCE



SepSolve Analytical Ltd  
[hello@sepsolve.com](mailto:hello@sepsolve.com)  
[www.sepsolve.com](http://www.sepsolve.com)

## SPECTRORADIOMETRY



ABB Measurement & Analytics  
[ftir@ca.abb.com](mailto:ftir@ca.abb.com)  
[abb.com/analytical](http://abb.com/analytical)



Gigahertz Optik GmbH  
[info@gigahertz-optik.de](mailto:info@gigahertz-optik.de)  
[www.gigahertz-optik.de](http://www.gigahertz-optik.de)

## SURFACE ANALYSIS



Hiden Analytical Ltd  
[info@hiden.co.uk](mailto:info@hiden.co.uk)  
[www.hidenanalytical.com](http://www.hidenanalytical.com)



Linkam Scientific Instruments  
[info@linkam.co.uk](mailto:info@linkam.co.uk)  
[www.linkam.co.uk](http://www.linkam.co.uk)



Ocean Insight  
[info@oceaninsight.com](mailto:info@oceaninsight.com)  
[oceaninsight.com](http://oceaninsight.com)

## TERAHERTZ



Edinburgh Instruments Ltd  
[alison.winn@edinst.com](mailto:alison.winn@edinst.com)  
[www.edinst.com](http://www.edinst.com)

Oxford Instruments  
 NanoScience

[nanoscience@oxinst.com](mailto:nanoscience@oxinst.com)  
[nanoscience.oxinst.com](http://nanoscience.oxinst.com)

## UV AND VISIBLE



AP Technologies Ltd  
[info@aptechnologies.co.uk](mailto:info@aptechnologies.co.uk)  
[www.aptechnologies.co.uk](http://www.aptechnologies.co.uk)



Edinburgh Instruments Ltd  
[alison.winn@edinst.com](mailto:alison.winn@edinst.com)  
[www.edinst.com](http://www.edinst.com)



Gigahertz Optik GmbH  
[info@gigahertz-optik.de](mailto:info@gigahertz-optik.de)  
[www.gigahertz-optik.de](http://www.gigahertz-optik.de)



Linkam Scientific Instruments  
[info@linkam.co.uk](mailto:info@linkam.co.uk)  
[www.linkam.co.uk](http://www.linkam.co.uk)



Medway Optics Ltd  
[medwayoptics@aol.com](mailto:medwayoptics@aol.com)  
[www.medwayoptics.com](http://www.medwayoptics.com)



Ocean Insight  
[info@oceaninsight.com](mailto:info@oceaninsight.com)  
[oceaninsight.com](http://oceaninsight.com)

Oxford Instruments  
 NanoScience

[nanoscience@oxinst.com](mailto:nanoscience@oxinst.com)  
[nanoscience.oxinst.com](http://nanoscience.oxinst.com)

Pro-Lite Technology  
 Ltd

[info@pro-lite.co.uk](mailto:info@pro-lite.co.uk)  
[www.pro-lite.co.uk](http://www.pro-lite.co.uk)



Starna Scientific Limited  
[sales@starna.com](mailto:sales@starna.com)  
[www.starna.com](http://www.starna.com)

## X-RAY DIFFRACTION

Bruker AXS GmbH

[info.BAXS@bruker.com](mailto:info.BAXS@bruker.com)  
[www.bruker.com/about-us.html](http://www.bruker.com/about-us.html)



Linkam Scientific Instruments  
[info@linkam.co.uk](mailto:info@linkam.co.uk)  
[www.linkam.co.uk](http://www.linkam.co.uk)



Rigaku Europe SE  
[rese@rigaku.com](mailto:rese@rigaku.com)  
[www.rigaku.com](http://www.rigaku.com)

## X-RAY SPECTROMETRY

Bruker AXS GmbH

[info.BAXS@bruker.com](mailto:info.BAXS@bruker.com)  
[www.bruker.com/about-us.html](http://www.bruker.com/about-us.html)



IM Publications Open LLP  
[info@impopen.com](mailto:info@impopen.com)  
[www.impopen.com](http://www.impopen.com)



Linkam Scientific Instruments  
[info@linkam.co.uk](mailto:info@linkam.co.uk)  
[www.linkam.co.uk](http://www.linkam.co.uk)



Quantum Design UK and Ireland Ltd  
[info@qd-uki.co.uk](mailto:info@qd-uki.co.uk)  
[www.qd-uki.co.uk](http://www.qd-uki.co.uk)



Rigaku Europe SE  
[rese@rigaku.com](mailto:rese@rigaku.com)  
[www.rigaku.com](http://www.rigaku.com)



Specac Ltd  
[sales@specac.co.uk](mailto:sales@specac.co.uk)  
[www.specac.com](http://www.specac.com)



XIA LLC  
[sales@xia.com](mailto:sales@xia.com)  
[www.xia.com](http://www.xia.com)

# Introduction to the Theory and Practice of Sampling

Kim H. Esbensen

with contributions from Claas Wagner, Pentti Minkkinen, Claudia Paoletti, Karin Engström, Martin Lischka and Jørgen Riis Pedersen

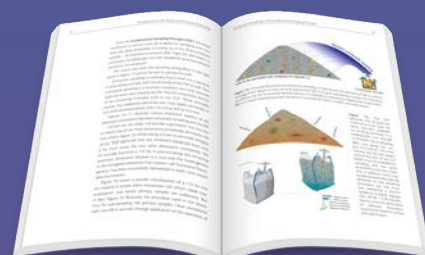
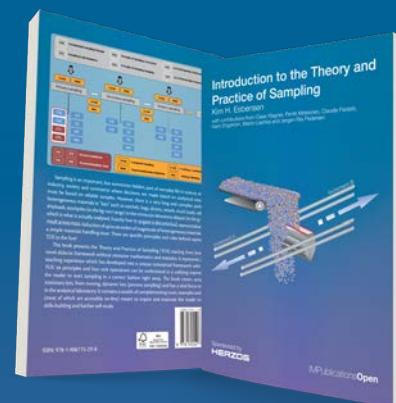
“Sampling is not gambling”. Analytical results forming the basis for decision making in science, technology, industry and society must be relevant, valid and reliable. However, analytical results cannot be detached from the specific conditions under which they originated. Sampling comes to the fore as a critical success factor before analysis, which should only be made on documented representative samples. There is a complex and challenging pathway from heterogeneous materials in “lots” such as satchels, bags, drums, vessels, truck loads, railroad cars, shiploads, stockpiles (in the kg–ton range) to the miniscule laboratory aliquot (in the g– $\mu$ g range), which is what is actually analysed.

This book presents the Theory and Practice of Sampling (TOS) starting from level zero in a novel didactic framework without excessive mathematics and statistics. The book covers sampling from stationary lots, from moving, dynamic lots (process sampling) and has a vital focus on sampling in the analytical laboratory.

“I recommend this book to all newcomers to TOS”

“This book may well end up being the standard introduction sourcebook for representative sampling.”

“One of the book’s major advantages is the lavish use of carefully designed didactic diagrams”



**[impopen.com/sampling](http://impopen.com/sampling)**

IMPublicationsOpen